TECHNICAL REPORT R-53

TRAJECTORIES WITH CONSTANT TANGENTIAL THRUST IN CENTRAL GRAVITATIONAL FIELDS

By W. E. MOECKEL

Lewis Research Center
Cleveland, Ohio

TECHNICAL REPORT R-53

TRAJECTORIES WITH CONSTANT TANGENTIAL THRUST IN CENTRAL GRAVITATIONAL FIELDS

By W. E. Moeckel

SUMMARY

Trajectories followed by vehicles propelled by a constant thrust directed parallel to the velocity vector were calculated in nondimensional form for a range of initial thrust-weight ratios from 10 to 10^{-4} and for a range of jet velocities from those attainable with chemical rockets to infinity. Trajectories are presented both for the departure outward from any circular orbit and the inward return to any circular orbit. Results are given in the form of curves of radial distance, energy per unit mass (hyperbolic velocity), trajectory inclination, and velocity and angular distance as functions of time. Utilization of these charts to estimate weight requirements for interplanetary missions is discussed.

INTRODUCTION

The trajectory followed by a space vehicle propelled by a constant thrust in a gravitational field is determined primarily by the initial acceleration (initial thrust-weight ratio) and the specific impulse (or jet velocity). For the many propulsion systems being considered for space missions, these parameters vary over very large ranges. Therefore, in order to evaluate performance, the propulsion time (and from this the propellant consumption) required to perform various space missions must be determined as a function of the propulsion-system parameters. This report presents results of generalized trajectory calculations in a form suitable for performance analyses for a range of parameters great enough to cover most propulsion systems of interest. These results were obtained by numerical integration with a digital computer.

Previous work on continuous-thrust trajectories is reported in references 1 to 4. In reference 1, the equations of motion are described, and some results of calculations are presented which compare propulsion times required to attain escape velocity using radial, circumferential, and tangential thrust. Tangential thrust was found to be the most efficient of the three, although there was little difference between tangential and circumferential thrust up to escape velocity.

In reference 2, calculations are presented for an Earth-Mars trajectory using tangential-thrust values appropriate for an electric space vehicle. This trajectory was a trial-and-error solution with constant thrust applied almost continuously (except for brief coasting periods to correct the trajectory) during an Earth-Mars transfer. Although no attempt was made to minimize the initial weight required for the mission, this paper was the first to show the feasibility of such a mission.

Another procedure is analyzed in reference 3. This procedure consisted of using an Earth-centered trajectory until the escape condition was reached on the outward trip. Beyond this point, trajectories were calculated on a heliocentric basis. The Earth-Mars transfer trajectories were determined by requiring that the vehicle match the speed and direction of Mars on reaching the Mars orbit. For a specified transfer time, it was shown that a single trajectory that minimizes the propellant consumption could be found. These optimum trajectories required constant applied jet power but not constant thrust; that is, both specific impulse and thrust were varied, but the product of the two was constant. Programing of the thrust direction, as well as magnitudes, was required to produce the optimum trajectory. It was found that, during the middle portion of the optimum transfer trajectory, the thrust required became quite small and the specific impulse correspondingly quite large. Such trajectories would therefore require propulsion systems capable of

rather wide ranges of operating conditions. However, since the required thrust and mass-flow consumptions are so low during the middle portions of the paths, it seems likely that an alternative trajectory consisting of somewhat higher thrust at the beginning and end of the trajectory with a coasting period between would be almost as satisfactory from the standpoint of propellant consumption. The procedure of reference 3 is excellent for determining minimum propulsion requirements for specified one-way-trip times, but it is not suited to rapid evaluation of round-trip missions, where waiting time must be considered and where optimum one-way trajectories do not necessarily produce minimum total trip time.

General trajectory charts, with which radial and angular distance and other parameters can be rapidly determined as functions of propulsion time for wide ranges of propulsion-system parameters, are extremely useful for preliminary mission analyses. Such charts have recently been presented in reference 4 for the case of constant thrust acceleration. Except for the special case of infinite specific impulse, a constant-thrust-acceleration trajectory requires that the thrust be reduced in proportion as the propellant mass is ejected. The correlation parameters developed in reference 4, however, have considerable generality and may be useful for other types of trajectory.

The charts presented in the present report provide in convenient form all trajectory variables required to analyze the motion and weight variation of vehicles propelled by constant tangential thrust in a central gravity field.

The types of missions for which the present charts are applicable are those in which continuous, constant thrust is applied at a fixed specific impulse until the energy required to follow a specified free-fall trajectory is attained. Thrust is then cut off and is not reapplied until the "capture" maneuver that produces the desired destination orbit is initiated. These missions are, therefore, similar to those usually considered for high-thrust propulsion systems, except that the assumption that thrust is applied impulsively at the start and end of the journey is not required.

The hyperbolic velocities required to produce a prescribed free-fall transfer time between the Earth and Mars or Venus are presented in reference 5 for several families of trajectories. With the charts of the present report, the propulsion time required to attain these hyperbolic velocities or to return to a prescribed circular orbit from an initial hyperbolic velocity can be determined for low-thrust, as well as high-thrust, propulsion systems. The principal restriction on missions that can be analyzed with these charts is that all portions of the powered trajectory must be realizable with constant tangential thrust. For very low thrust systems, this requirement limits the types of mission to those requiring hyperbolic velocities only moderately greater than those needed for minimum-energy transfer; but the restriction becomes less severe as the thrust is increased.

EQUATIONS OF MOTION WITH APPLIED THRUST

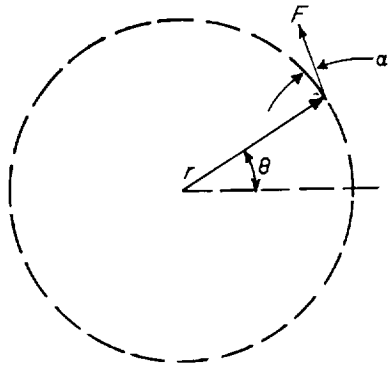

(a)

The equations of motion with continuous thrust are the same as for zero thrust except for the additional term representing the thrust along each component:

$$\ddot{r}-r\dot{\theta}^2=-\frac{\mu}{r^2}+\frac{F}{m}\sin\alpha \tag{1a}$$

$$2\dot{r}\dot{\theta}+r\ddot{\theta}\equiv\frac{1}{r}\frac{\mathrm{d}(r^2\dot{\theta})}{\mathrm{d}t}=\frac{F}{m}\cos\alpha \tag{1b}$$

(All symbols are defined in appendix A.)

The equations can be simplified immediately by introducing nondimensional radii and times defined as follows:

$$\rho=\frac{r}{r_0};\ \tau=\frac{v_{c0}}{r_0}\,t\equiv\sqrt{\frac{\mu}{r_0^3}}\,t\equiv\sqrt{\frac{g_0}{r_0}}\,t \tag{2}$$

where r_0, v_{c0}, and g_0 are the radius, circular velocity, and gravitational acceleration at a reference point

(usually the starting point of an outward trajectory or the destination orbit for inward trajectories). Equations (1a) and (1b) then become

$$\rho'' - \rho\theta'^2 + \frac{1}{\rho^2} = \frac{F}{mg_0}\sin\alpha \tag{3a}$$

$$\frac{(\rho^2\theta')'}{\rho} = \frac{F}{mg_0}\cos\alpha \tag{3b}$$

where m is the instantaneous mass and the primes now denote differentiation with respect to τ.

Now, the mass m decreases during the trip because of propellant ejection and because of the expulsion of waste material and excess tankage. For very high specific impulses, such as are attainable with electric propulsion systems, these sources of mass reduction may be of equal magnitude. It is convenient to consider the discontinuous mass reductions, such as disposal of propellant tanks and other large masses, separately from the continuous mass reductions, such as propellant consumptions and, possibly, human waste disposal. The latter is basically discontinuous also, but over a long period of time it can be effectively considered as a continuous process. The instantaneous mass, therefore, is represented by

$$m = m_0 - \dot{m}t \tag{4}$$

where $\dot{m}$ is assumed to be constant. This is the case when the ship is operating at constant thrust and constant specific impulse and the crew is eliminating wastes at a rather constant rate. The rate of mass consumption can then be represented as

$$\dot{m} = \frac{F}{Ig_{00}} \tag{5}$$

where g_{00} is the gravitational acceleration at the Earth's surface (since I is, by definition, thrust per unit Earth-weight flow) and I is the effective specific impulse, considering both propellant consumption and waste disposal. An example will clarify the possible importance of the distinction between propellant and effective specific impulse: If the thrust is 50 pounds and the propellant specific impulse I_p is 30,000 seconds, the propellant consumption rate is

$$\dot{m}g_{00} = \frac{50}{30{,}000}\times 24\times 3600 = 144 \text{ lb/day}$$

If the crew consists of 8 men, each consuming 10 pounds per day of water, food, and oxygen, then

$$I = \frac{F}{\dot{m}g_{00}} = \frac{50}{144+80}\times 24\times 3600 = 19{,}300 \text{ sec}$$

Thus, the effective specific impulse, assuming that the waste expulsion produces no thrust, is about two-thirds of the propellant specific impulse.

Now, some of the 10 pounds per man per day is probably reusable; in fact, a closed-cycle system might be developed with which almost all the waste is utilized. Also, a means might be developed for using these wastes as propellant. At any rate, it should be noted that the specific impulse now introduced is not necessarily only the propellant specific impulse.

In terms of the nondimensional variables used throughout this paper, the mass used during propulsion becomes

$$\frac{m_p}{m_0} = \frac{Ft}{Ig_{00}m_0} = \frac{F}{m_0g_0}\frac{g_0t}{v_j} = \frac{a_0\tau}{V_j}$$

where a_0 is initial acceleration or thrust-weight ratio (in terms of gravitational acceleration at the reference radius), v_j is the jet velocity (and is equal to Ig_{00} since $\dot{m}v_j \equiv \dot{m}g_{00}I = F$), and $V_j = v_j/v_{c0}$.

Introducing equation (5) into (4) and (4) into (3) yields

$$\rho'' - \rho\theta'^2 + \frac{1}{\rho^2} = \frac{a_0\sin\alpha}{1-\frac{a_0}{V_j}\tau} \tag{6a}$$

$$\frac{(\rho^2\theta')'}{\rho} = \frac{a_0\cos\alpha}{1-\frac{a_0}{V_j}\tau} \tag{6b}$$

The quantity V_j is herein referred to as the specific impulse, or jet velocity, parameter. Equations (6) determine the trajectory of a vehicle propelled by a constant thrust in a gravitational field. Three particular cases are of interest for future application: one in which the thrust is applied circumferentially ($\alpha = 0$), one in which F is parallel to the instantaneous velocity vector (tangential thrust), and one in which the thrust is applied radially

Case A, circumferential thrust ($\alpha=0$):

For this case, equations (6) become

$$\rho''-\rho\theta'^2+\frac{1}{\rho^2}=0 \tag{7a}$$

$$(\rho^2\theta')'=\frac{\rho a_0}{1-\frac{a_0}{V_j}\tau} \tag{7b}$$

These can be reduced to a single differential equation by differentiating equation (7a) and substituting for the derivatives of θ:

$$\rho'''-\rho'\theta'^2-2\rho\theta'\theta''-2\frac{\rho'}{\rho^3}=0 \tag{8a}$$

$$\theta'^2=\frac{1}{\rho}\left(\rho''+\frac{1}{\rho^2}\right) \tag{8b}$$

From (7b),

$$\theta''=\frac{1}{\rho}\left[\frac{a_0}{1-\frac{a_0}{V_j}\tau}-2\rho'\theta'\right]$$

$$=\frac{1}{\rho}\left[\frac{a_0}{1-\frac{a_0}{V_j}\tau}-2\rho'\sqrt{\frac{1}{\rho}\left(\rho''+\frac{1}{\rho^2}\right)}\right]$$

Thus, equation (8a) becomes

$$\rho'''+\frac{3\rho'\rho''}{\rho}+\frac{\rho'}{\rho^3}=\frac{2a_0}{1-\frac{a_0}{V_j}\tau}\sqrt{\frac{\rho''}{\rho}+\frac{1}{\rho^3}} \tag{9}$$

This determines the distance against time curve, and the corresponding trajectory angle is, from equation (8b),

$$\theta=\int_0^\tau\sqrt{\frac{\rho''}{\rho}+\frac{1}{\rho^3}}\,d\tau+\theta_0 \tag{10}$$

The velocity is given by

$$V^2=\rho'^2+\rho^2\theta'^2=\rho'^2=\rho'^2+\rho\rho''+\frac{1}{\rho} \tag{11}$$

and the angle α_1 of the trajectory relative to the circumferential direction is given by

$$\tan\alpha_1=\frac{\rho'}{\rho\theta'}=\frac{\rho'}{\sqrt{\rho\rho''+\frac{1}{\rho}}} \tag{12}$$

Case B, thrust parallel to velocity vector ($\tan\alpha=\dot{r}/r\dot{\theta}$):

For this case, the angle α is equal to α_1 and is given by

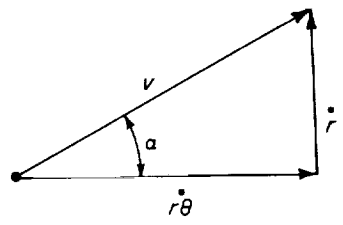

$$\tan\alpha=\frac{\dot{r}}{r\dot{\theta}}=\frac{\rho'}{\rho\theta'}$$

It is convenient, in this case, to change from derivatives of ρ and θ to derivatives of V and α. For this purpose the following relations are needed:

$$\dot{r}=\sqrt{r_0g_0}\rho'=v\sin\alpha=v_{c0}V\sin\alpha=\sqrt{g_0r_0}V\sin\alpha$$

or

$$\rho'=V\sin\alpha;\ \rho''=(V\sin\alpha)' \tag{13a}$$

Similarly,

$$\rho\theta'=V\cos\alpha;\ \theta'=\frac{V}{\rho}\cos\alpha \tag{13b}$$

Substituting into equations (6) yields

$$(V\sin\alpha)'=\frac{V^2}{\rho}\cos^2\alpha-\frac{1}{\rho^2}+\frac{a_0\sin\alpha}{1-\frac{a_0}{V_j}\tau} \tag{14}$$

and

$$(\rho V\cos\alpha)'\equiv\rho'(V\cos\alpha)+\rho(V\cos\alpha)'$$

$$=V^2\sin\alpha\cos\alpha+\rho(V\cos\alpha)'=\frac{\rho a_0\cos\alpha}{1-\frac{a_0}{V_j}\tau}$$

or

$$(V\cos\alpha)'=\frac{a_0\cos\alpha}{1-\frac{a_0}{V_j}\tau}-\frac{V^2}{\rho}\sin\alpha\cos\alpha \tag{15}$$

Equations (14) and (15) can be written

$$\sin\alpha\,dV+V\cos\alpha\,d\alpha=\left(\frac{V^2}{\rho}\cos^2\alpha-\frac{1}{\rho^2}+\frac{a_0\sin\alpha}{1-\frac{a_0}{V_j}\tau}\right)d\tau \tag{16a}$$

$$\cos\alpha\,dV - V\sin\alpha\,d\alpha = \left(\frac{a_0\cos\alpha}{1-\frac{a_0}{V_j}\tau} - \frac{V^2}{\rho}\sin\alpha\cos\alpha\right)d\tau \tag{16b}$$

Multiply (16a) by sin α and (16b) by cos α and add:

$$dV = \left(\frac{a_0}{1-\frac{a_0}{V_j}\tau} - \frac{\sin\alpha}{\rho^2}\right)d\tau \tag{17a}$$

Multiply (16a) by cos α and (16b) by sin α and subtract:

$$V\,d\alpha = \left(\frac{V^2}{\rho} - \frac{1}{\rho^2}\right)\cos\alpha\,d\tau \tag{17b}$$

The final equations for this case are, therefore,

$$dV = \left(\frac{a_0}{1-\frac{a_0}{V_j}\tau} - \frac{\sin\alpha}{\rho^2}\right)d\tau \tag{18a}$$

$$d\alpha = \frac{1}{\rho V}\left(V^2 - \frac{1}{\rho}\right)\cos\alpha\,d\tau \tag{18b}$$

with

$$\left.\begin{aligned} d\rho &= V\sin\alpha\,d\tau \\ d\theta &= \frac{V}{\rho}\cos\alpha\,d\tau \end{aligned}\right\} \tag{19}$$

Case C, radial thrust ($\alpha=90°$):

For this case, the equations of motion become

$$\rho'' - \rho\theta'^2 + \frac{1}{\rho^2} = \frac{a_0}{1-\frac{a_0}{V_j}\tau} \tag{20a}$$

$$\rho^2\theta' = \text{constant} = \rho_0^2\theta_0' \equiv H \tag{20b}$$

where $H=h/r_0v_{c0}$ is the nondimensional angular momentum. For radial acceleration, therefore, the angular momentum is constant, as it is for zero applied thrust. If the trip starts or ends in the circular orbit at reference radius r_0, then $H=1$ since ρ_0 and θ_0' are unity.

For the more general case, $\theta'=H/\rho^2$ and equation (20a) becomes

$$\rho'' - \frac{H^2}{\rho^3} + \frac{1}{\rho^2} = \frac{a_0}{1-\frac{a_0}{V_j}\tau} \tag{21}$$

The corresponding values of θ, V, and α are

$$\theta = H\int_0^\tau \frac{d\tau}{\rho^2} + \theta \tag{22}$$

$$V^2 = \rho'^2 + \rho^2\theta'^2 = \rho'^2 + \frac{H^2}{\rho^2} \tag{23}$$

$$\tan\alpha_1 = \frac{\rho'}{\rho\theta'} = \frac{\rho\rho'}{H} \tag{24}$$

ATTAINMENT OF ESCAPE VELOCITY AND ANY HYPERBOLIC VELOCITY

The energy required to reach the orbit of another planet along a least-energy, or any given excess-energy, free-fall trajectory is usually given in terms of the required hyperbolic velocity (see, for example, ref. 5). The relation between energy, velocity, radius, and hyperbolic velocity is

$$E = \frac{v^2}{2} - \frac{\mu}{r} = \frac{v_h^2}{2} \tag{25}$$

Thus, $v_h^2/2$ is the energy per unit mass and is positive if escape velocity is exceeded. If any specified hyperbolic velocity v_h is to be achieved, the thrust must be cut off when

$$v^2 = v_h^2 + 2\frac{\mu}{r} \tag{26}$$

or

$$V^2 = V_h^2 + \frac{2}{\rho} \tag{27}$$

Obviously, the local escape velocity is attained when $V^2=2/\rho$. From a plot of V_h^2 against τ, the thrust cutoff time required to follow any desired trajectory to another orbit can be determined.

COMPARISON OF CIRCUMFERENTIAL AND TANGENTIAL THRUST

Typical curves of V_h^2 as a function of τ are compared in figure 1 for circumferential and tangential thrust. As pointed out previously (refs. 1 and 3), there is little difference between the two methods of operation for energies up to escape velocity ($V_h^2=0$); but tangential thrust becomes increasingly more advantageous, in terms of propulsion time required to attain a prescribed hyperbolic velocity, as higher values of hyperbolic velocity are required. Radial thrust is less efficient than either of the other methods (ref. 1) but may be useful for special applications where constant angular momentum is desired. The remainder of the report is concerned only with tangential thrust.

RETURN TRAJECTORIES

To compute the return path from any hyperbolic velocity to a prescribed circular orbit using constant tangential thrust would, for direct computation, require an iterative procedure in choosing initial location and trajectory angle such that the desired orbit is finally attained. A simpler procedure, and one that is amenable to general treatment, consists of computing backward in time from the desired final orbit to the initial hyperbolic velocity. The final orbit then serves as the reference orbit. In practice, such a computation is equivalent to a forward computation (positive τ) from an initial orbit, as before, but with the difference that propellant mass is added during the computation instead of subtracted. For the tangential thrust computation, therefore, it is only necessary to change the term $\left(1-\frac{a_0\tau}{V_j}\right)$ in equation (18a) to $\left(1+\frac{a_0\tau}{V_j}\right)$, where a_0 is the final acceleration when the vehicle attains its desired circular orbit. This number is not known at the start, but it can be easily estimated and subsequently corrected if the final mass is different from the value initially assumed. The time parameter τ is now interpreted as $\tau_0-\tau$, where τ_0 is the total propulsion time parameter. Thus, in following the inward trajectory, $\tau_0-\tau=\tau_0$ when the approach is started (i.e., $\tau=0$) and $\tau_0-\tau=0$, or $\tau=\tau_0$, when the destination orbit is attained.

TRAJECTORY CHARTS

Results of the trajectory computations are shown in chart form in figures 2 to 11. Figures 2 to 6 show ρ, V_h^2, V, α, and θ, respectively, as functions of τ for outward trajectories. Figures 7 to 11 show the same parameters as functions of $\tau_0-\tau$ for the inward trajectories. For each case, a_0 ranges from 10 to 10^{-4} and V_j from ∞ to 1.0 (or 0.5 in some cases). Very slight oscillations were obtained during the initial phases of the low-thrust trajectories, but their amplitude was so small as to be barely visible in the plotted form. These oscillations disappeared as the computation proceeded.

The most useful charts for general mission studies are figures 3 and 8, which plot V_h^2 as a function of τ. These charts yield propulsion time required, and consequently propellant weight, for prescribed values of the hyperbolic velocity.

Because of the value of the V_h^2 against τ functions, figures 3 and 8 have been cross-plotted in figures 12 and 13, respectively, to present total propulsion time parameter τ_0 as a function of initial or final acceleration for fixed values of V_h^2 and V_j. These charts are useful if intermediate values of a_0 are encountered. For these charts, calculations were made for values of a_0 intermediate between 10^{-2}, 10^{-1}, and 1.0 to obtain better fairing accuracy in this range of rapidly changing values of $a_0\tau_0$. Since $a_0\tau_0/V_j$ is the propellant-weight ratio, the curves of figures 12 and 13 also show relative propellant weight required to attain a given V_h^2 as the initial acceleration is varied. These curves show, as might be expected, that for $a_0>1.0$ the propellant needed is essentially equal to the value calculated assuming impulsive thrust $\left(\frac{m_1}{m_0}=e^{-\Delta v/v_j}\right)$. As the acceleration is reduced, more propellant is needed because of the gravitational loss associated with long propulsion times in gravitational fields.

An example of the use of the charts for a mission analysis is given in appendix B.

TRANSITION FROM PLANETARY TO HELIOCENTRIC COORDINATES

For low thrust-weight ratios, the distance ratio becomes quite large before escape velocity, or any real hyperbolic velocity, is attained. It is therefore necessary to consider whether, even for the minimum-energy path, the effect of the solar field becomes greater than that of the departure planet before the desired transfer velocity is attained. If it does, then the last part of the accelerating process should be computed in heliocentric coordinates instead of the planetary coordinates. Particularly for excess-energy paths where, with low a_0, thrust may be required for very long periods of time, it is important to try to determine when the original geocentric, or planet-centered, system should be abandoned to switch to the solar field. Of course, an exact computation would consider continuous transition, utilizing the exact effect of both the planet's and the sun's field; but for approximate estimates of propulsion and weight requirements, the two-body equations are sufficient.

To estimate where the change should be made, the equations for the three-body problem must be considered briefly. The point where the planet's

and sun's gravitational fields are equal is not particularly significant because the spaceship shares the planet's circular motion as it starts to move in or out of the planet's field, so that a large part of the effect of the sun's field is canceled out by the centrifugal force of the planetary motion.

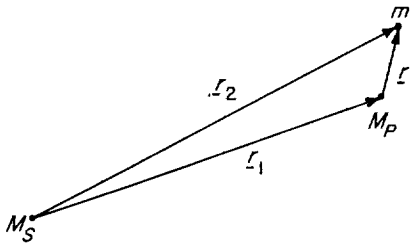

(b)

In sketch (b) let M_S, M_P, and m be the masses of the sun, the planet, and the spaceship, respectively. The vector $\underline{r}_2$ is the distance from the ship to the sun, $\underline{r}$ is the distance from the ship to the planet, and $\underline{r}_1$ is the distance from the planet to the sun. Then, in vector form (and assuming $M_P \ll M_S$),

$$\underline{r}_2 \equiv r_2\hat{r}_2 = \underline{r}_1 + \underline{r} \equiv r_1\hat{r}_1 + r\hat{r} \tag{28}$$

$$\ddot{\underline{r}}_2 = \ddot{\underline{r}}_1 + \ddot{\underline{r}} = -\frac{\mu_S}{r_2^2}\hat{r}_2 - \frac{\mu_P}{r^2}\hat{r} \tag{29}$$

where the circumflex indicates the unit vector. Equation (29) expresses the motion in terms of coordinates relative to the sun.

To determine the motion relative to M_P, note that

$$\ddot{\underline{r}}_1 = -\frac{\mu_S}{r_1^2}\hat{r}_1 = -\frac{\mu_S}{r_1^2}\left[\frac{r_2}{r_1}\hat{r}_2 - \frac{r}{r_1}\hat{r}\right] \tag{30}$$

where $\hat{r}_1$ has been replaced by its equivalent from equation (28). Hence, the equation of motion relative to M_P becomes

$$\ddot{\underline{r}} = \ddot{\underline{r}}_2 - \ddot{\underline{r}}_1 = -\frac{\mu_S}{r_2^2}\hat{r}_2 - \frac{\mu_P}{r^2}\hat{r} + \frac{\mu_S}{r_1^2}\left[\frac{r_2}{r_1}\hat{r}_2 - \frac{r}{r_1}\hat{r}\right]$$

$$= -\frac{\mu_S}{r_2^2}\left[1 - \frac{r_2^3}{r_1^3}\right]\hat{r}_2 - \left[\frac{\mu_P}{r^2} + \frac{\mu_S}{r_1^2}\frac{r}{r_1}\right]\hat{r} \tag{31}$$

With equations (29) and (31), several "spheres of influence," at the boundary of which the strength of a perturbing force becomes of the same order of magnitude as that of the primary force field, can be arbitrarily defined. Thus, if the path of a vehicle is being computed in heliocentric coordinates, equation (29) indicates that the perturbing acceleration due to the planet becomes equal to the acceleration due to the sun when

$$\left(\frac{r}{r_2}\right) \approx \frac{r}{r_1} = \left(\frac{M_P}{M_S}\right)^{1/2} \tag{32}$$

If the path is being computed in planetary coordinates, a similar "sphere of influence" can be found from equation (31) by considering the extremes; that is, when $\underline{r}$ is parallel to $\underline{r}_1$ but is either positive or negative. For these cases (and assuming $r \ll r_1$), the perturbing acceleration due to the sun is found to be equal to the acceleration due to the planet when

$$\frac{r}{r_1} = \left(\frac{1}{2}\frac{M_P}{M_S}\right)^{1/3} \tag{33}$$

Both of these spheres of influence (eqs. (32) and (33)) differ from the one defined by Tisserand in reference 6, which is obtained by setting the ratio of perturbation force to primary force in heliocentric coordinates equal to the same ratio in planetary coordinates. From equations (29) and (31) (with the same approximations as before), these ratios are found to be equal when

$$\frac{\mu_P/r^2}{2\dfrac{\mu_S}{r_1^2}\dfrac{r}{r_1}} = \frac{\mu_S/r_1^2}{\mu_P/r^2}$$

This method yields

$$\frac{r}{r_1} = \left(\frac{1}{2}\right)^{1/5}\left(\frac{M_P}{M_S}\right)^{2/5} \tag{34}$$

This result differs from that of reference 6 only by the factor $\left(\frac{1}{2}\right)^{1/5} = 0.871$. An advantage of a "sphere of influence" defined in this manner is that a single "sphere" applies for both coordinate systems. This advantage, however, appears to be chiefly an aesthetic one. Which "sphere" best approximates the exact trajectory can be determined only by comparison with exact solutions of the three-body problem for a variety of trajectories.

For the interplanetary missions discussed in the present report, it appears that equation (33) may be most appropriate, since the primary fields for most of the powered trajectories are those of the departure or destination planet. Furthermore, the equation of motion relative to the planet

(eq. (31)) includes the effect of the planet's motion around the sun, for which the gravitational acceleration is approximately balanced by centrifugal force. For a vehicle moving at speeds comparable with the planet's speed, this effect should be included in defining the magnitude of the perturbations. Equation (29), on the other hand, contains simply the gravitational attraction of the sun and planet.

Using equation (33), the distances from each planet at which the effective acceleration due to the solar field is equal to that of the planet's field are shown in table I. Values from equation (34) are also shown for comparison. These distances are less than one-tenth of the sun-planet distances, so that the assumption $r \ll r_1$ is a good approximation. For the last column of table I, M_S in equations (33) and (34) was taken to be the Earth's mass and r_1 the Earth-Moon distance. The resulting values of r/r_1 are greater than 0.1, so that the approximation is not as valid as for the planet-sun relations.

Also shown in table I are values of r at which the solar effect is one-tenth of the planet's effect, and the value of r for which the planet's effect is less than one-tenth of the solar effect. These values were obtained by changing the 1/2 in equation (33) to 1/20 and 5, respectively. These values are intended to define the range of distances where the effects of both gravitational fields are comparable.

If two-body computations are used, the switch from planetary coordinates to heliocentric coordinates should be made when the effect of the sun's and the planet's fields are about equal. However, it is generally simpler (and more conservative) to follow an alternative procedure, in which planet-centered coordinates are used until escape velocity is attained. The remainder of the acceleration is then computed on a heliocentric basis. In this manner, the heliocentric trajectory starts in a circular orbit at the planet's circular velocity, so that use of the charts is facilitated. Of course, this switch to heliocentric coordinates is not necessary if the required hyperbolic velocity is attained well within the "sphere of influence" of the planet.

TRANSFER BETWEEN TWO CIRCULAR ORBITS

It should be noted that hyperbolic velocities required for orbit transfer are based on free-fall conic trajectories between the orbits. Consequently, if the powered portion of the trajectory produces values of ρ significantly greater than unity before the hyperbolic velocity is attained, the required free-fall transfer trajectory is no longer the same, and therefore the required hyperbolic velocity becomes a function of the distance at which thrust cutoff occurs. An extreme example of this is the case for which the hyperbolic velocity is so great, or the acceleration so low, that the vehicle reaches the destination orbit before the free-fall hyperbolic velocity is attained. In this case, of course, thrust should have been cut off, or reversed, long before in order to match the circular velocity of the destination orbit. The actual required hyperbolic velocity is thus much less than calculated on the basis of free-fall trajectories, and a mission analysis based on hyperbolic velocities needed for free-fall transfer would be unnecessarily pessimistic with regard to required propulsion time.

TABLE I. –DISTANCES IN MILES FROM PLANET'S CENTER WHERE THIRD-BODY EFFECT BECOMES SIGNIFICANT

Planet		Mercury	Venus	Earth	Mars	Jupiter	Saturn	Uranus	Neptune	Moon	
										M_S=Sun	M_S=Earth
Value of r for which solar and planet's effects are about equal.	Eq. (33)	157,000	720,000	1,064,000	768,000	37.8×10^6	46.3×10^6	50×10^6	83.2×10^6	246,000	43,700
	Eq. (34)	61,000	333,000	502,000	311,000	26×10^6	29.5×10^6	28×10^6	45×10^6	86,600	35,900
Value of r for which solar effect is 0.1 planet's effect (eq. (33))		73,000	334,000	494,000	357,000	17.5×10^6	21.5×10^6	23.2×10^6	38.6×10^6	114,000	20,300
Value of r for which planet's effect is 0.1 solar effect (eq. (33))		338,000	1.55×10^6	2.29×10^6	1.65×10^6	81.5×10^6	94×10^6	108×10^6	180×10^6	530,000	94,200

Sketches (c) and (d) illustrate the types of trajectories that must be calculated for transfers between circular orbits when propulsion time is a significant portion of the total transfer time.

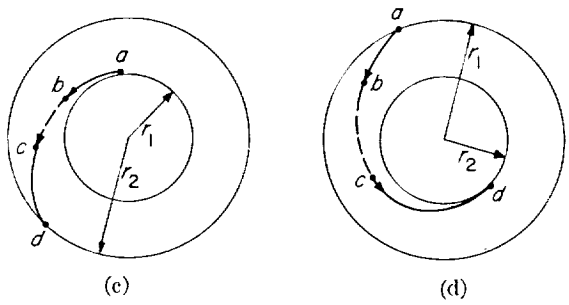

In transferring from an inner to an outer orbit (sketch (c)), the charts of figures 2 to 6 can be used to evaluate the departure portion *ab* of the powered trajectory. If the powered arrival segment *cd* were available in chart form, the two segments could be matched, by iteration, with an appropriate free-fall segment *bc*. Attempts were made to calculate trajectories of the type *cd* by using constant tangential thrust. These attempts were unsuccessful, in that the trajectories moved to larger values of ρ instead of toward the center. This result indicates that approach trajectories to a circular orbit from lower values of r are not possible with constant tangential thrust and cannot, therefore, be represented in general charts of the type contained herein.

For the case of transfer from an outer to an inner circular orbit (sketch (d)), the powered arrival portion *cd* can be evaluated with the charts of figures 7 to 11. Again, if powered departure trajectories of type *ab* were available, the two powered portions could be matched with an appropriate free-fall segment *bc*. Computations attempted for trajectories of type *ab* (departure from circular orbit with constant tangential braking thrust) showed them to be highly oscillatory in nature and therefore probably undesirable for actual use. It appears, therefore, that a thrust programing (in magnitude and/or direction) is necessary for successful completion of a powered transfer between two circular orbits. A technique such as that developed in reference 3 is ideal for this purpose, except that it requires rather elaborate trial and error computations and also requires quite large variations in magnitude of the thrust and jet velocity. Actual engines may not be able to cover such large ranges of parameters.

Another possible procedure is to prescribe reasonable-looking transfer paths and calculate the thrust programing needed to follow these paths. This method is now being investigated, although it is fundamentally rather unsatisfactory because of the large number of trial trajectories required before an acceptable solution is found.

These remarks illustrate that a satisfactory procedure for missions that require transfers between two circular orbits is at present available only for vehicles that require propulsive thrust only in the immediate vicinity of the departure and arrival orbits. These restrictions imply near-minimum-energy transfer for very low thrust vehicles, but increasingly fast transfers can be handled as the thrust is increased.

CORRELATION OF TRAJECTORY PARAMETERS

The equations of motion for constant tangential thrust can be expressed in a form similar to that of reference 4 as follows:

$$\rho''=\frac{V^2}{\rho}-\frac{\rho'^2}{\rho}-\frac{1}{\rho^2}+\frac{a_0\rho'}{V\left(1-\frac{a_0}{V_j}\tau\right)} \tag{35}$$

$$V'=\frac{a_0}{1-\frac{a_0}{V_j}\tau}-\frac{\rho'}{\rho^2 V} \tag{36}$$

These equations are obtained from equations (6a) and (6b) by evaluating θ', θ'', $\sin\alpha$, and $\cos\alpha$ from equations (11), (13a), and (13b). With the parameters of reference 4,

$$X=a_0^{1/2}\rho,\ Y=a_0^{-1/4}V,\ T=a_0^{3/4}\tau$$

Equations (35) and (36) become

$$\ddot{X}=\frac{Y^2-\dot{X}^2}{X}-\frac{1}{X^2}+\frac{\dot{X}}{Y\left(1-\frac{T}{Y_j}\right)} \tag{37}$$

$$\dot{Y}=\frac{1}{1-\frac{T}{Y_j}}+\frac{\dot{X}}{X^2Y} \tag{38}$$

where $Y_j=a_0^{-1/4}V_j$. These equations are identical

with those of reference 4, except for the term

$$\left(1-\frac{T}{Y_j}\right)$$

which is unity either for $Y_j=\infty$ or for constant thrust acceleration.

In reference 4 it was shown that, for $a_0 \leqq 10^{-2}$, a single curve of Y as function of X and Y as function of $T-T_E$ was obtained for all a_0, where T_E is the value of the time parameter when escape velocity is obtained. It might be expected from equations (37) and (38) that similar single curves would result for a specified value of Y_j. Figures 14 and 15 show curves of Y against X and Y against $T-T_E$, respectively, for several selected values of a_0 and V_j (or Y_j). The curves for $V_j=\infty$ agree with those of reference 4. For other values of V_j (or Y_j), there appears to be no correlation in terms of Y_j for various values of a_0. Thus, the curve for $a_0=10^{-3}$, $Y_j=28.1$ does not fall as close to the curve for $a_0=10^{-4}$, $Y_j=30$ as does the curve $a_0=10^{-3}$, $Y_j=16.85$. For the $X-Y$ plot, in fact (fig. 14), the correlation is somewhat better in terms of V_j than Y_j, though this may be coincidental. The reason for the lack of correlation in terms of Y_j is probably the same as the reason noted in reference 4 for lack of correlation of $V_j=\infty$ curves for values of $a_0 \geq 10^{-1}$; that is, for different values of a_0, the circular-velocity points occur at different values of the parameters. Consequently, the differences in the initial conditions produce different integral curves. With finite V_j, these differences appear to be more pronounced than for infinite V_j.

CONCLUDING REMARKS

Charts that describe the trajectories followed by space vehicles powered with continuous tangential thrust in a central gravity field are presented for a wide range of thrust-weight ratios and specific impulse. These charts permit rapid calculation of propulsion time required to attain any prescribed hyperbolic velocity starting outward from a circular orbit, or to return to a circular orbit from any prescribed hyperbolic velocity. Although the charts are not valid in regions significantly affected by more than one gravitational field, they can be used to compute trajectories through successions of single fields. Thus, the departure from an orbit around the Earth, or other planets, can be followed by another period of applied thrust in the heliocentric field.

The charts can also be applied for transfer between two circular orbits, provided that the required transfer energies are attained close to the circular orbits. This restriction arises because no general curves can be plotted, using purely tangential thrust, either for the inward departure from a circular orbit or for the arrival from within at a circular orbit. The former trajectories are found to be oscillatory, while the latter apparently do not exist. Thrust programing (either in magnitude or direction or both) appears to be required for these cases.

For interplanetary missions, these restrictions mean that only near-minimum-energy transfers can be handled with these charts if the initial thrust-weight ratio is less than about 10^{-4}. For higher values of thrust-weight ratio, however, progressively faster transfers can be handled until, for a ratio of 1, the propulsion period is equivalent to an impulsive thrust, and the restrictions no longer exist.

LEWIS RESEARCH CENTER
NATIONAL AERONAUTICS AND SPACE ADMINISTRATION
CLEVELAND, OHIO, *July 15, 1959*

APPENDIX A

SYMBOLS

a_0	initial acceleration, $F/m_0 g_0$
E	energy per unit mass
F	constant applied thrust
G	universal gravitational constant
g_0	gravitational acceleration at $r=r_0(\rho=1)$
g_{00}	gravitational acceleration at Earth's surface
H	nondimensional angular momentum, $h/r_0 v_{c0}$
h	angular momentum
I	specific impulse
I_{eff}	effective specific impulse
M	mass of body producing central gravitational field
m	mass
P_j	jet power
r	radial distance of body from center of force field
r_0	radius of circular orbit of departure or return
T	$a_0^{3/4}\tau$
t	time
V	v/v_{c0}
V_h	v_h/v_{c0}: $V_h^2=V^2-\frac{2}{\rho}$
V_j	v_j/v_{c0}, nondimensional jet velocity
v	velocity
v_{c0}	circular velocity at $r=r_0(v_{c0}^2=\mu/r_0)$
v_h	hyperbolic velocity $\left(v_h^2=v^2-2\frac{\mu}{r}=2E\right)$
v_j	jet velocity
W	weight, mg_{00}
W_{PP}	powerplant weight
X	$a_0^{1/2}\rho$
Y	$a_0^{-1/4}V$
Y_j	$a_0^{-1/4}V_j$
α	inclination of thrust vector relative to circumferential, deg
α_1	inclination of velocity vector relative to circumferential, deg
θ	angular distance, radians
μ	gravitational constant, GM
ρ	r/r_0
τ	$v_{c0}t/r_0$, nondimensional time

Subscripts:

a	at beginning of phase
b	at end of phase
E	Earth
M	Mars
P	planet
p	propellant
S	sun
0	reference or initial conditions (except in τ_0)
1,2 . . . 7	phases of interplanetary mission

APPENDIX B

ANALYSIS OF MARS MISSION

As an example of the use of the charts, vehicle weights needed for an 8-man round-trip expedition to Mars using an electric propulsion system are estimated. It is assumed that the vehicle is launched into an Earth-satellite orbit at a radius 1.1 times the Earth radius. The electric propulsion system then propels the vehicle out of the Earth's field until the minimum-energy-transfer hyperbolic velocity is attained. At Mars, the vehicle settles into a circular orbit at altitude about 400 miles ($r=2500$ miles) above the surface. A chemical-rocket landing vehicle takes part of the crew to the surface for exploration during this waiting period and returns them to the mother ship before departure time. The electric propulsion system then propels the vehicle out of Mars' gravitational field, attaining the hyperbolic velocity needed for a minimum-energy transfer to the Earth's orbit. The vehicle then settles again into the initial orbit around the Earth. This mission is similar to the one discussed in reference 7, except that an initial acceleration of 2×10^{-4} gravity units instead of 10^{-4} will be assumed. A detailed analysis must start with a preliminary rough estimate of the initial total vehicle weight. Such preliminary estimates are readily made by methods described in reference 7. The basic constants and assumed parameters for the analysis are as follows:

For orbit near Earth:	
$r_{0,E}$, miles	4360
$v_{c0,E}$, miles/sec	4. 69
$g_{0,E}$, ft/sec^2	26. 6
t, $(r_{0,E}/v_{c0,E})\tau$, days	0.01075τ
For orbit near Mars:	
$r_{0,M}$, miles	2500
$v_{c0,M}$, miles/sec	2. 05
$g_{0,M}$, ft/sec^2	8. 87
t, $(r_{0,M}/v_{c0,M})\tau$, days	0.0141τ
For heliocentric trajectory near Earth's orbit:	
$r_{0,SE}$, miles	92.9×10^6
$v_{c0,SE}$, miles/sec	18. 5
$g_{0,SE}$, ft/sec^2	0. 0196
t, $(r_{0,SE}/v_{c0,SE})\tau$, days	58.1τ
For heliocentric trajectory near Mars' orbit:	
$r_{0,SM}$, miles	141.5×10^6
$v_{c0,SM}$, miles/sec	15. 0
$g_{0,SM}$, ft/sec^2	0. 0084
t, $(r_{0,SM}/v_{c0,SM})\tau$, days	109.1τ
Minimum-energy hyperbolic velocities:	
$v_{h,E}$, miles/sec	1. 85
$V^2_{h,E}$, $(1.85/4.69)^2$	0. 155
$v_{h,M}$, miles/sec	−1. 65
$V^2_{h,M}$, $(1.65/2.05)^2$	0. 65
$v^2_{h,SE}$, $[(18.5+1.85)/18.5]^2-2$	−0. 79
$V^2_{h,SM}$, $[(15.0-1.65)/15]^2-2$	−1. 207
Assumed initial weight, $W_{1,a}\equiv m_{1,a}g_{00}$, lb	450, 000
Initial mass, $m_{1,a}=450{,}000/32.2$, slugs	14, 000
Assumed initial acceleration, $a_{0,1}\equiv F/m_{1,a}g_0$	2×10^{-4}
Thrust, $F=2\times10^{-4}\times14{,}000\times26.6$, lb	74. 5
Assumed specific impulse, I, sec	10, 000
Jet power, $P_j=FI/45.9=(74.5\times10{,}000)/45.9$, kw	16, 200
Assumed specific powerplant weight, lb/jet kw	10
Powerplant weight, $W_{PP}=10P_j$, lb	162, 000
Propellant weight flow, $\dot{W}_p=F/I$, lb/sec	0. 00745
lb/day	642
Disposal rate of subsistence supplies (10 lb/man-day), $\dot{W}_s$, lb/day	80
Effective specific impulse, $I_{eff}=F/(\dot{W}_p+\dot{W}_s)$, sec	8900
Effective jet velocity, $v_j=g_{00}I_{eff}=32.2\times8900$, ft/sec	286, 000
miles/sec	54. 2
Jet velocity parameters:	
$V_{j,E}$, 54.2/4.69	11. 55
$V_{j,M}$, 54.2/2.05	26. 43
$V_{j,SE}$, 54.2/18.5	2. 93
$V_{j,SM}$, 54.2/15	3. 61

The computation can be divided into several phases, as follows:

Phase 1, propulsion from orbit around Earth to $v_h=1.85$ miles/sec:

$$a_0=2\times10^{-4};\ V_h^2=0.155;\ V_j=11.55$$

From figure 3(a) for $a_0=10^{-4}$,

$$a_0\tau_0=1.15$$

From figure 3(b) for $a_0=10^{-3}$,

$$a_0\tau_0=1.03$$

Therefore, for $a_0=2\times10^{-4}$,

$$a_0\tau_0\approx1.11$$

$$\tau_0=\frac{1.11}{2\times10^{-4}}=5550$$

$$t_{1,a}=0.01075\times5550=59.7 \text{ days}$$

From a cross plot (fig. 2(a)) of ρ against a_0 for $a_0\tau_0=1.11$, $\rho_{1,a}$, at the end of the propulsion period, is found to be about 350.

This is considerably beyond the value for which a change to heliocentric coordinates should be made (table I), so it is well to check the propulsion time by the alternative procedure, consisting of propulsion in the Earth's field to $V_h^2=0$, and then propulsion in the heliocentric field to $V_{h,SE}^2=-0.79$.

From figures 3(a) for $a_0=10^{-4}$,

$$a_0\tau_0=0.88$$

From figure 3(b) for $a_0=10^{-3}$,

$$a_0\tau_0=0.83$$

Therefore,

$$a_0\tau_0\approx0.86;\ \tau_0=4300$$

$$t_{escape}=46.2 \text{ days}$$

For heliocentric coordinates,

$$a_0=\frac{2\times10^{-4}}{0.926}\times\frac{26.6}{0.0196}=0.293;\ V_j=2.93$$

where 0.926 is the mass ratio on attainment of escape velocity.

From figure 3(d) for $a_0=10^{-1}$,

$$a_0\tau_0=0.10$$

From figure 3(c) for $a_0=1.0$,

$$a_0\tau_0=0.10$$

Therefore,

$$a_0\tau_0=0.1;\ \tau_0=\frac{0.1}{0.293}=0.341$$

$$t_h=58.1\times0.341=19.8 \text{ days}$$

Thus, $t_{1,a}=46.2+19.8=66.0$ days, or about 6 days longer than before. The correct value is between those obtained by the two computation methods. It can be assumed, therefore, that $t_{1,a}=64$ days. Then,

$$W_{p,1}=642\times64=41{,}100 \text{ lb}$$

and the weight and mass at the end of phase 1 are

$$W_{1,b}=450{,}000-41{,}100-80\times64=404{,}000 \text{ lb}$$

$$m_{1,b}=\frac{404{,}000}{32.2}=12{,}530 \text{ slugs}$$

Phase 2, coast along minimum-energy path to Mars orbit (259 days):

At the end of this phase, weight and mass are

$$W_{2,b}=403{,}820-80\times259=383{,}000 \text{ lb}$$

$$m_{2,b}=11{,}900 \text{ slugs}$$

Phase 3, settle into orbit around Mars from $V_{h,M}^2=0.65$:

Assume that $m_{3,b}\approx11{,}000$ slugs; then,

$$a_0=\frac{F}{m_{3,b}g_{0,M}}=\frac{74.3}{11{,}000\times8.87}=7.4\times10^{-4}$$

$$V_j=26.43$$

From figure 8(a) for $a_0=10^{-4}$,

$$a_0\tau_0=1.68$$

From figure 8(b) for $a_0=10^{-3}$,

$$a_0\tau_0=1.53$$

Therefore,

$$a_0\tau_0\approx1.56;\ \tau_0=2110$$

$$t_{p,2}=0.0141\times2110=29.8 \text{ days}$$

From a cross plot of ρ against a_0 for $a_0\tau=1.56$, it is found that $\rho_3=430$, or the distance at which propulsion is initiated is $430\times2500=1{,}075{,}000$ miles. This is considerably beyond the value (table I) at which the effects of the solar field and the Martian field are equal, but no charts are available for approach to circular orbit from inside, which is the heliocentric path followed in this phase. Consequently, the approximation involved in remaining in Martian coordinates will be accepted at this point.

The propellant weight required for phase 3 is, therefore,

$$W_{p,2}=30\times642=19{,}260 \text{ lb}$$

and the weight and mass at the end of this phase are

$$W_{3,b}=383{,}000-19{,}300-80\times30.6=360{,}000 \text{ lb}$$

$$m_{3,b}=11{,}200 \text{ slugs}$$

This mass is quite close to the value assumed to determine a_0 for this phase, so there is no need to repeat the calculation with the new value.

Phase 4, wait period and exploration at Mars:

For a high-thrust system, following the minimum-energy trajectory, the required wait period at Mars is 455 days. For the low-thrust system, the propulsion time of phase 3 and that of phase 5 must be subtracted from this value. An estimate of the phase 5 time is therefore needed at this point. Since the weight will be less for departure than for arrival, the propulsion time will also be less. If the required time is assumed to be 25 days, the net waiting and exploration time is 455−25−30=400 days. At the end of this phase, the weight and mass are, therefore,

$$W_{4,b}=360{,}000-W_{ex}-80\times400=288{,}000 \text{ lb}$$

$$m_{4,b}=8940 \text{ slugs}$$

where, as in reference 7, a weight W_{ex} of 40,000 pounds is allowed for auxiliary descent and ascent vehicle and for exploration equipment that is left on Mars.

Phase 5, propulsion from orbit around Mars to $V_h^2=0.65$:

$$a_0=\frac{F}{m_{4,b}g_{0,M}}=\frac{74.3}{8940\times8.87}=9.4\times10^{-4};\ V_f=26.43$$

From figure 3(a) for $a_0=10^{-4}$,

$$a_0\tau=1.58$$

From figure 3(b) for $a_0=10^{-3}$,

$$a_0\tau=1.47$$

Therefore,

$$a_0\tau\approx1.48;\ \tau=\frac{1.48}{9.40\times10^{-4}}=1570$$

$$t_{p,3}=1570\times0.0141=22.1 \text{ days}$$

The value is close enough to the 25 days assumed in phase 4 that no repeat calculation is needed. The propellant required in this phase is

$$W_{p,3}=22.1\times642=14{,}200 \text{ lb}$$

and the weight and mass at the end of phase 5 are

$$W_{5,b}=288{,}000-14{,}200-80\times23=272{,}000 \text{ lb}$$

$$m_{5,b}=8440 \text{ slugs}$$

Phase 6, coast along minimum-energy ellipse to Earth's orbit (259 days):

The weight and mass at the end of this phase are

$$W_{6,b}=272{,}000-80\times259=251{,}000 \text{ lb}$$

$$m_{6,b}=7800 \text{ slugs}$$

Phase 7, settle into orbit around Earth at $r_{0,E}=4360$ miles from $V_h^2=0.155$:

Assume that $m_{7,b}=7000$ slugs; then,

$$a_0=\frac{74.3}{7000\times26.6}=4\times10^{-4};\ V_f=11.55$$

From figure 8(a) for $a_0=10^{-4}$,

$$a_0\tau_0=1.28$$

From figure 8(b) for $a_0=10^{-3}$,

$$a_0\tau_0=1.14$$

Therefore,

$$a_0\tau_0\approx1.20;\ \tau_0=3000$$

$$t_{p,4}=0.01075\times3000=32.3 \text{ days}$$

The propellant weight required for this phase is

$$W_{p,}4=32.3\times642=20{,}800 \text{ lb}$$

and the weight and mass at the end of this phase are

$$W_{7,b}=251{,}000-20{,}800-80\times32=227{,}500$$

$$m_{7,b}=6940$$

This value, again, is sufficiently close to the assumed value that no iteration is needed.

The weight $W_{7,b}$ at the end of the mission includes the powerplant W_{PP}, the basic payload W_{pay}, and reserves W_{res}. As in reference 7, the basic payload, which consists of the cabins, crew,

navigation and communication equipment, and environment control, is assumed to be about 50,000 pounds. The amount available for reserves is, therefore,

$$W_{res}=W_{7.b}-W_{PP}-W_{pay}=227{,}500-161{,}800-50{,}000=15{,}700 \text{ lb}$$

This value is rather small and indicates that a somewhat larger initial weight $W_{1,a}$ should have been assumed.

The final weight breakdown for this mission is as follows:

Powerplant	162, 000
Propellant	96, 000
Subsistence supplies	86, 000
Basic payload	50, 000
Exploration vehicle and supplies	40, 000
Reserves	16, 000
Total, lb	450, 000

The total time required for the mission is 1068 days. Comparable figures using $a_0=10^{-4}$ as the initial acceleration for the same mission are: total initial weight, 322,000 pounds; total trip time, 1160 days. The time saving, purchased at the expense of over 100,000 pounds additional weight, is simply the reduced time required to spiral out of and back into the circular orbit around the Earth when $a_0=2\times10^{-4}$ instead of 10^{-4}. The remainder of the trip time is not reduced, since both missions followed minimum-energy transfer paths.

The fact that the powerplant weight is considerably greater than the propellant weight indicates that the specific impulse chosen (10,000 sec) is not the optimum value for this mission. As pointed out in reference 7, for optimum specific impulse, the powerplant and propellant weights are nearly equal. In fact, from the elementary analysis of reference 7, and using the total propulsion time from the preceding example (about 150 days), the optimum specific impulse is about 7700 seconds. By using this value, a lower total powerplant plus propellant weight would be obtained, and the reserve weight would be larger.

To obtain large reductions in round-trip time using low-thrust propulsion will probably require, as with high-thrust systems, that trajectories other than direct-transfer be followed. No procedure other than trial and error is as yet available for analyzing such trajectories.

REFERENCES

1. Tsien, H. S.: Take-Off from Satellite Orbit. Jour. Am. Rocket Soc., vol. 23, no. 4, July–Aug. 1953, pp. 233–236.
2. Stuhlinger, E. Ernst: The Flight Path of an Electrically-Propelled Space Ship. Jet Prop., vol. 27, no. 4, Apr. 1957, pp. 410–414.
3. Irving, J. H., and Blum, E. K.: Comparative Performance of Ballistic and Low-Thrust Vehicles for Flight to Mars. Paper presented at AFOSR Astronautics Symposium, Denver (Col.), Apr. 1959.
4. Perkins, Frank M.: Flight Mechanics of Low-Thrust Spacecraft. Jour. Aero/Space Sci., vol. 26, no. 5, May 1959, pp. 291–297.
5. Moeckel, W. E.: Interplanetary Trajectories with Excess Energy. Paper presented at North Int. Astronautical Cong., Amsterdam (Holland), Aug. 23–30, 1958.
6. Tisserand, Francois Félix: Théories des satellites de Jupiter et de Saturne Perturbations des petites planétes. Traité de Mechanique Céleste, T. 4, Gauthier-Villars (Paris), 1896.
7. Moeckel, W. E.: Propulsion Methods in Astronautics. Paper presented at Int. Cong. of Aero. Sci., Madrid (Spain), Sept. 8–13, 1958.

532584—60 ---3

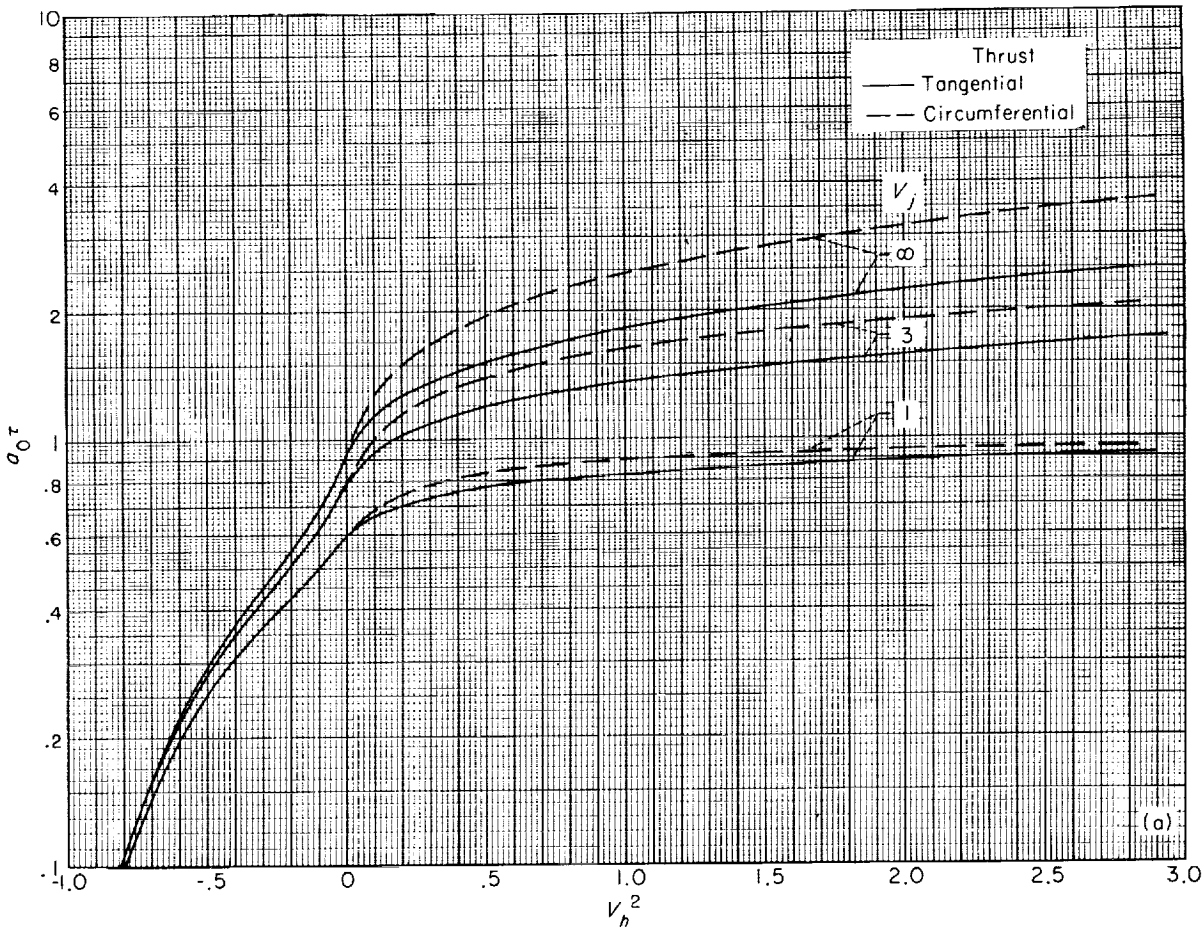

(a) a_0, 10^{-4}.

FIGURE 1.—Comparison of tangential and circumferential thrust.

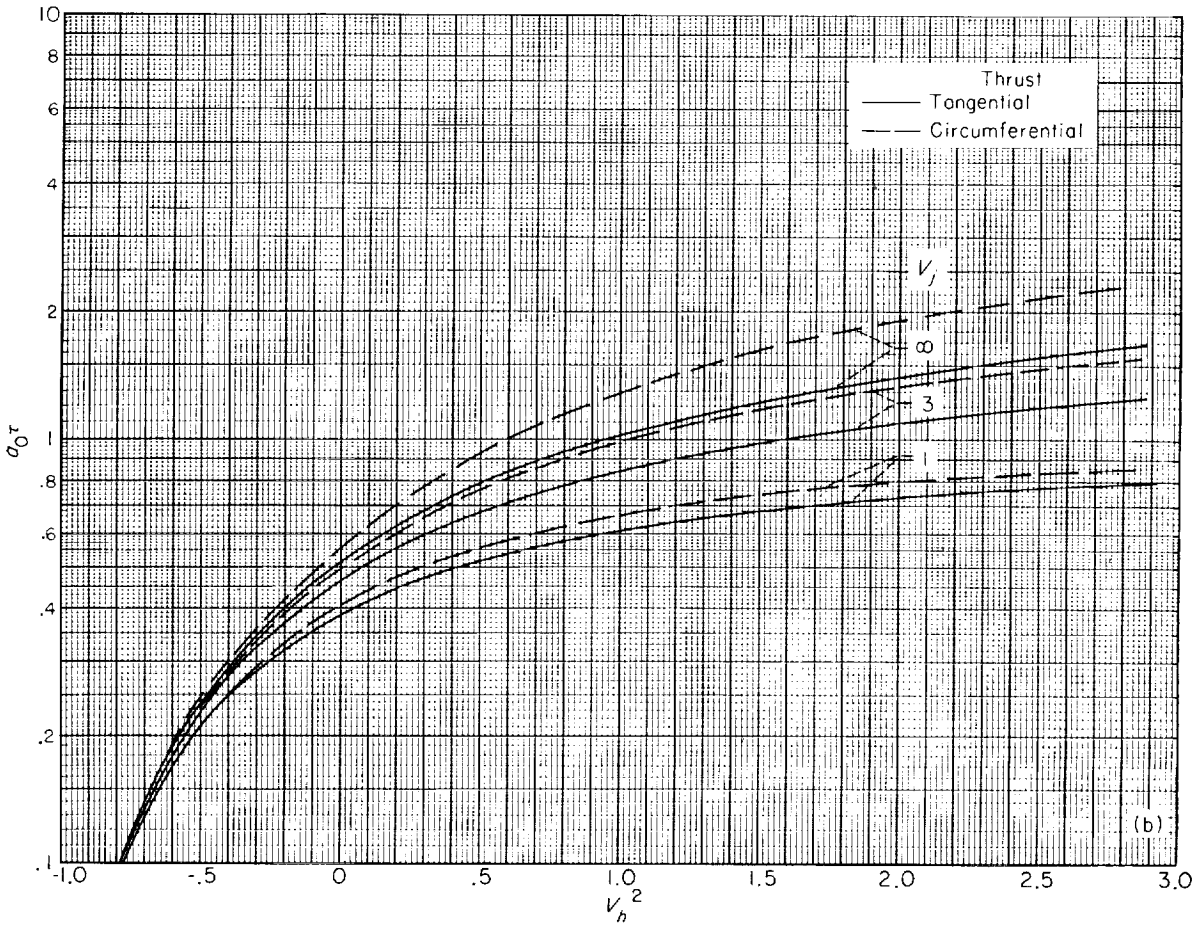

(b) a_0, 10^{-1}.

FIGURE 1.—Concluded. Comparison of tangential and circumferential thrust.

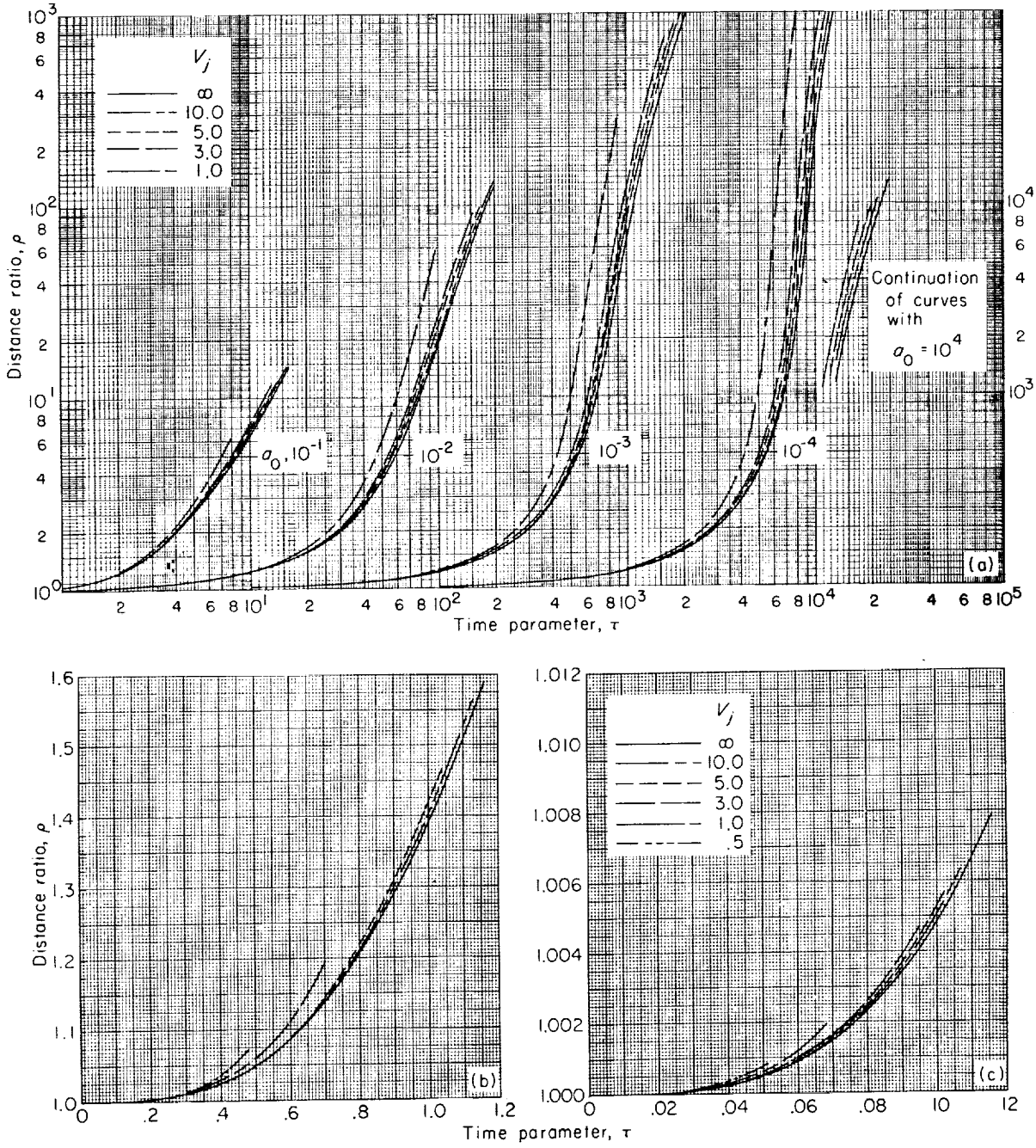

(a) a_0, 10^{-4} to 10^{-1}.

(b) a_0, 1.0.

(c) a_0, 10.0.

FIGURE 2.—Radial distance as a function of time for outward paths.

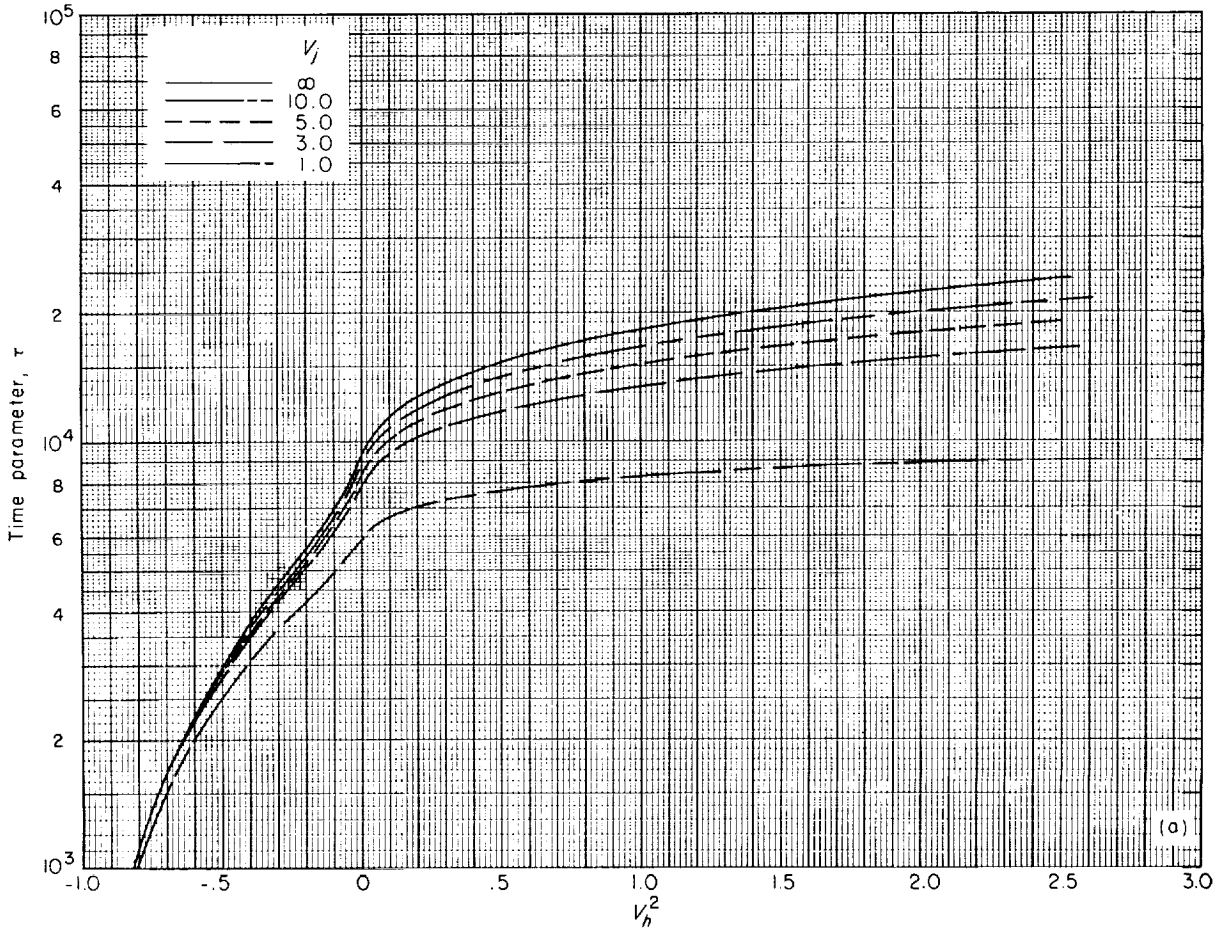

(a) a_0, 10^{-4}.

FIGURE 3.—Local hyperbolic velocity as a function of time for outward paths.

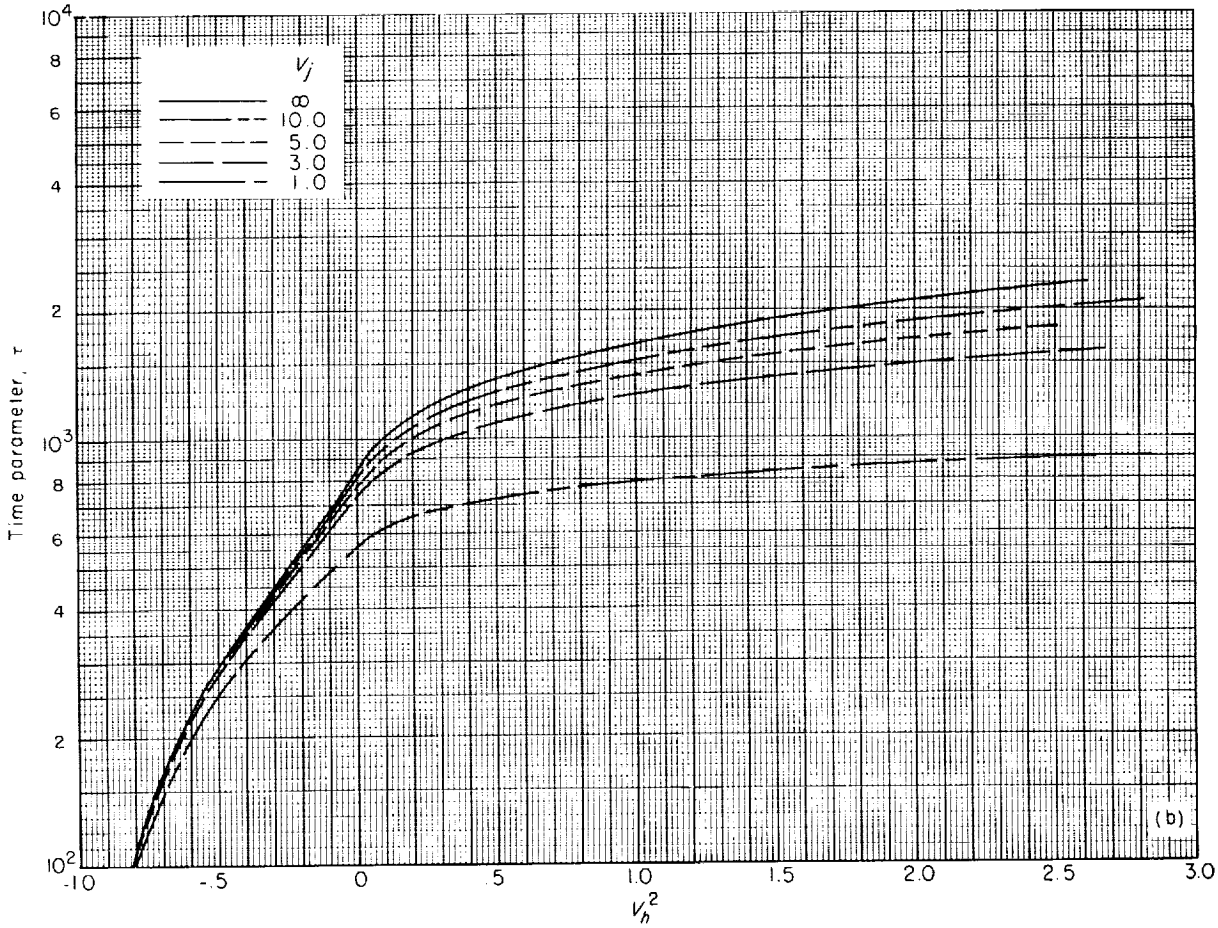

(b) a_0, 10^{-3}.

FIGURE 3. Continued. Local hyperbolic velocity as a function of time for outward paths.

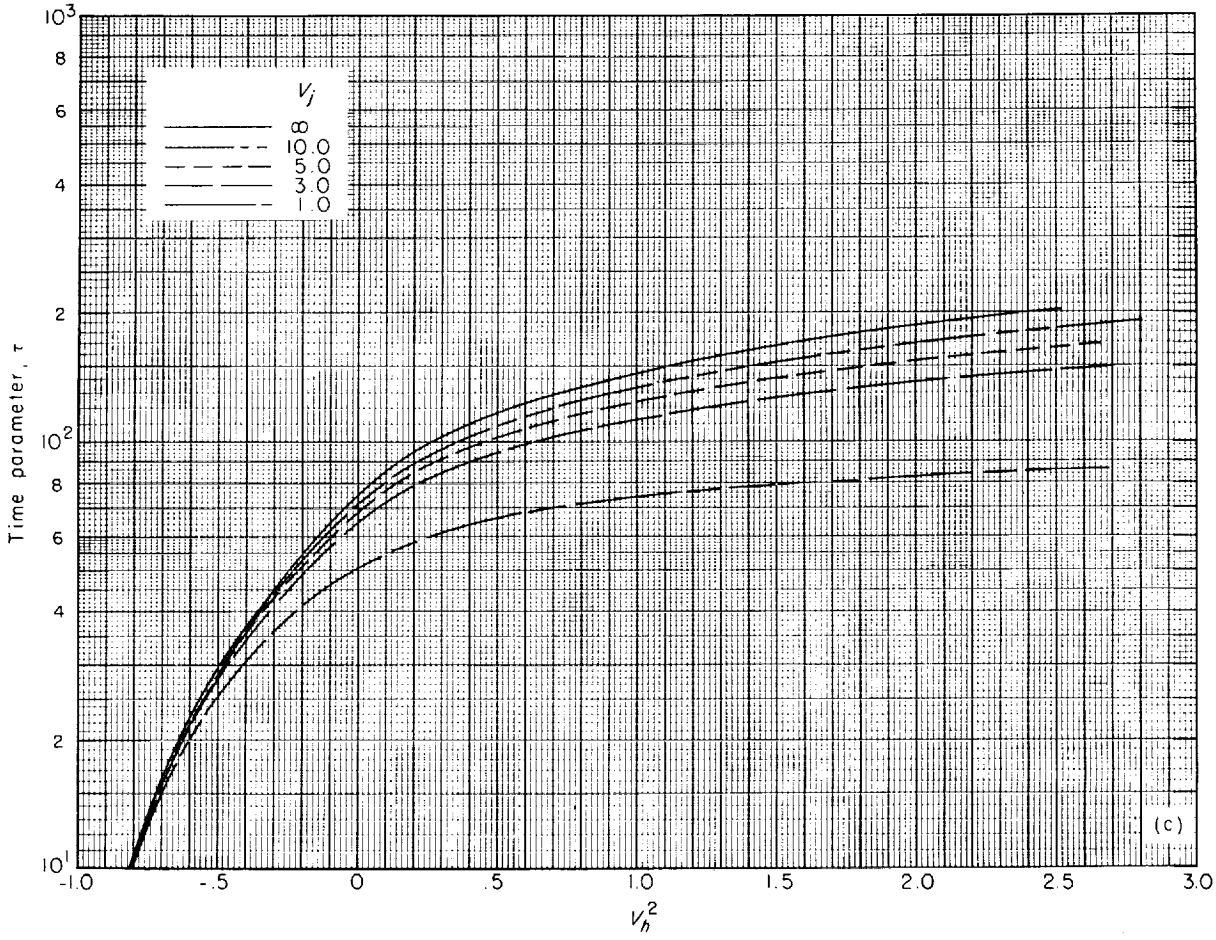

(c) a_0, 10^{-2}.

FIGURE 3.—Continued. Local hyperbolic velocity as a function of time for outward paths.

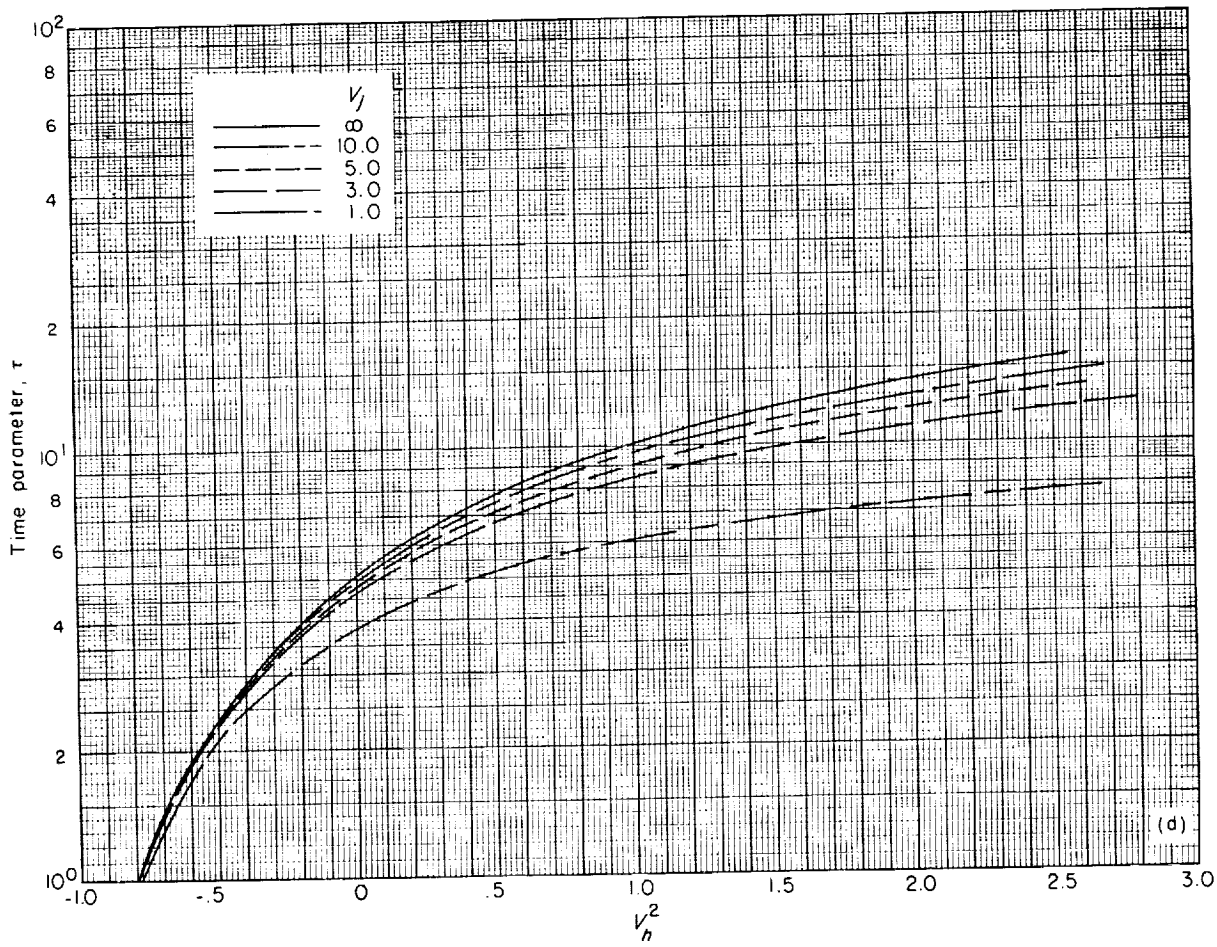

(d) a_0, 10^{-1}.

FIGURE 3.—Continued. Local hyperbolic velocity as a function of time for outward paths.

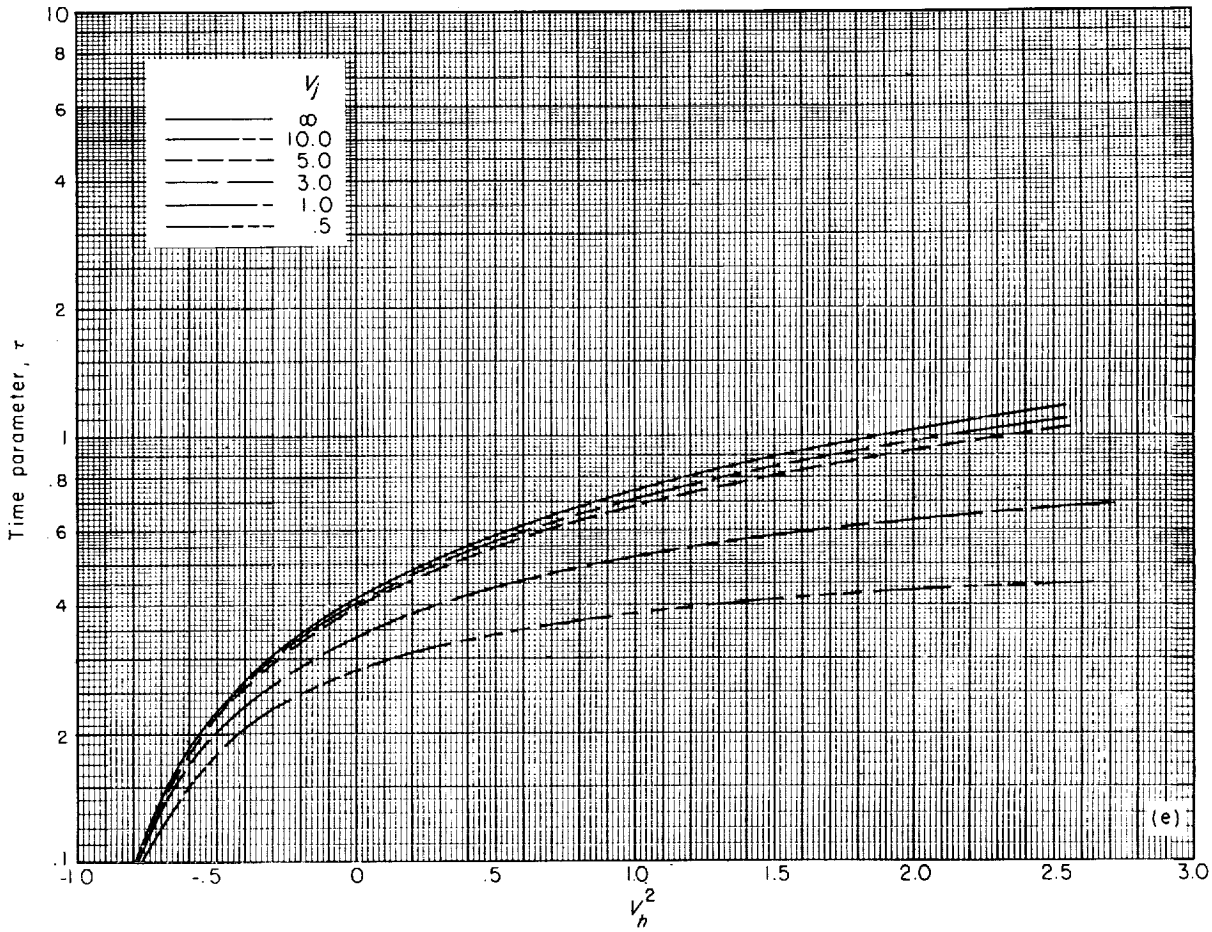

(e) a_0, 1.0.

FIGURE 3.—Continued. Local hyperbolic velocity as a function of time for outward paths.

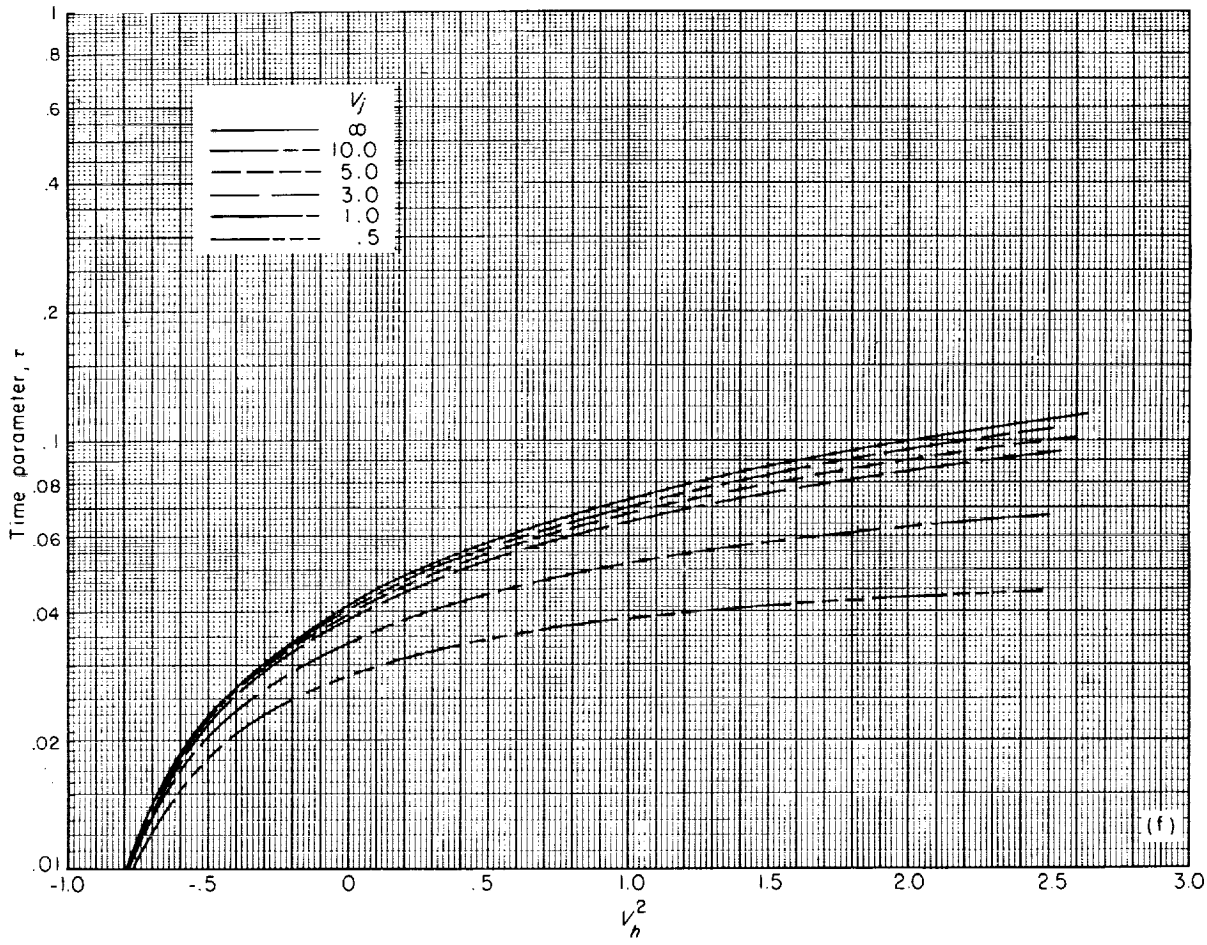

(f) a_0, 10.0.

FIGURE 3.—Concluded. Local hyperbolic velocity as a function of time for outward paths.

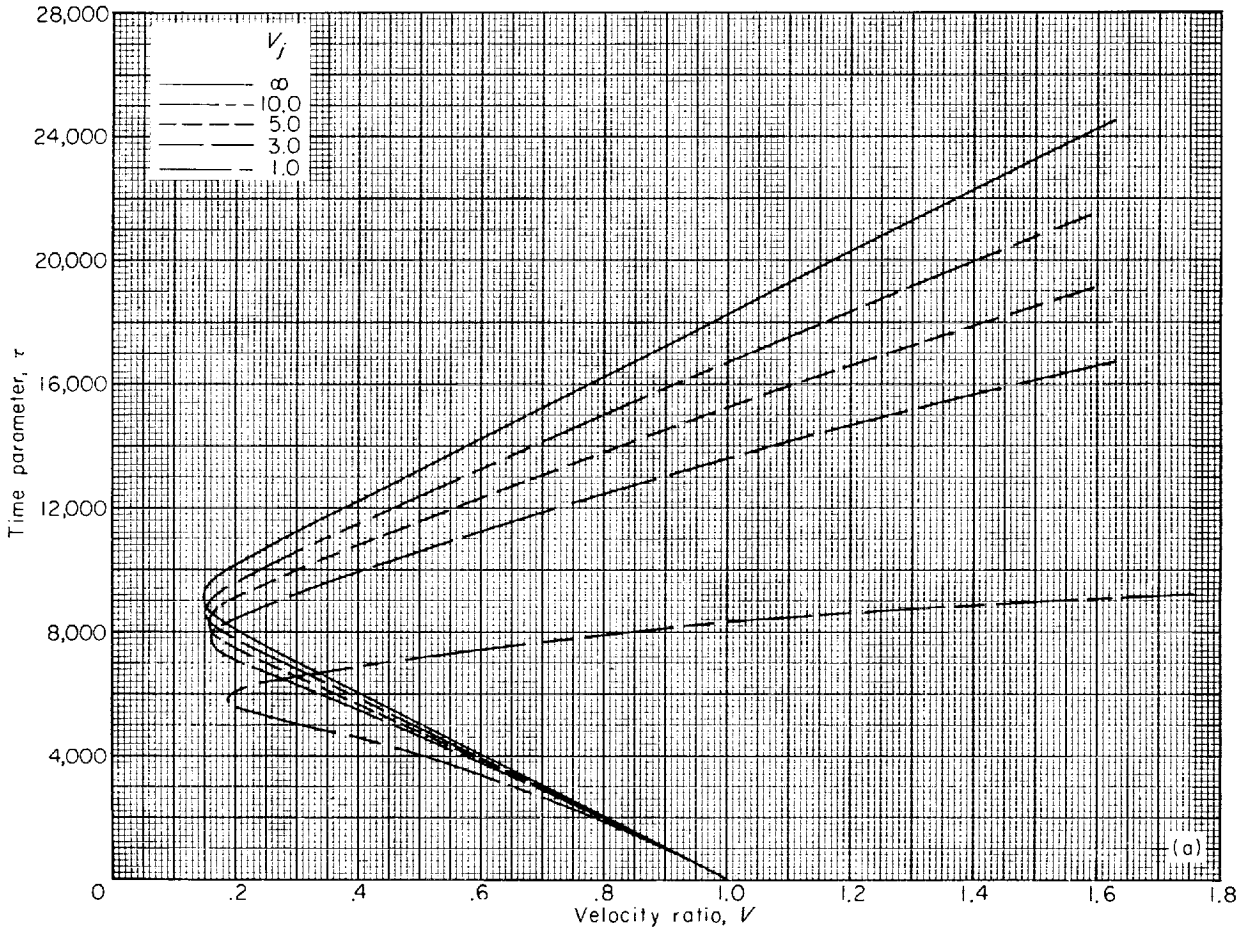

(a) a_0, 10^{-4}.

FIGURE 4.--Velocity as a function of time for outward paths.

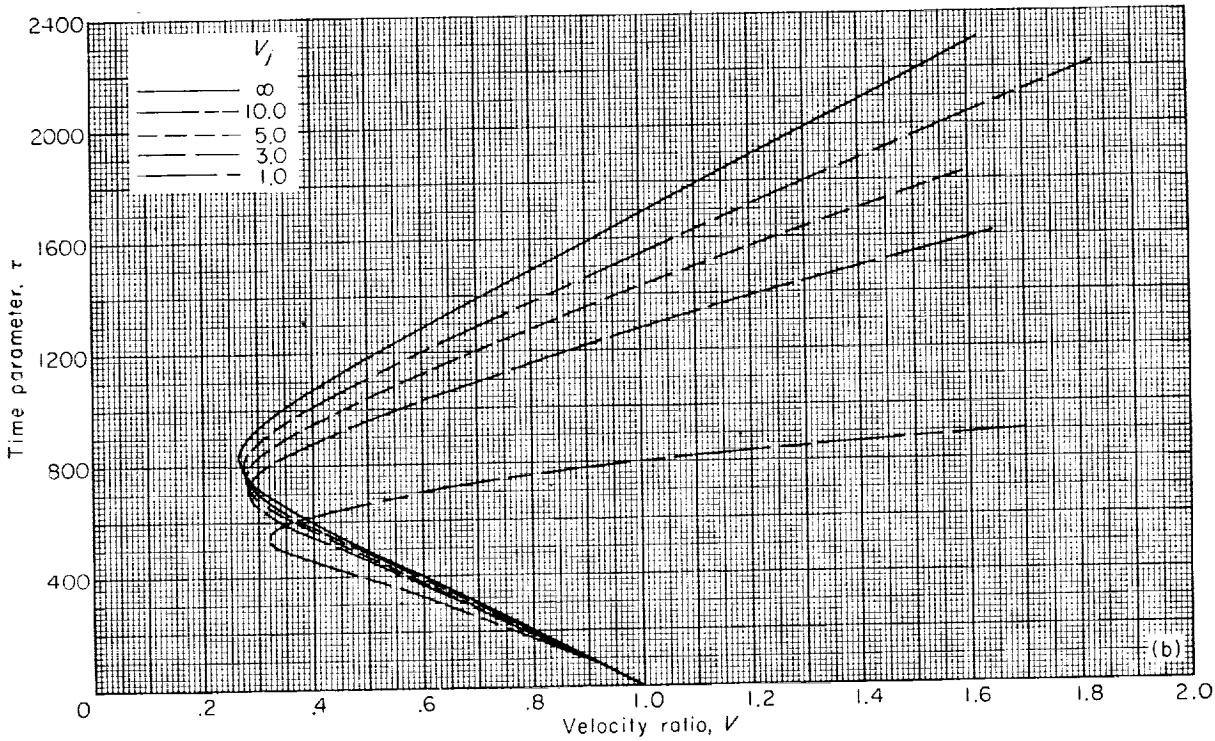

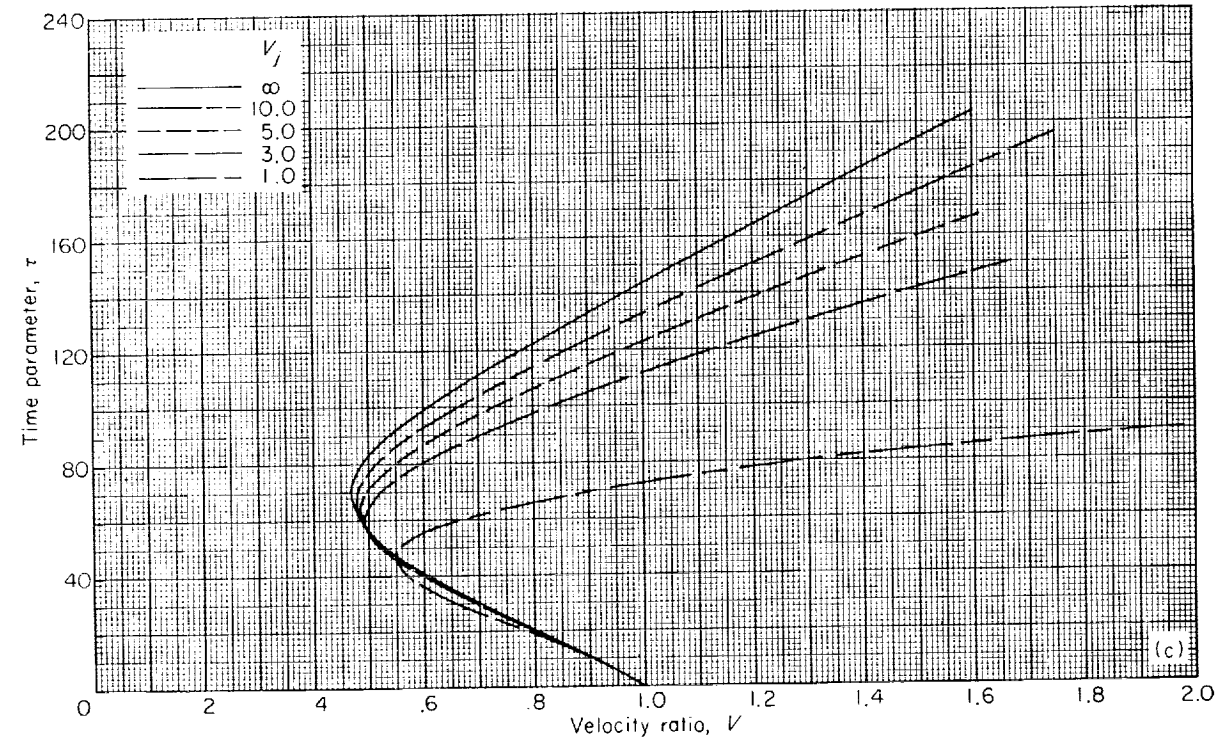

(b) a_0, 10^{-3}.
(c) a_0, 10^{-2}.

FIGURE 4.—Continued. Velocity as a function of time for outward paths.

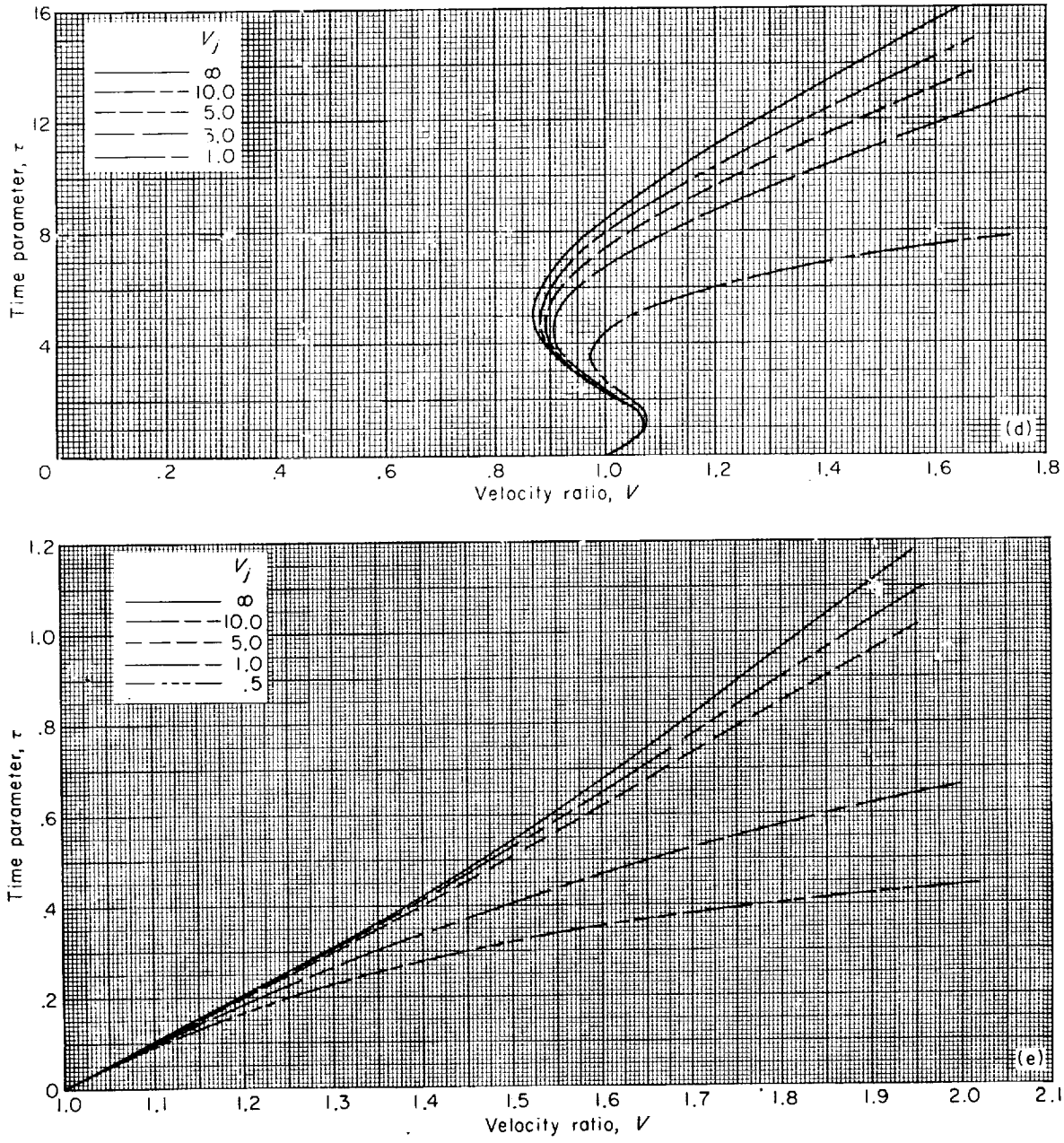

(d) a_0, 10^{-1}.
(e) a_0, 1.0.

FIGURE 4. Continued. Velocity as a function of time for outward paths.

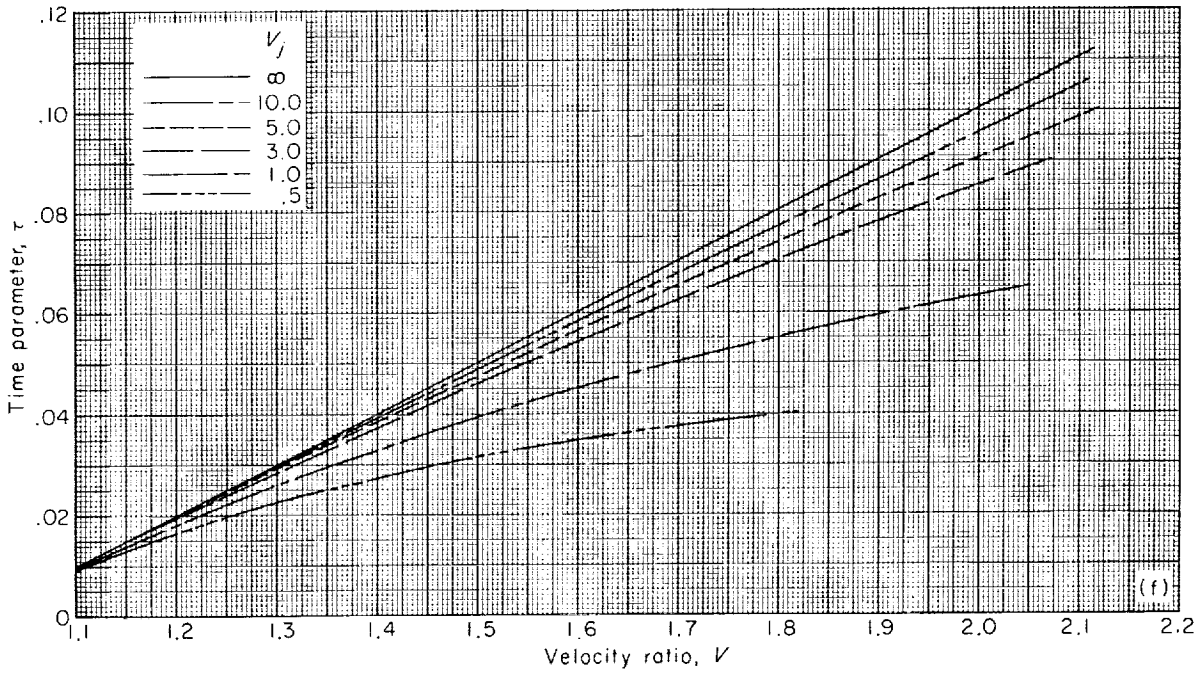

(f) a_0, 10.0.

FIGURE 4.—Concluded. Velocity as a function of time for outward paths.

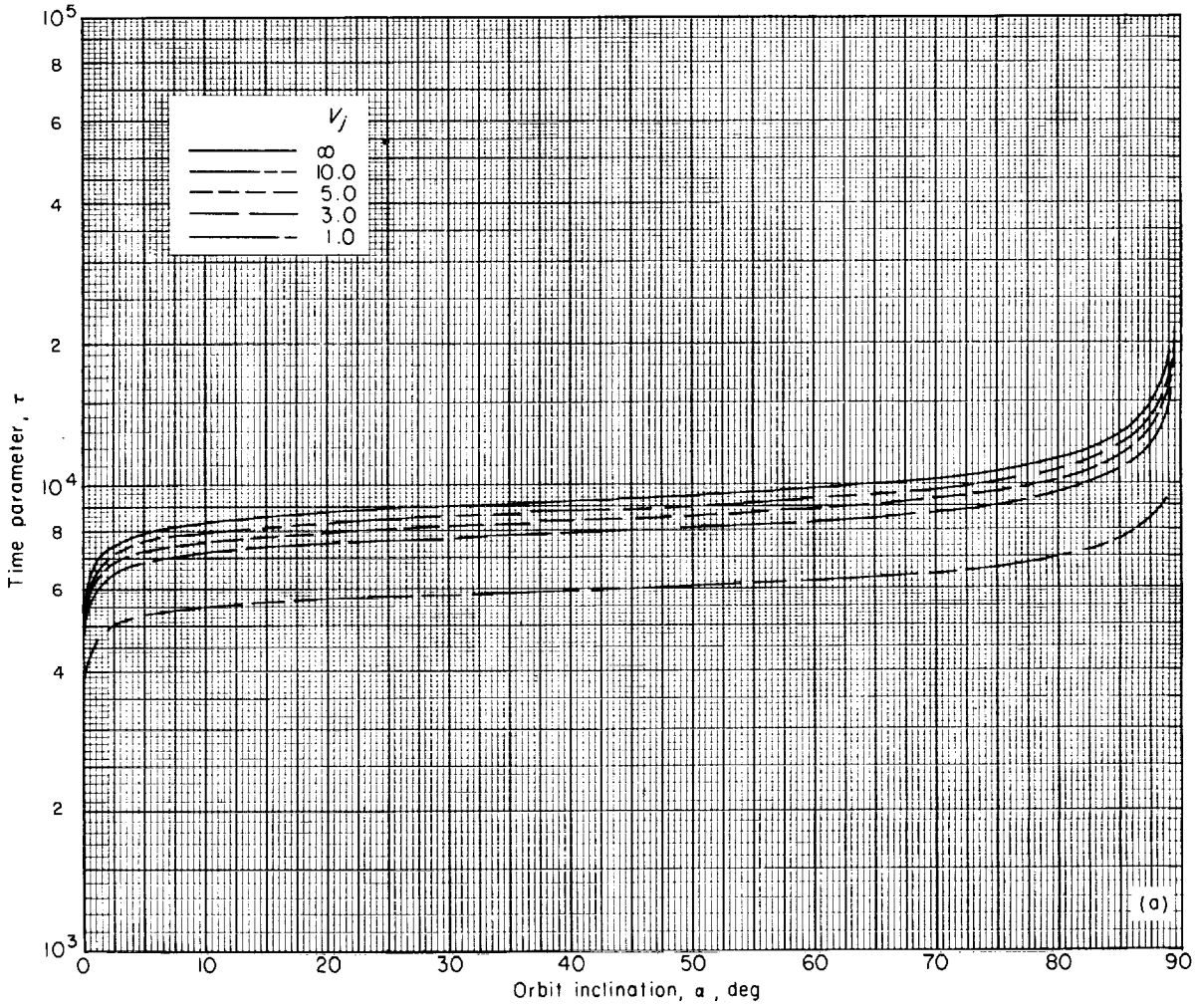

(a) a_0, 10^{-4}.

FIGURE 5.—Inclination to circumferential direction as a function of time for outward paths.

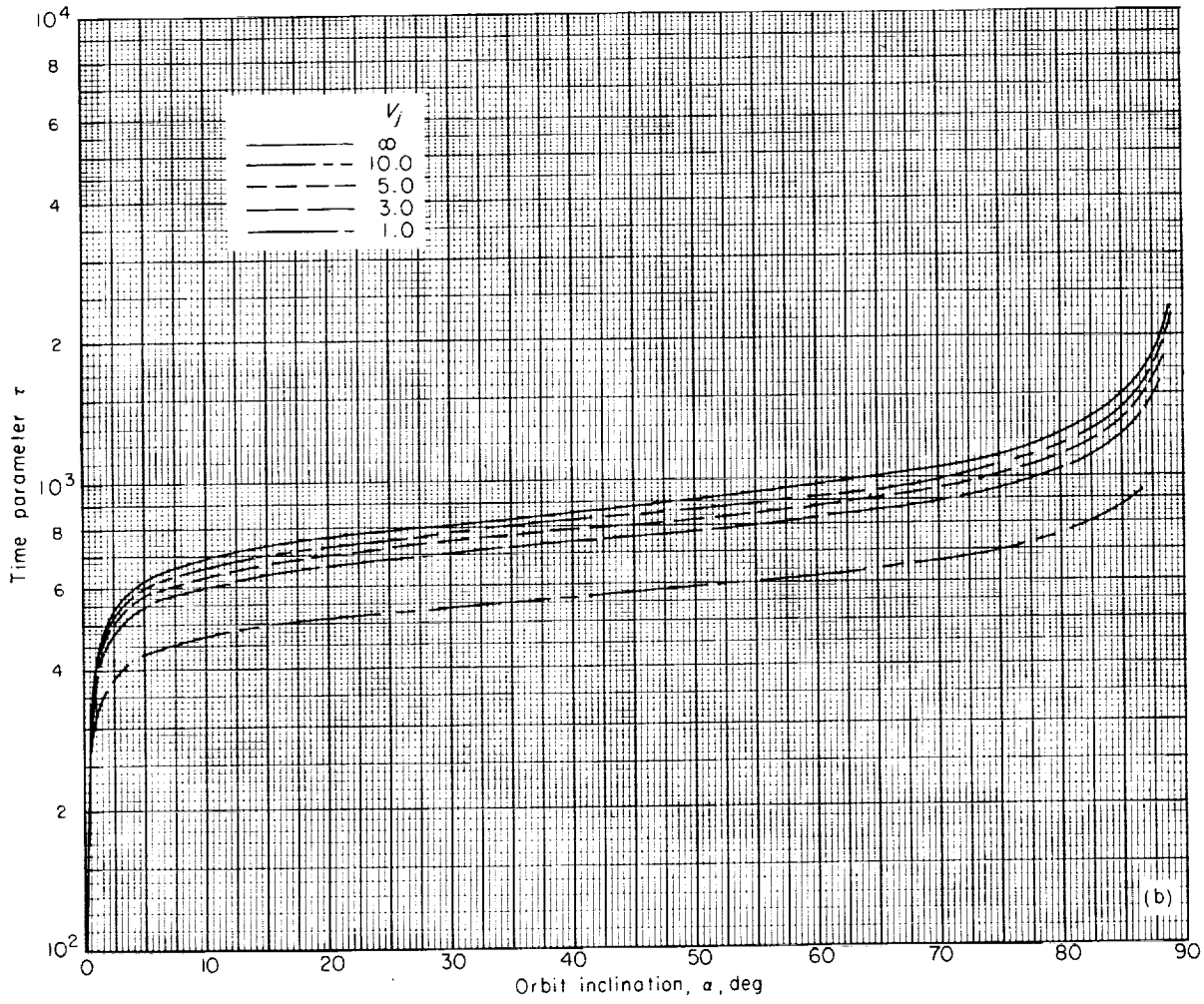

(b) a_0, 10^{-3}.

FIGURE 5.—Continued. Inclination to circumferential direction as a function of time for outward paths.

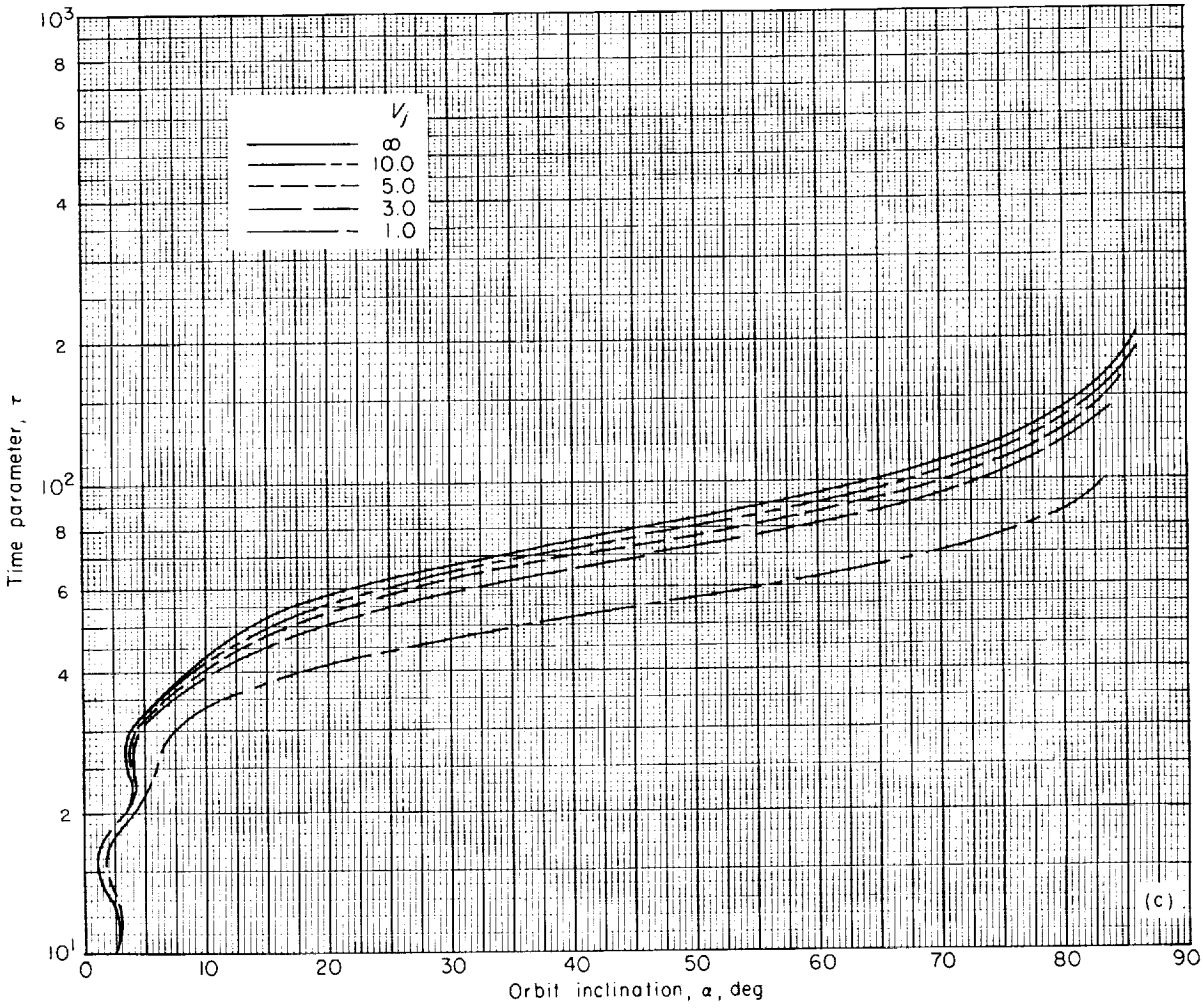

(c) a_0, 10^{-2}.

FIGURE 5.—Continued. Inclination to circumferential direction as a function of time for outward paths.

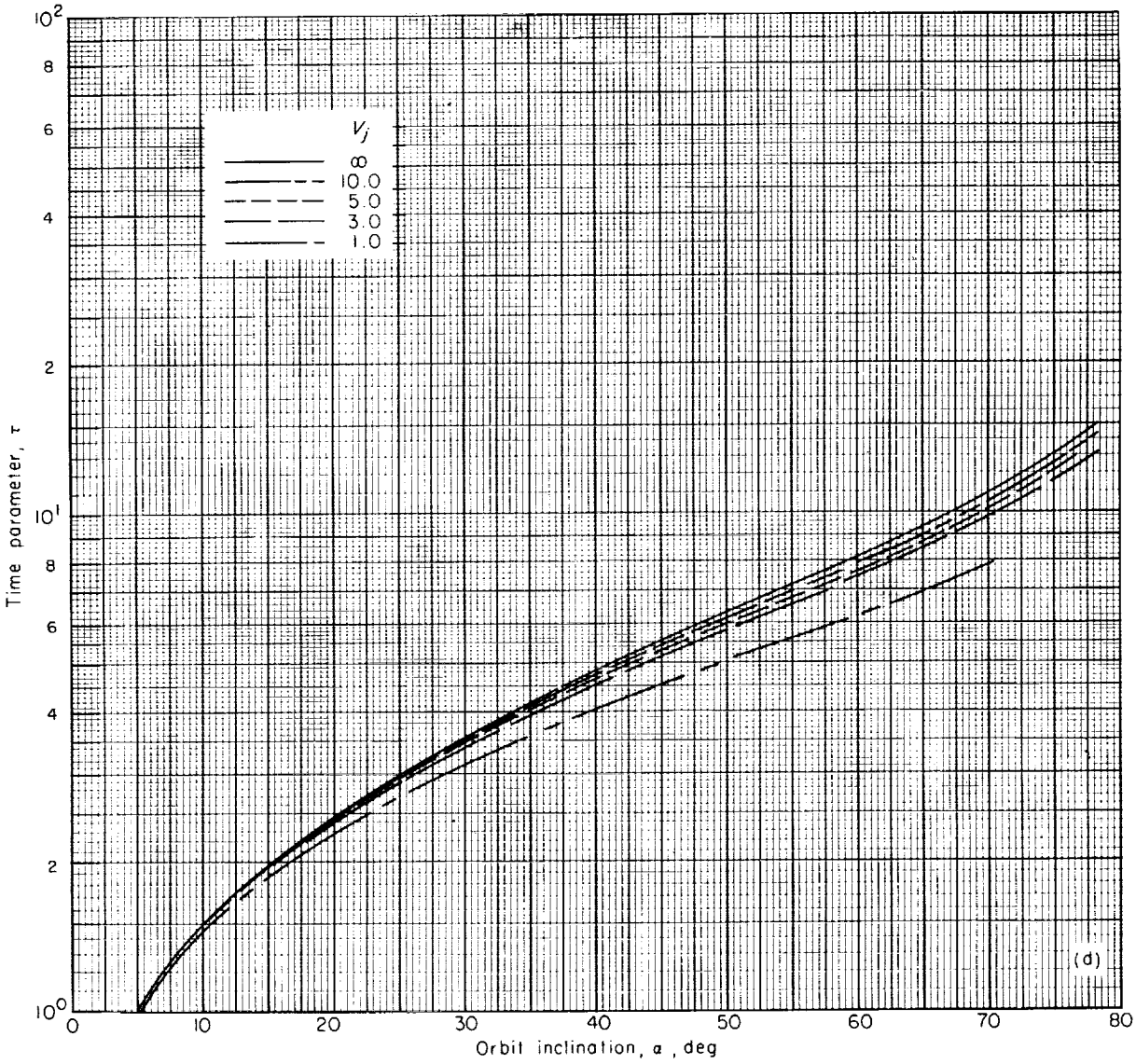

(d) a_0, 10^{-1}.

FIGURE 5. –Continued. Inclination to circumferential direction as a function of time for outward paths.

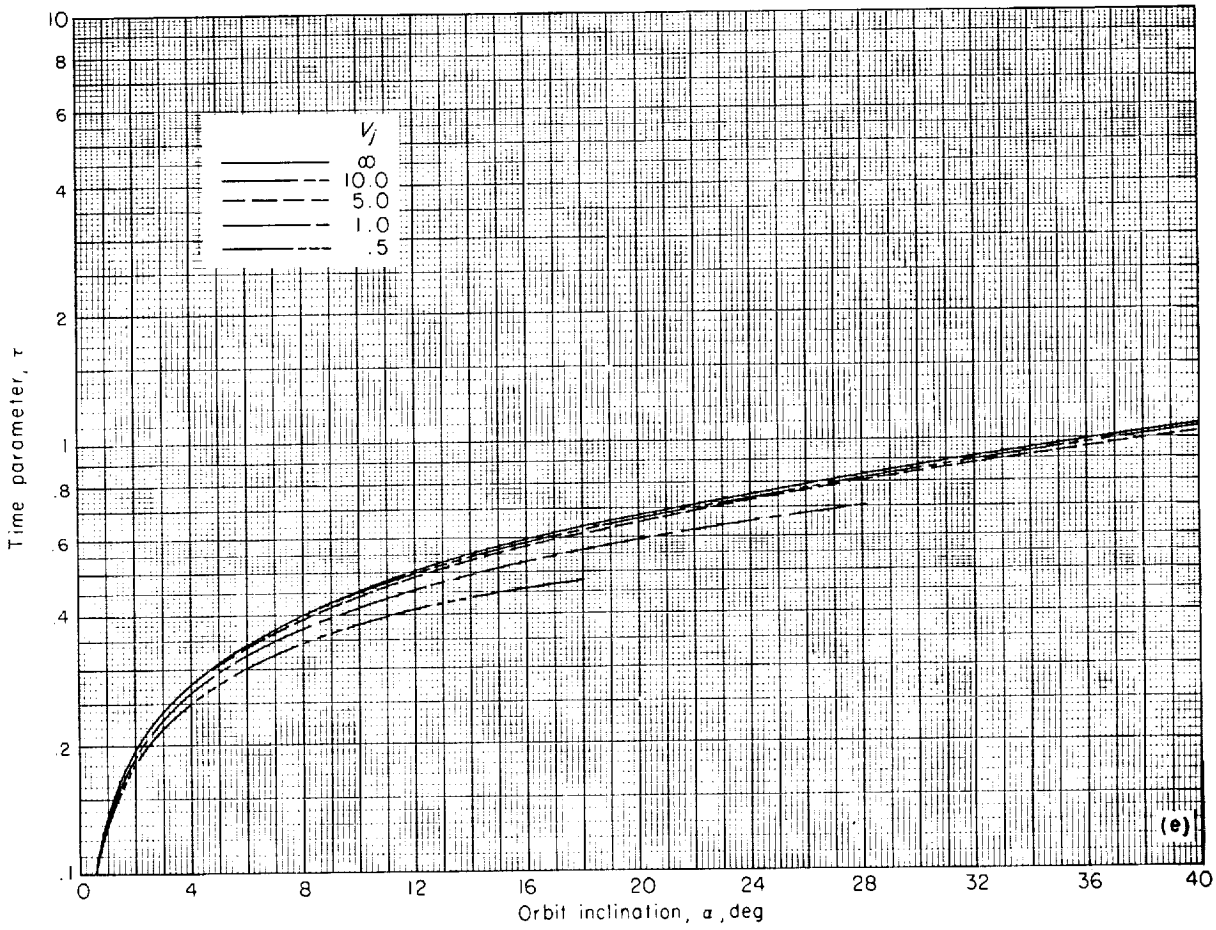

(e) a_0, 1.0.

FIGURE 5.—Continued. Inclination to circumferential direction as a function of time for outward paths.

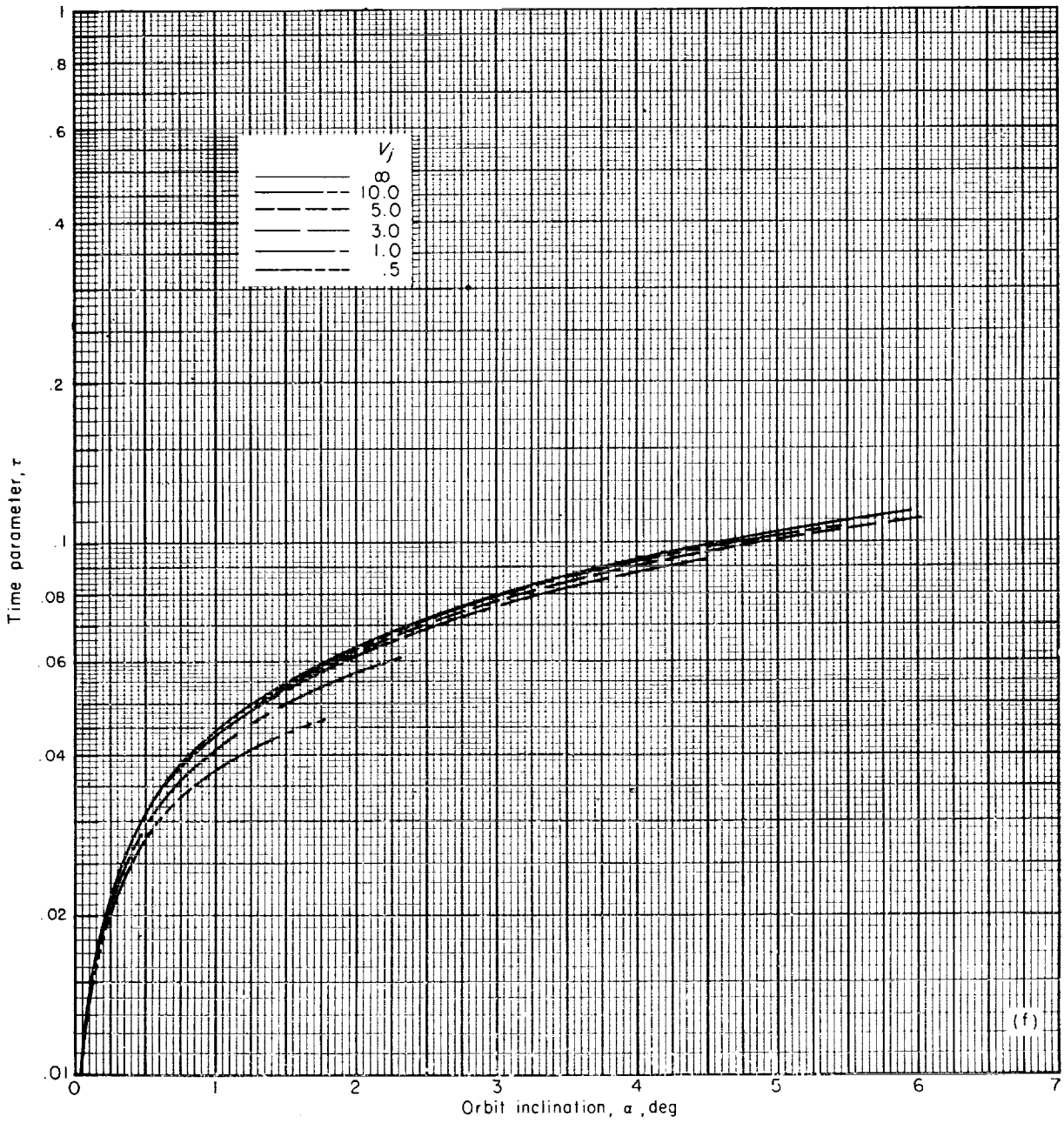

(f) a_0, 10.0.

FIGURE 5.—Concluded. Inclination to circumferential direction as a function of time for outward paths.

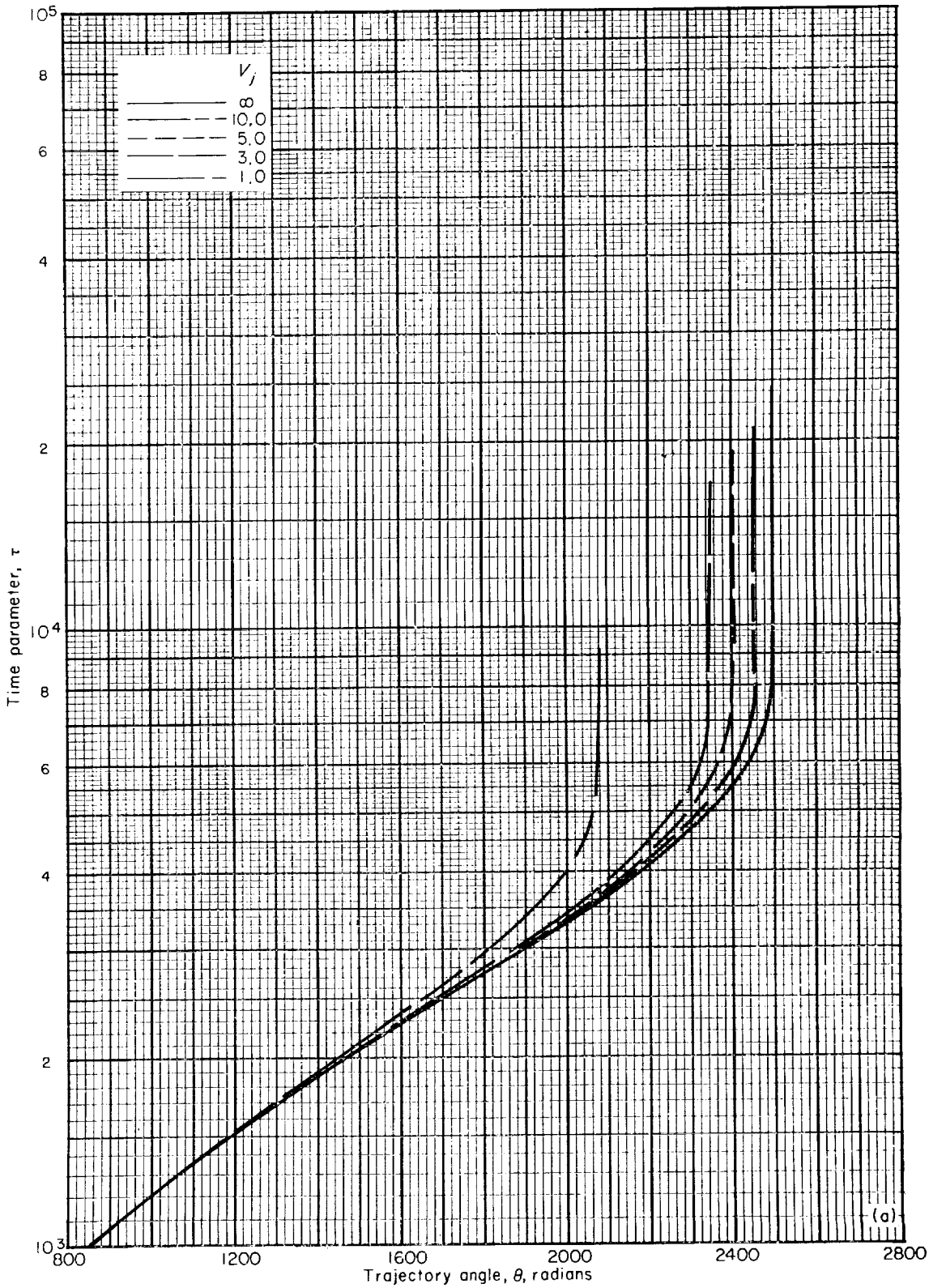

(a) a_0, 10^{-4}.

FIGURE 6.—Trajectory angle as a function of time for outward paths.

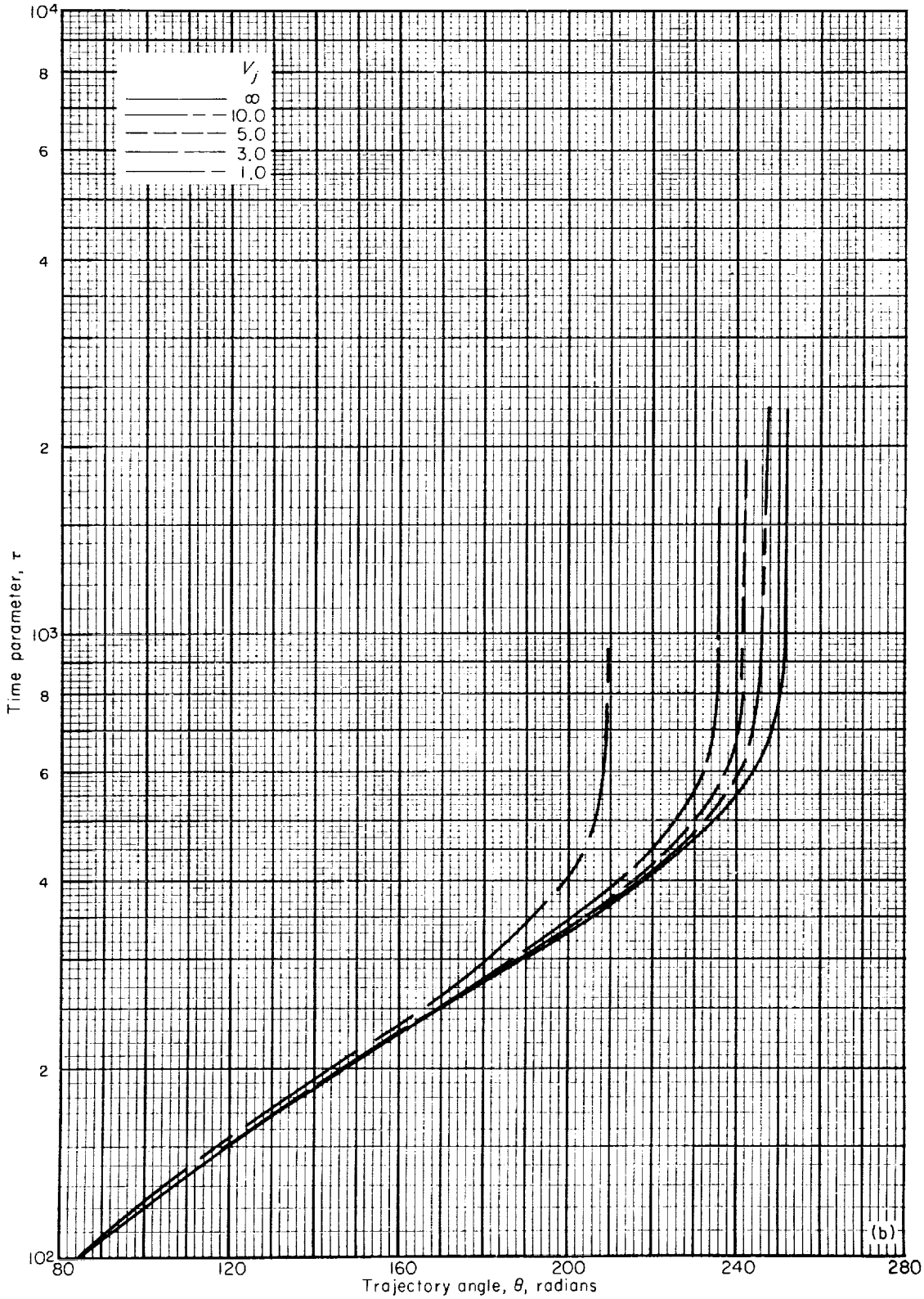

(b) a_0, 10^{-3}.

FIGURE 6.- Continued. Trajectory angle as a function of time for outward paths.

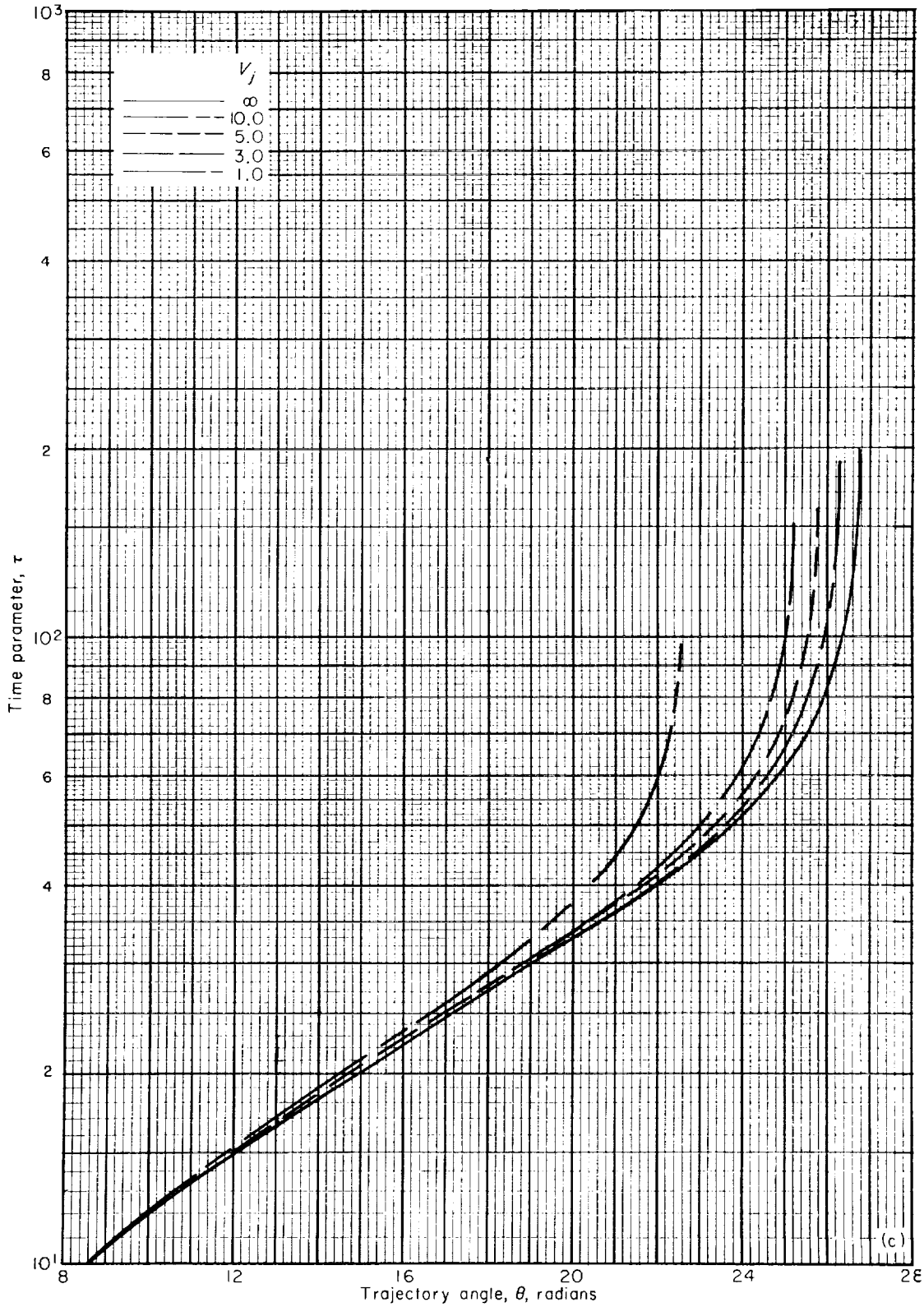

(c) a_0, 10^{-2}.

FIGURE 6. Continued. Trajectory angle as a function of time for outward paths.

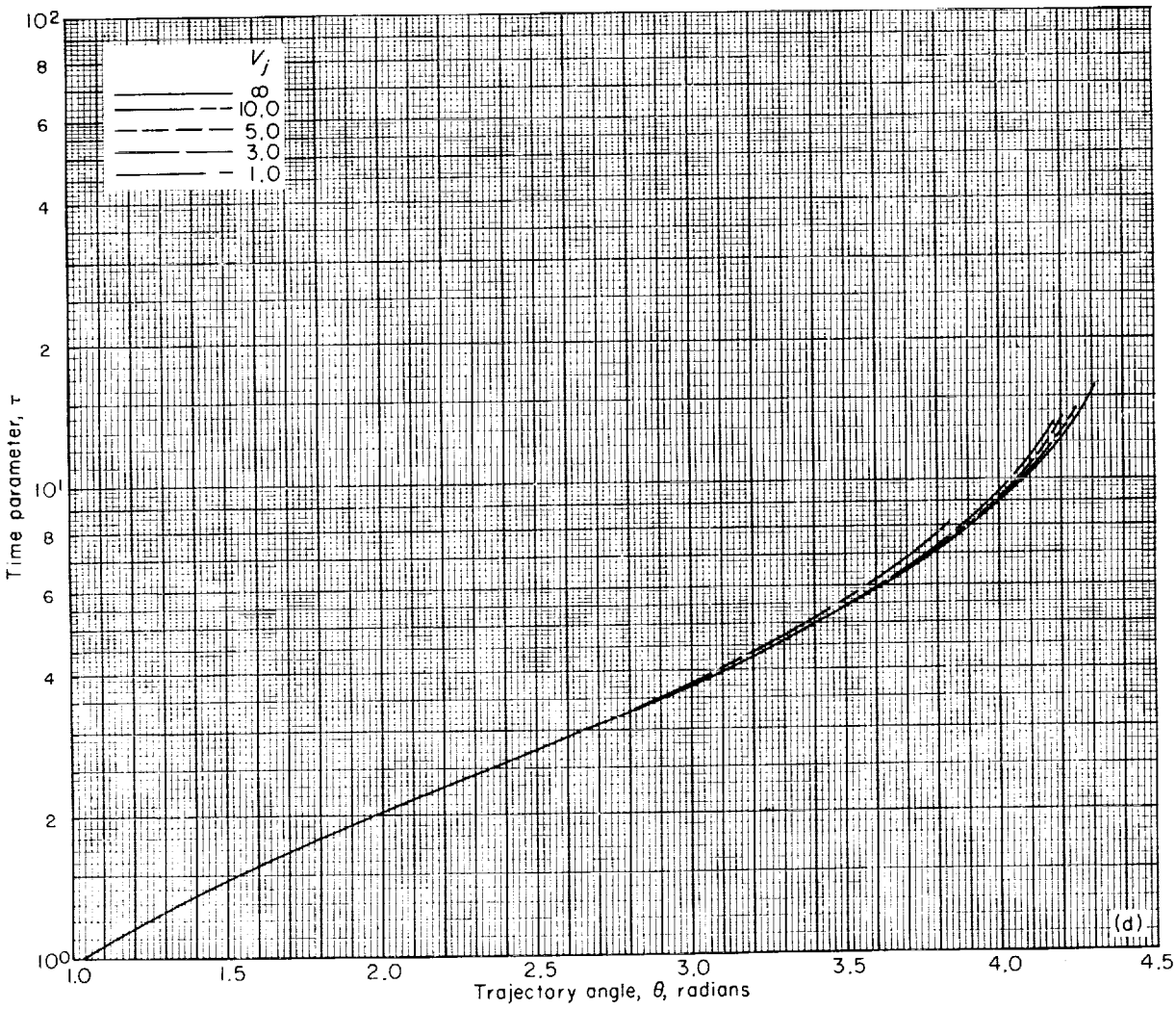

(d) a_0, 10^{-1}.

FIGURE 6.—Continued. Trajectory angle as a function of time for outward paths.

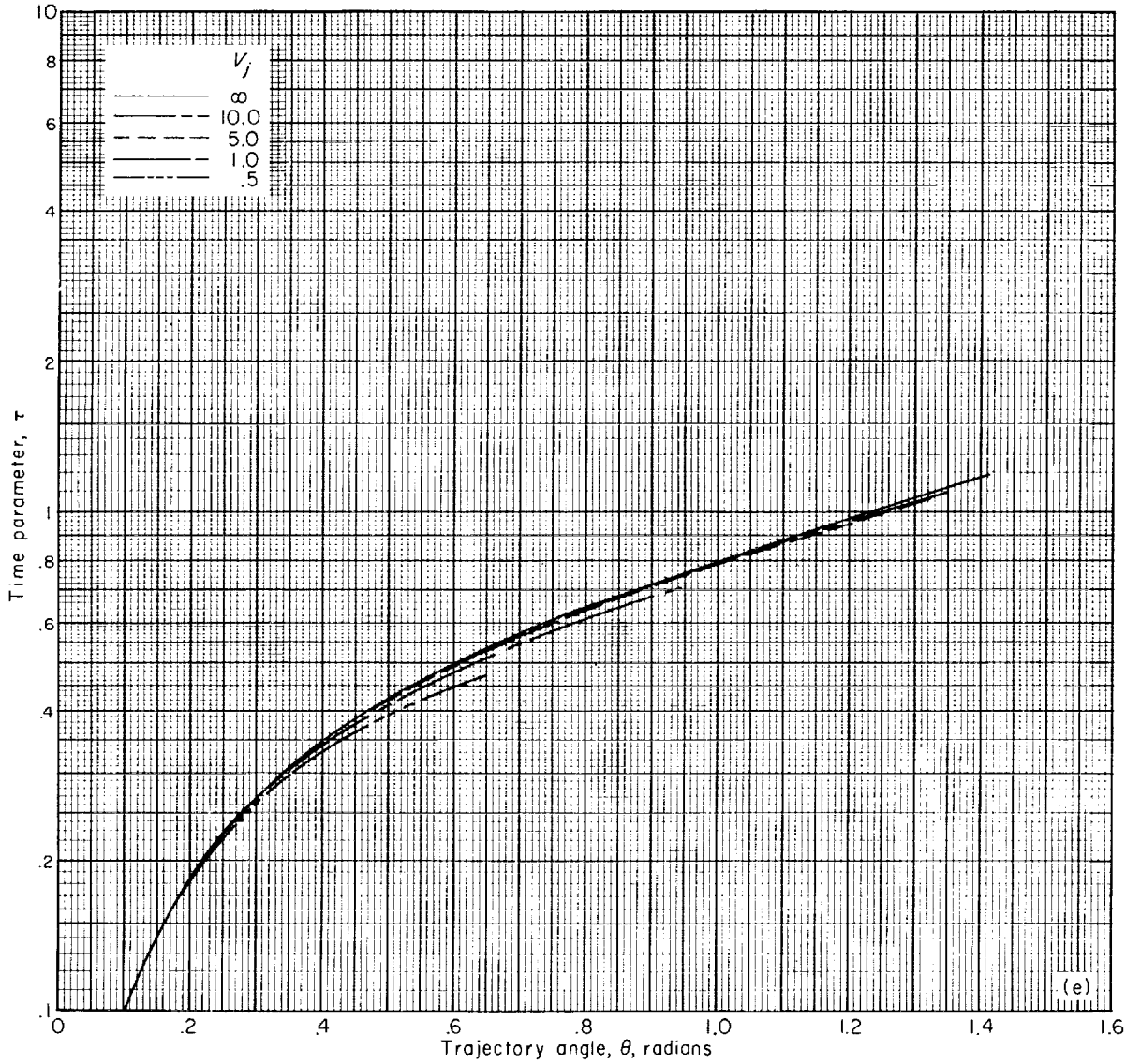

(c) a_0, 1.0.

FIGURE 6. Continued. Trajectory angle as a function of time for outward paths.

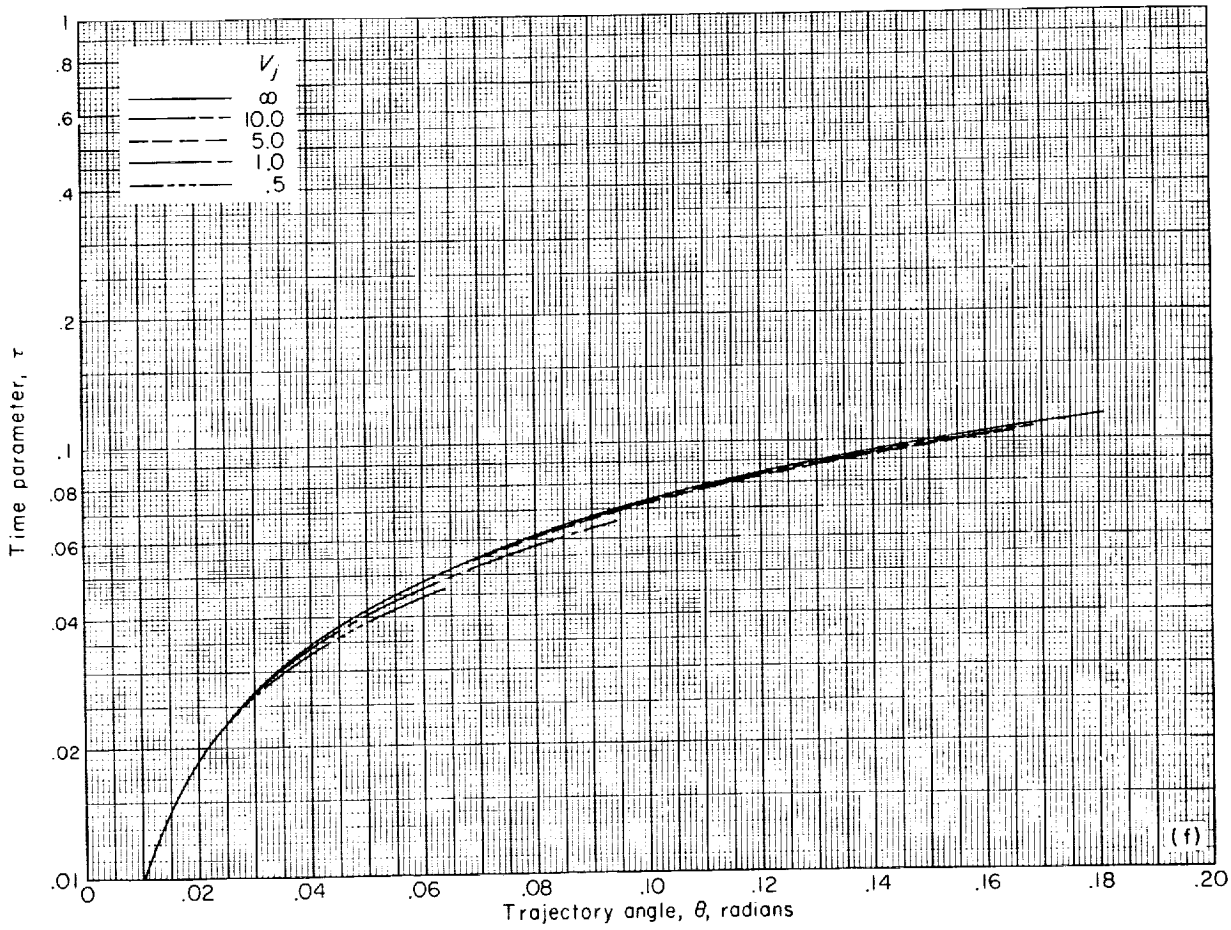

(f) a_0, 10.0.

FIGURE 6. Concluded. Trajectory angle as a function of time for outward paths.

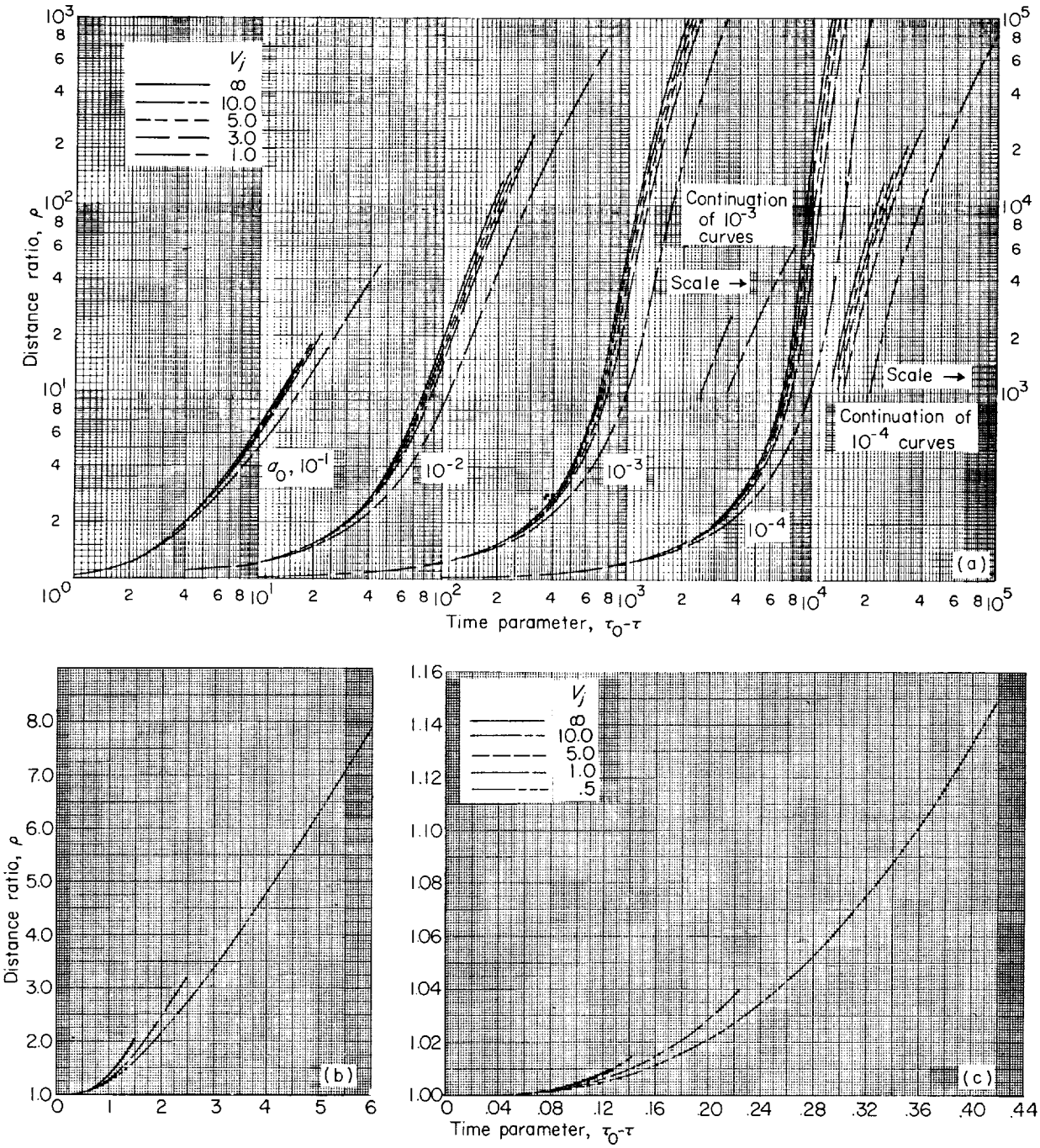

(a) a_0, 10^{-4} to 10^{-1}.

(b) a_0, 1.0. (c) a_0, 10.0.

FIGURE 7.—Radial distance as a function of time for inward paths.

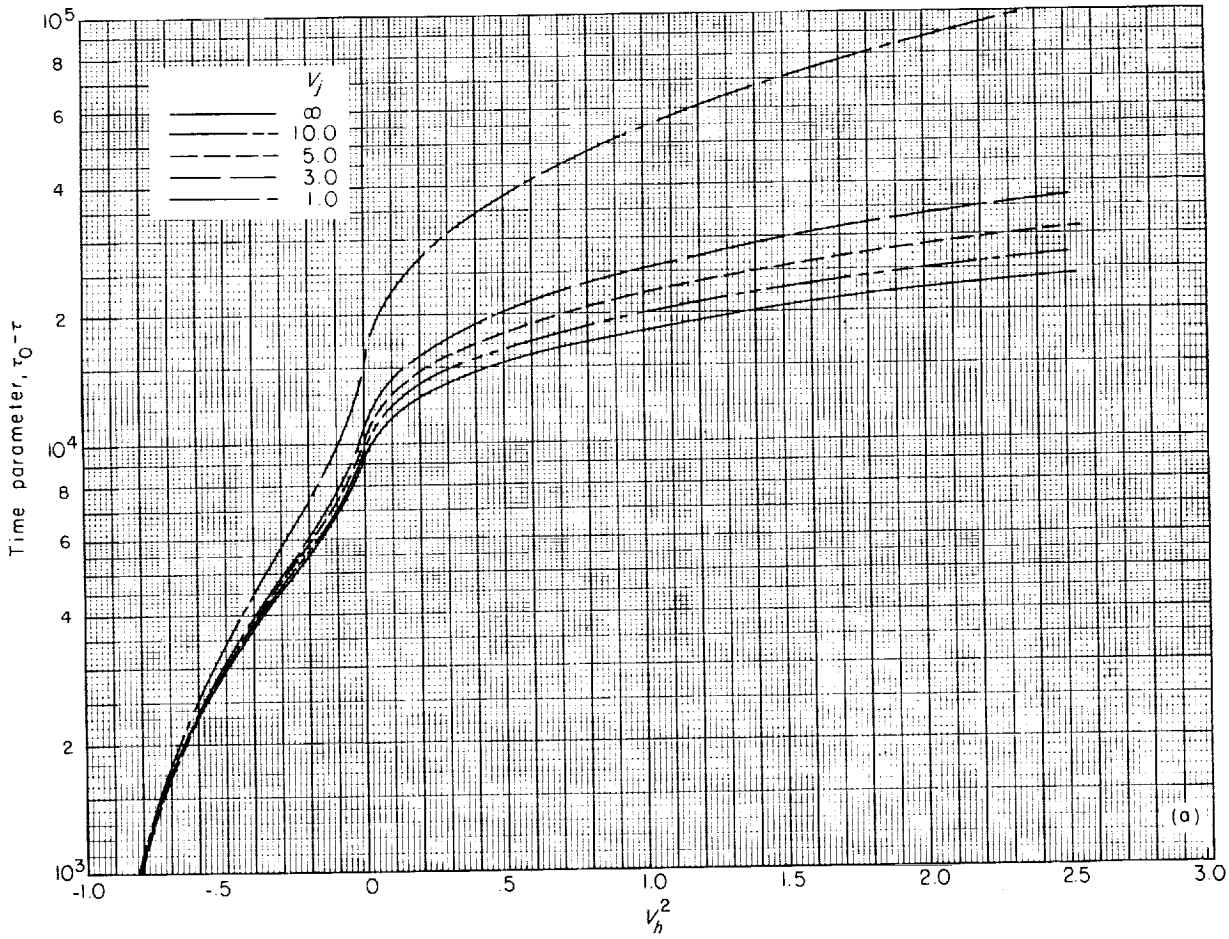

(a) a_0, 10^{-4}.

FIGURE 8.—Local hyperbolic velocity as a function of time for inward paths.

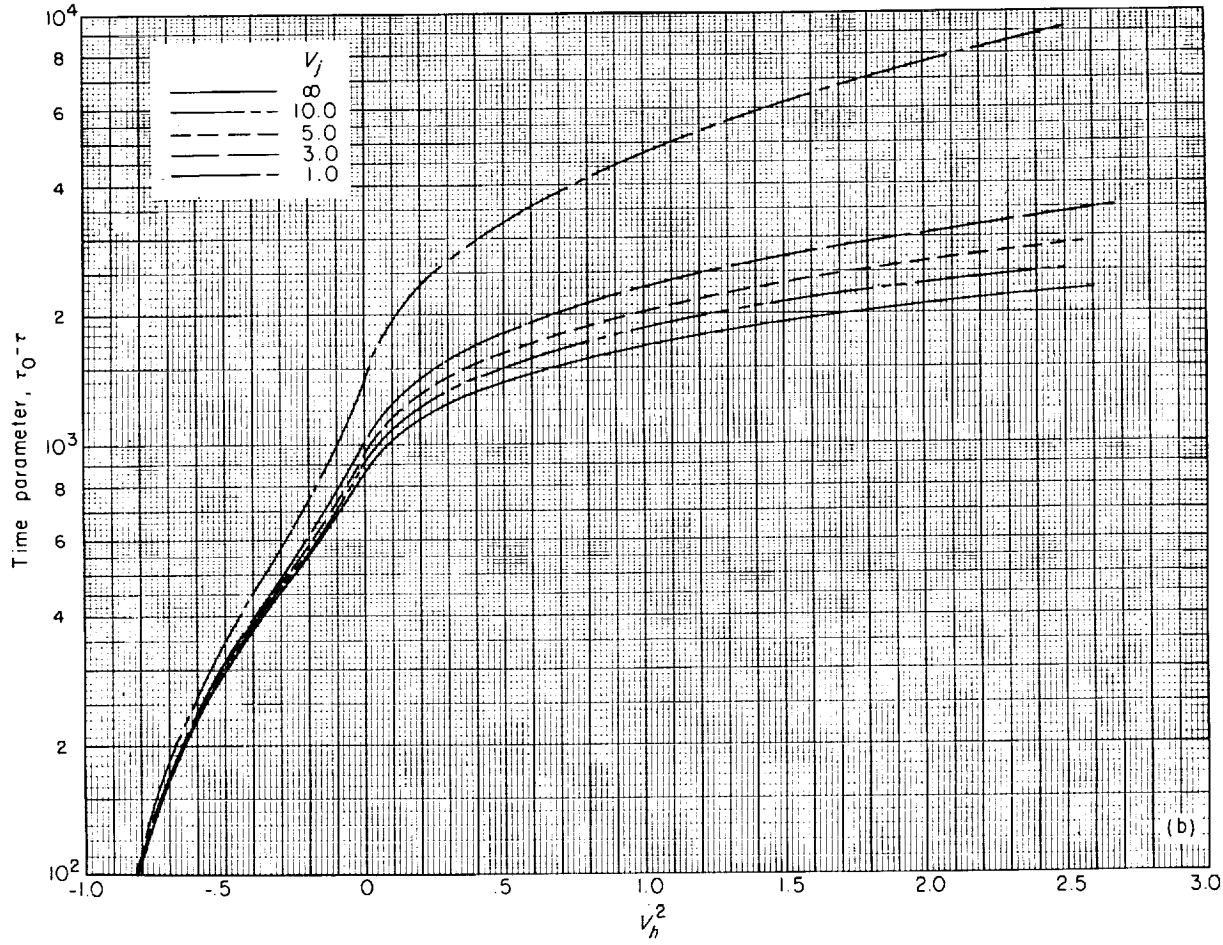

(b) a_0, 10^{-3}.

FIGURE 8.—Continued. Local hyperbolic velocity as a function of time for inward paths.

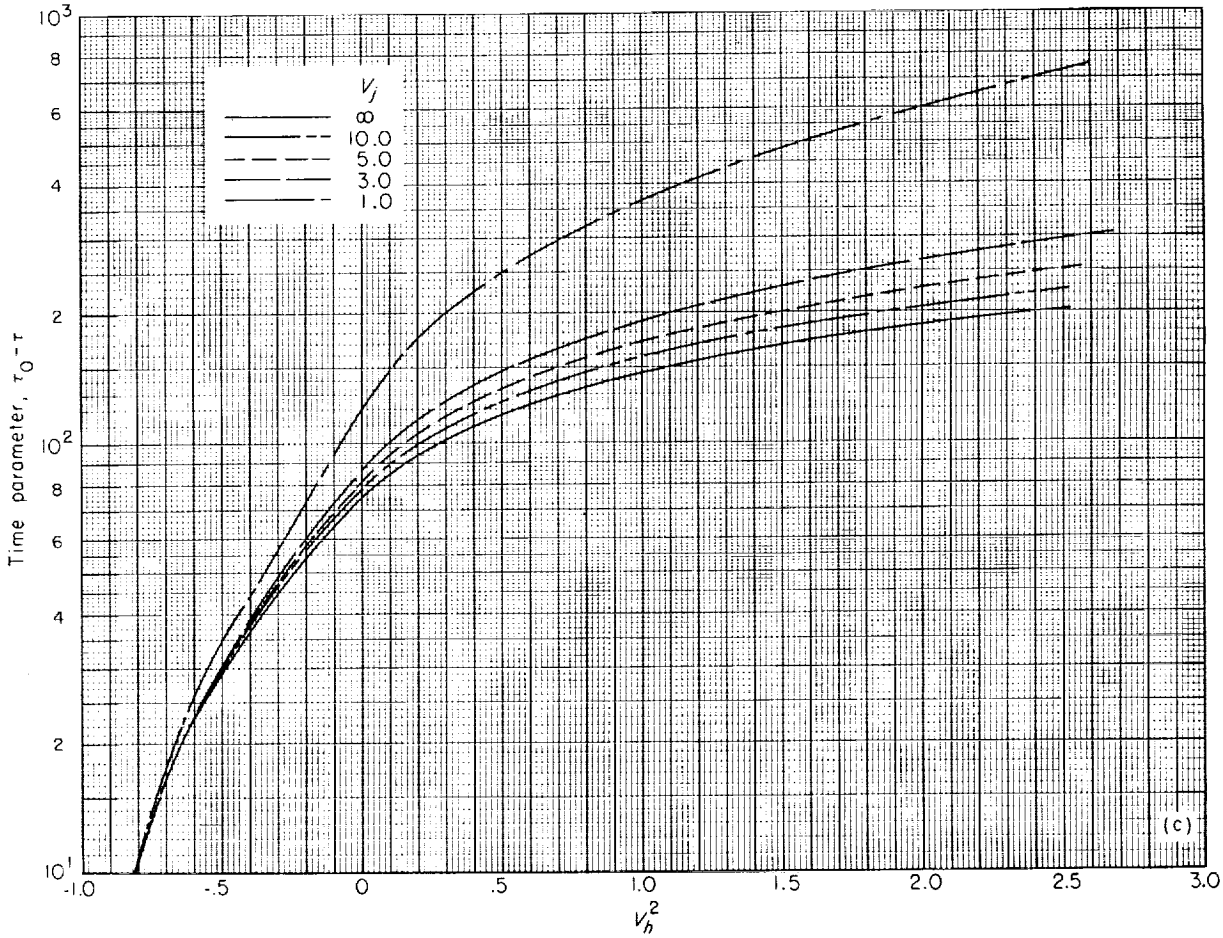

(c) a_0, 10^{-2}.

FIGURE 8.—Continued. Local hyperbolic velocity as a function of time for inward paths.

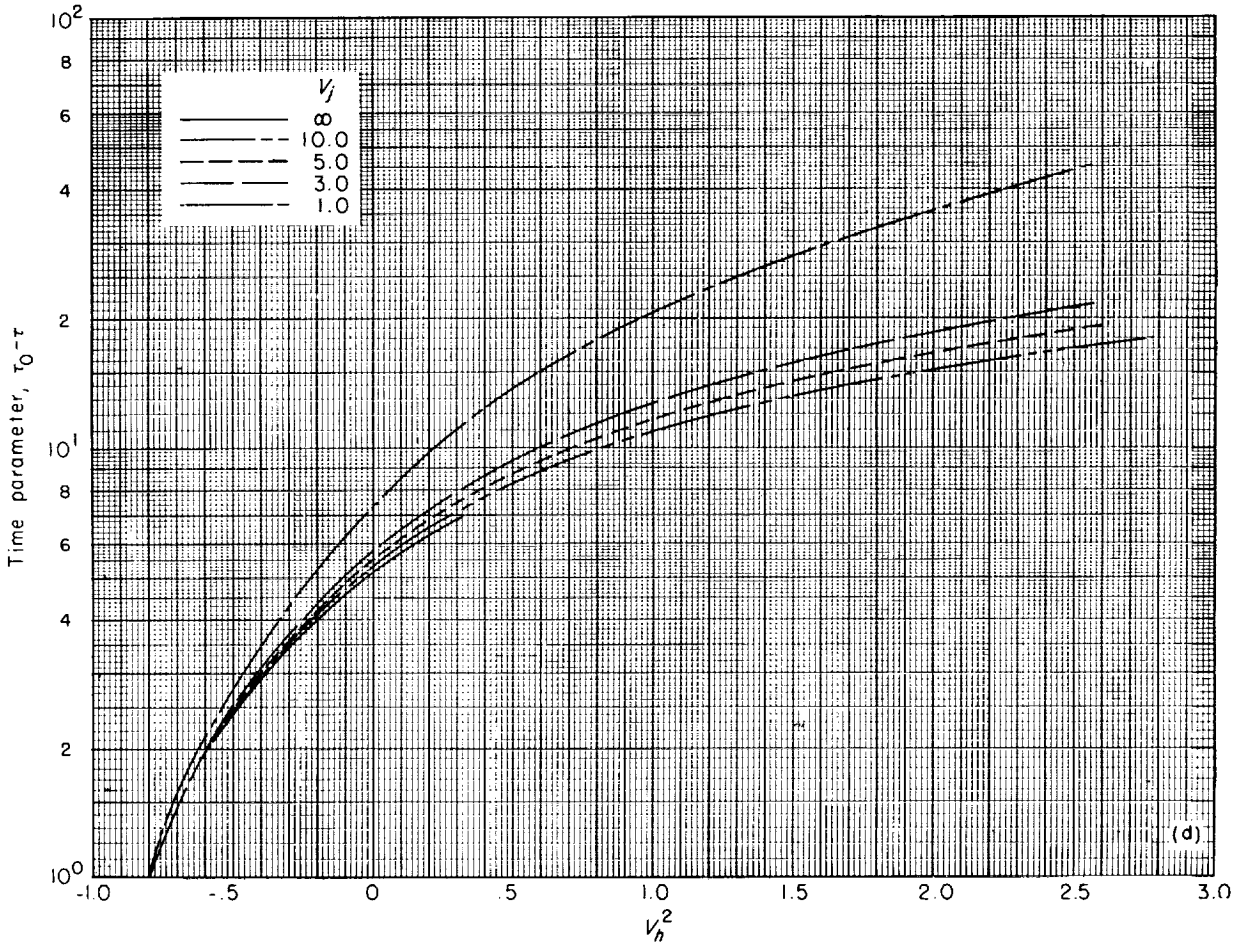

(d) a_0, 10^{-1}.

FIGURE 8.—Continued. Local hyperbolic velocity as a function of time for inward paths.

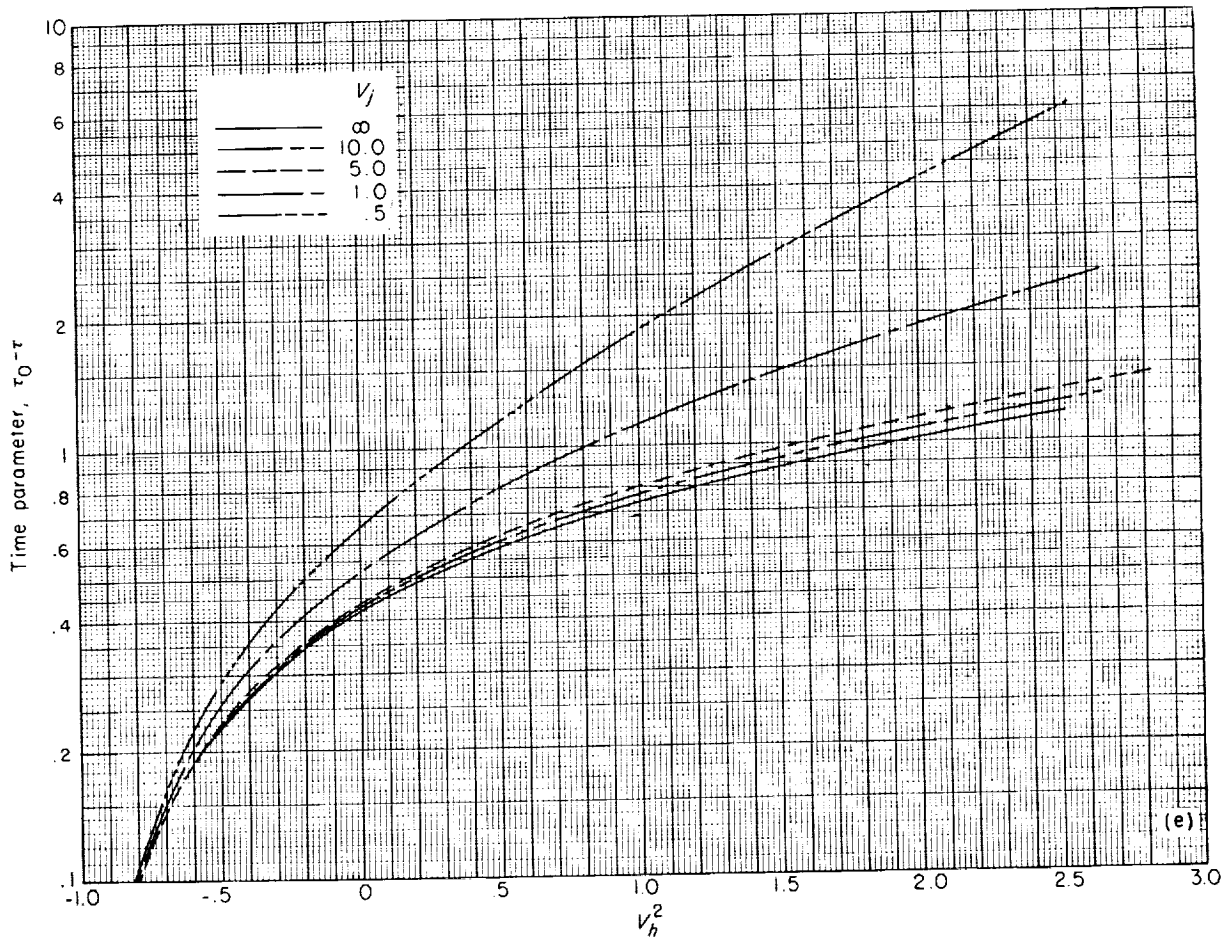

(c) a_0, 1.0.

FIGURE 8.—Continued. Local hyperbolic velocity as a function of time for inward paths.

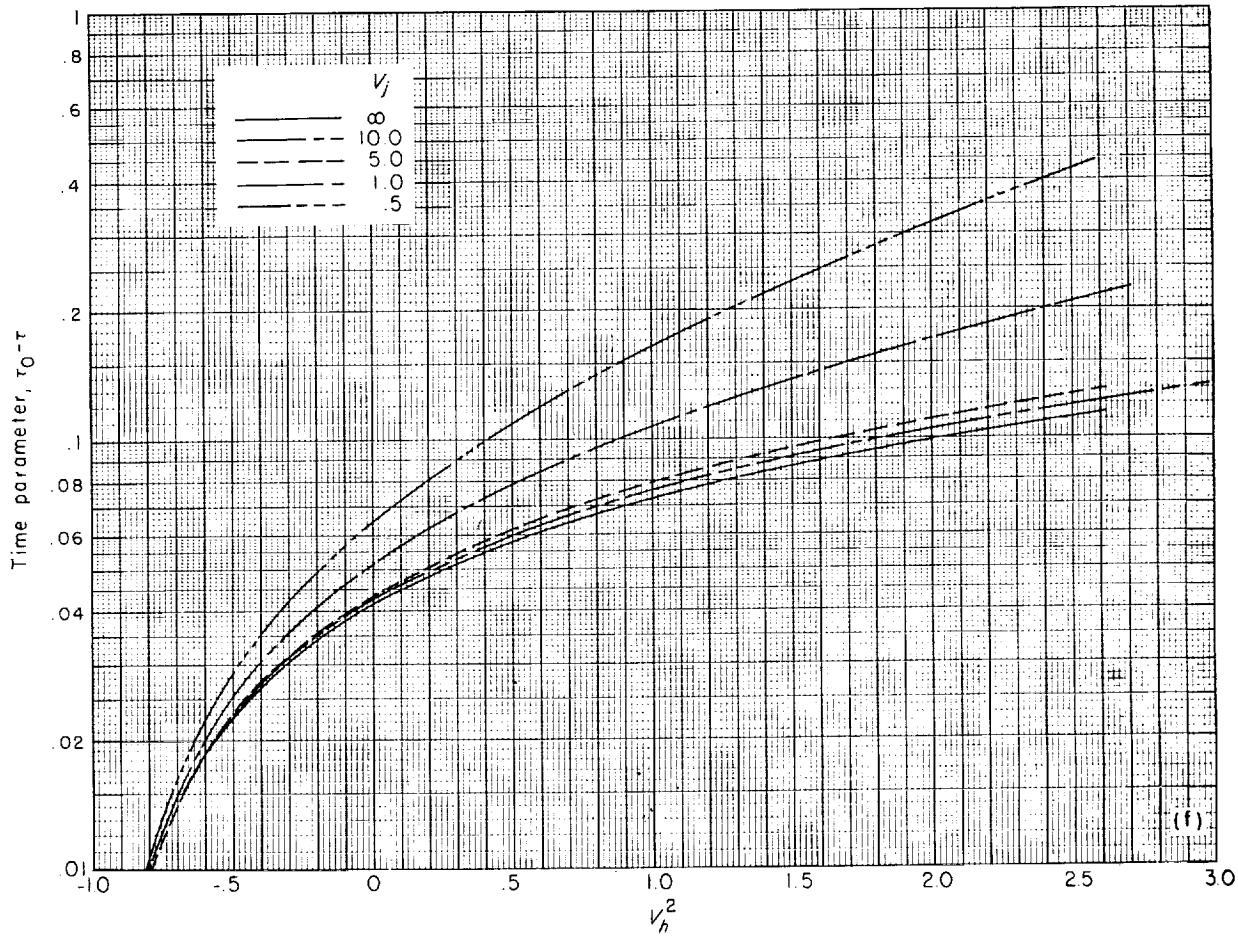

(f) a_0, 10.0.

FIGURE 8. Concluded. Local hyperbolic velocity as a function of time for inward paths.

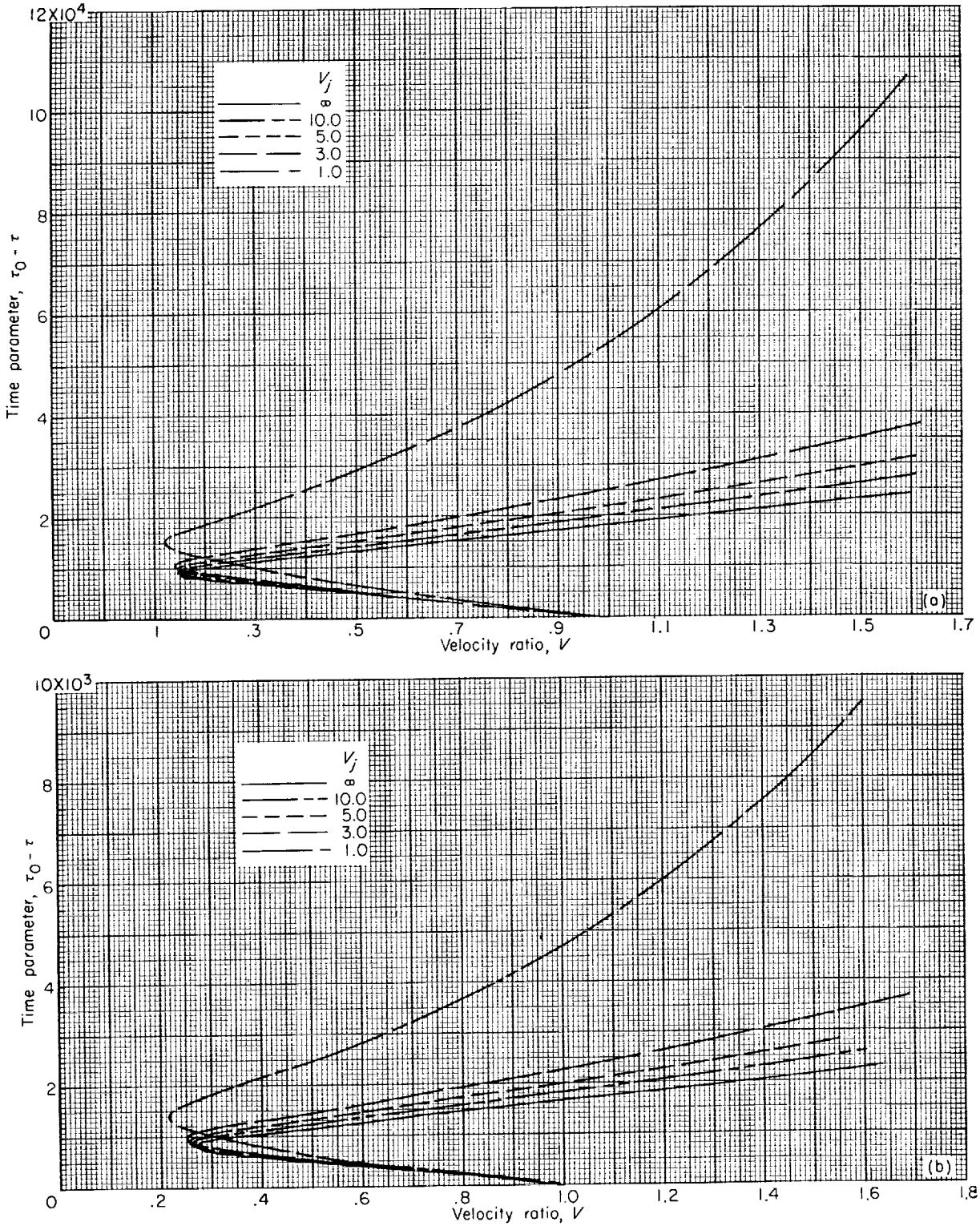

(a) a_0, 10^{-4}.
(b) a_0, 10^{-3}.

FIGURE 9.—Velocity as a function of time for inward paths.

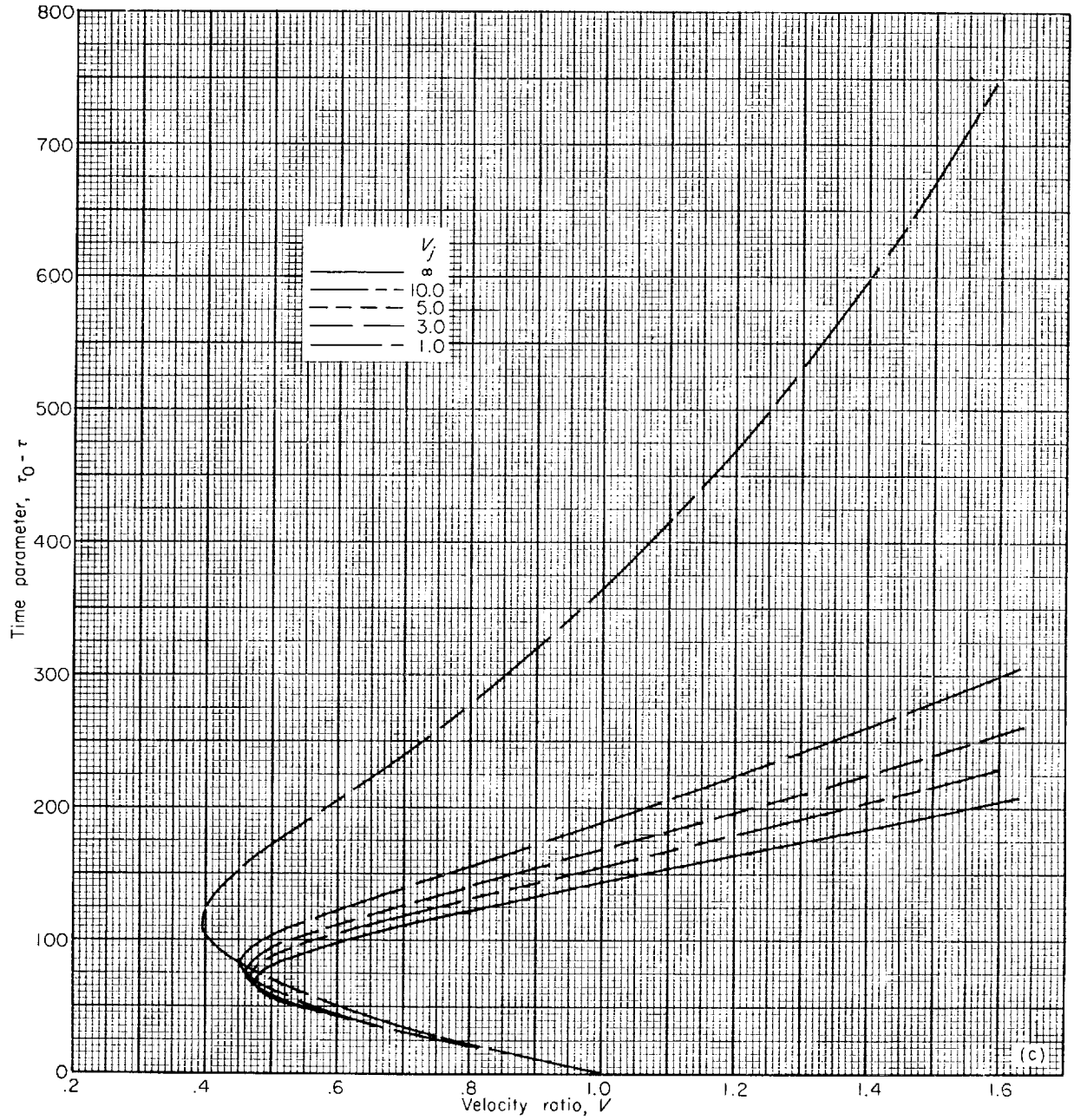

(c) a_0, 10^{-2}.

FIGURE 9.—Continued. Velocity as a function of time for inward paths.

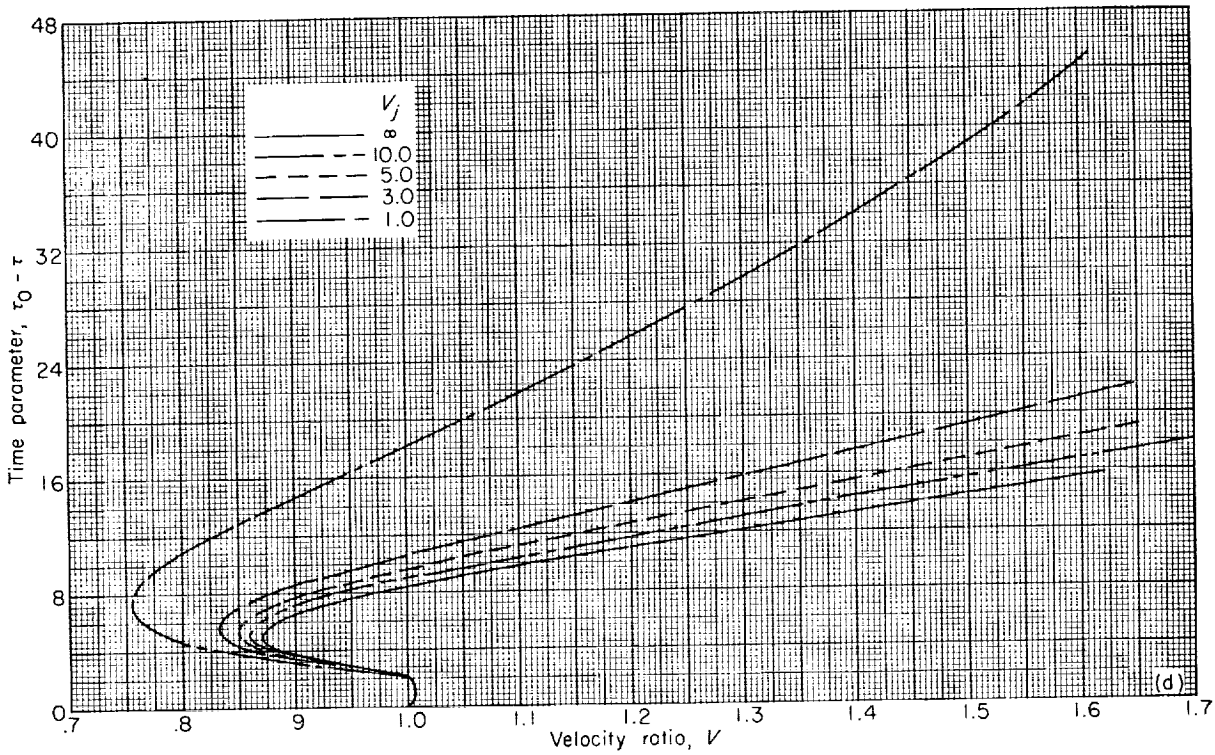

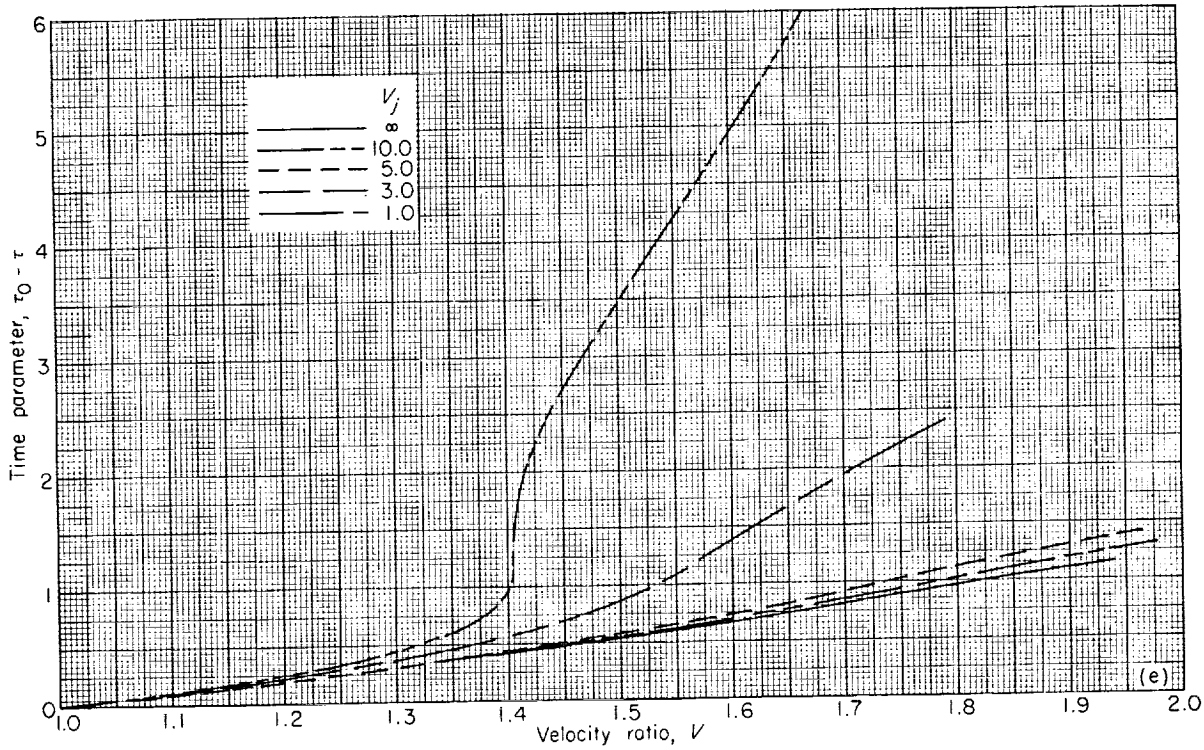

(d) a_0, 10^{-1}.
(e) a_0, 1.0.

FIGURE 9.—Continued. Velocity as a function of time for inward paths.

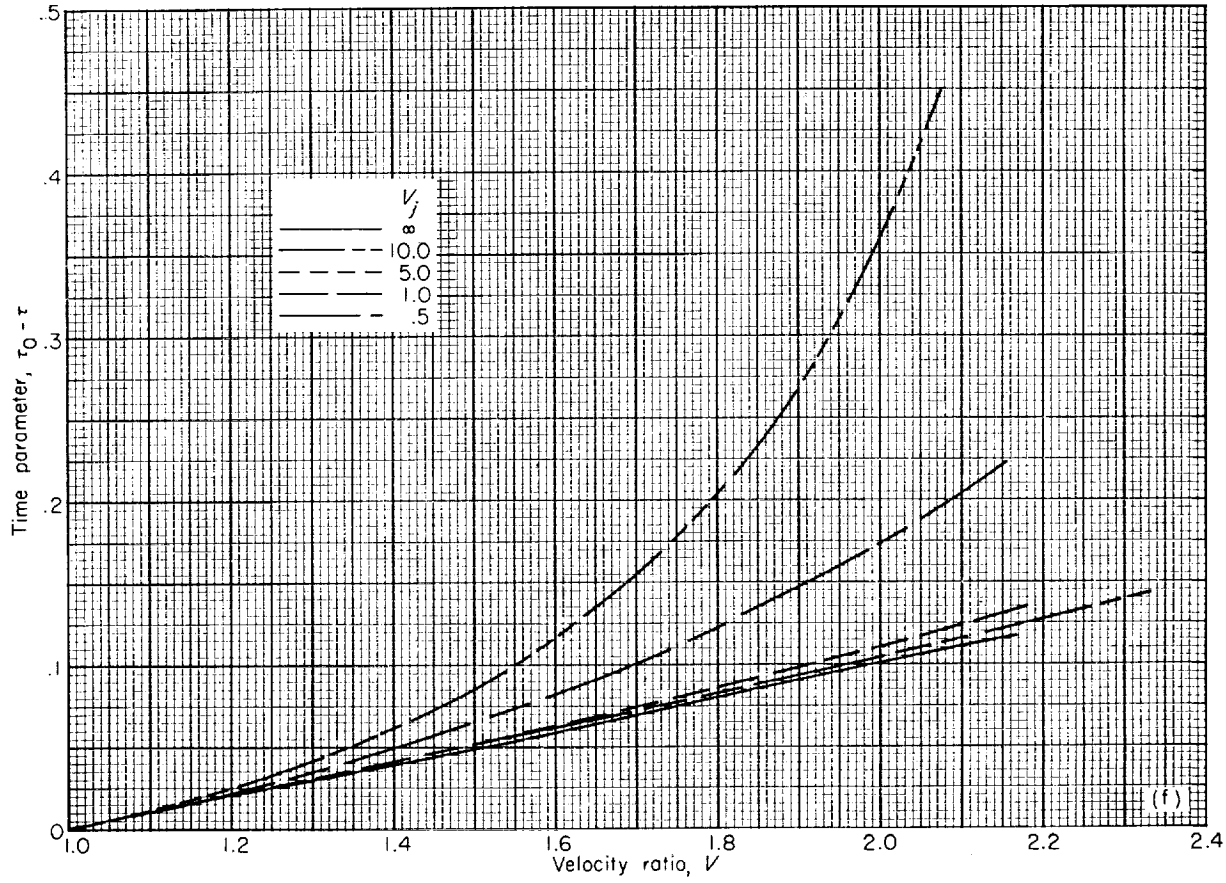

(f) a_0, 10.0.

FIGURE 9.—Concluded. Velocity as a function of time for inward paths.

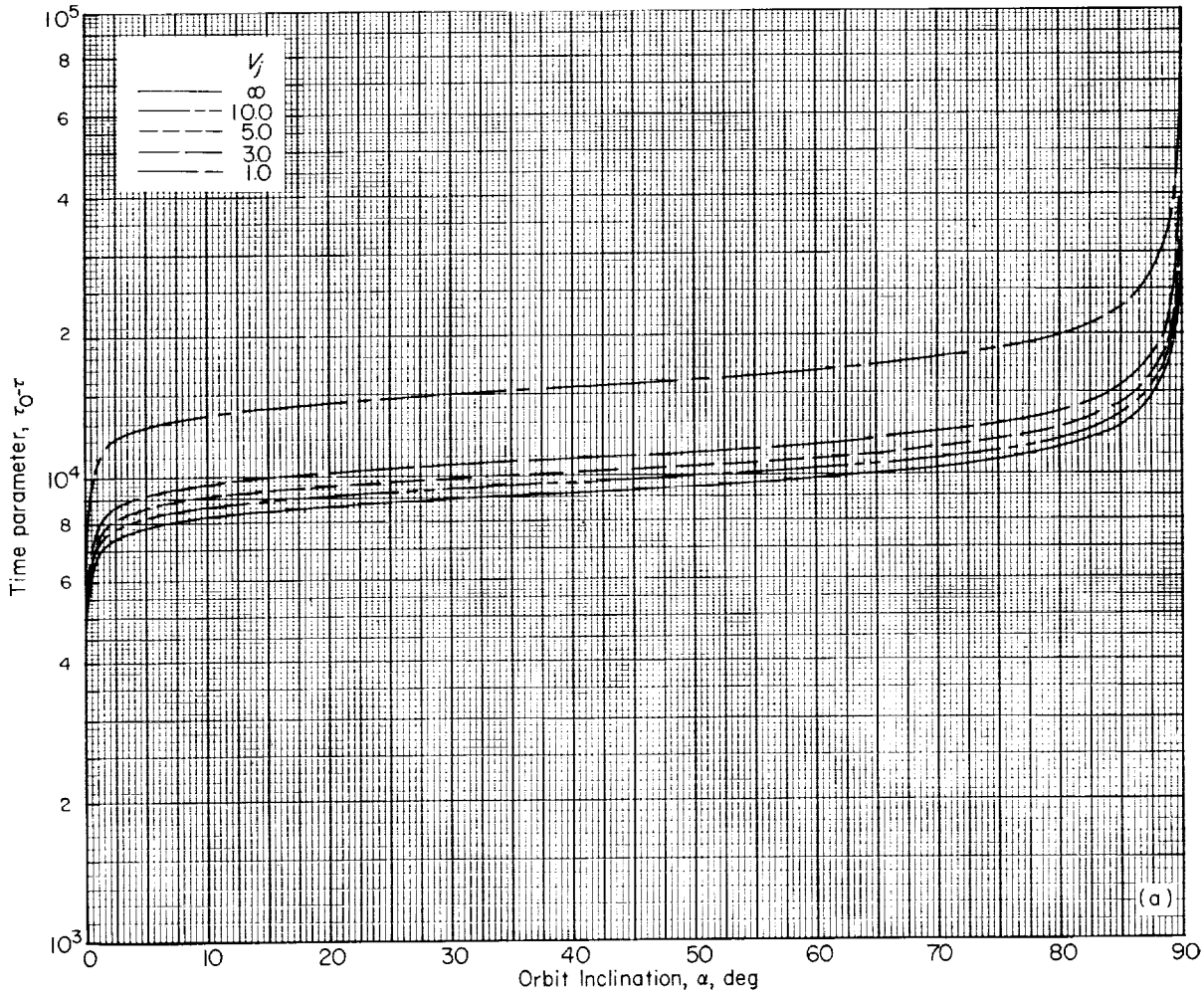

(a) a_0, 10^{-4}.

FIGURE 10. –Inclination to circumferential direction as a function of time for inward paths.

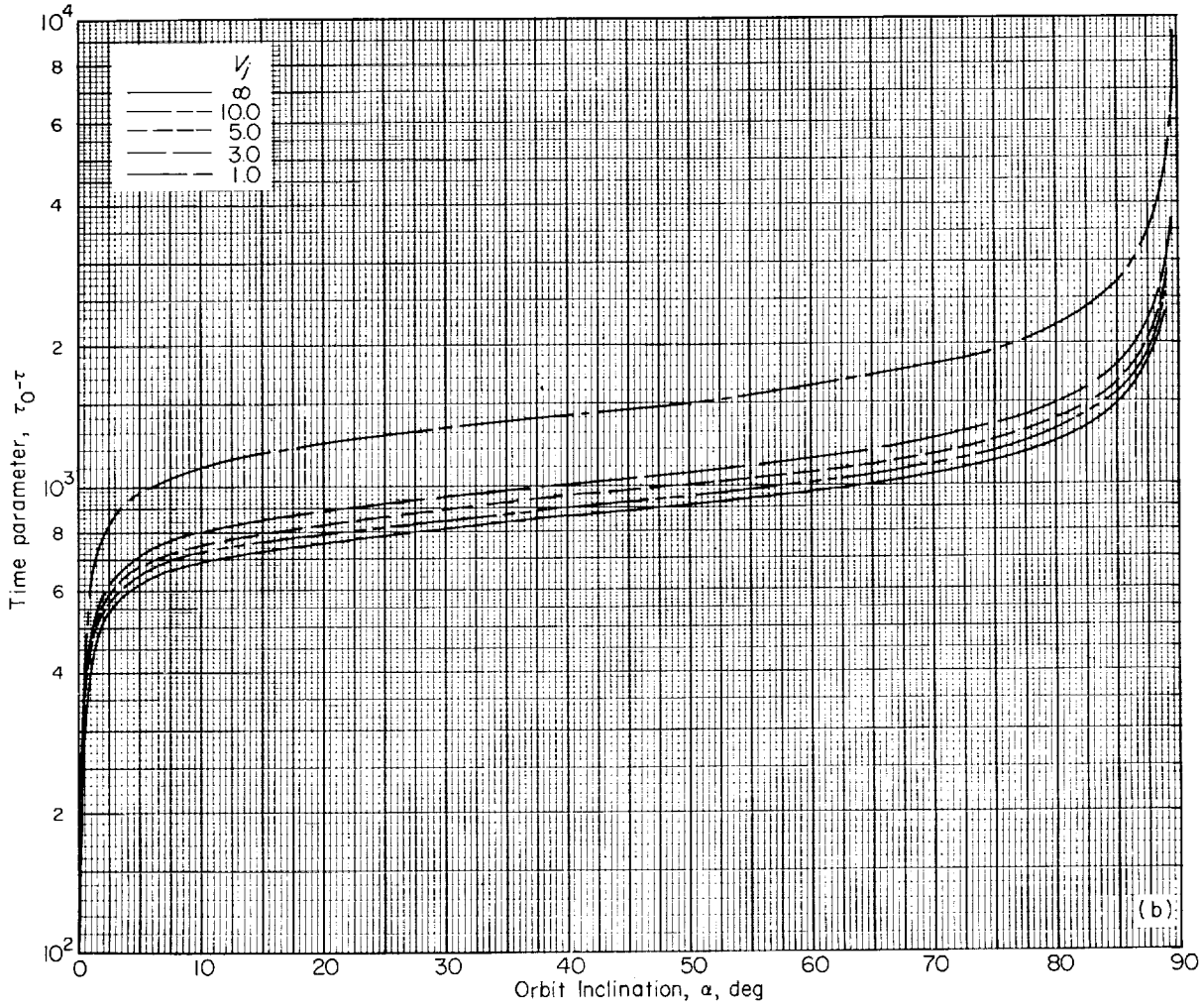

(b) a_0, 10^{-3}.

FIGURE 10. Continued. Inclination to circumferential direction as a function of time for inward paths.

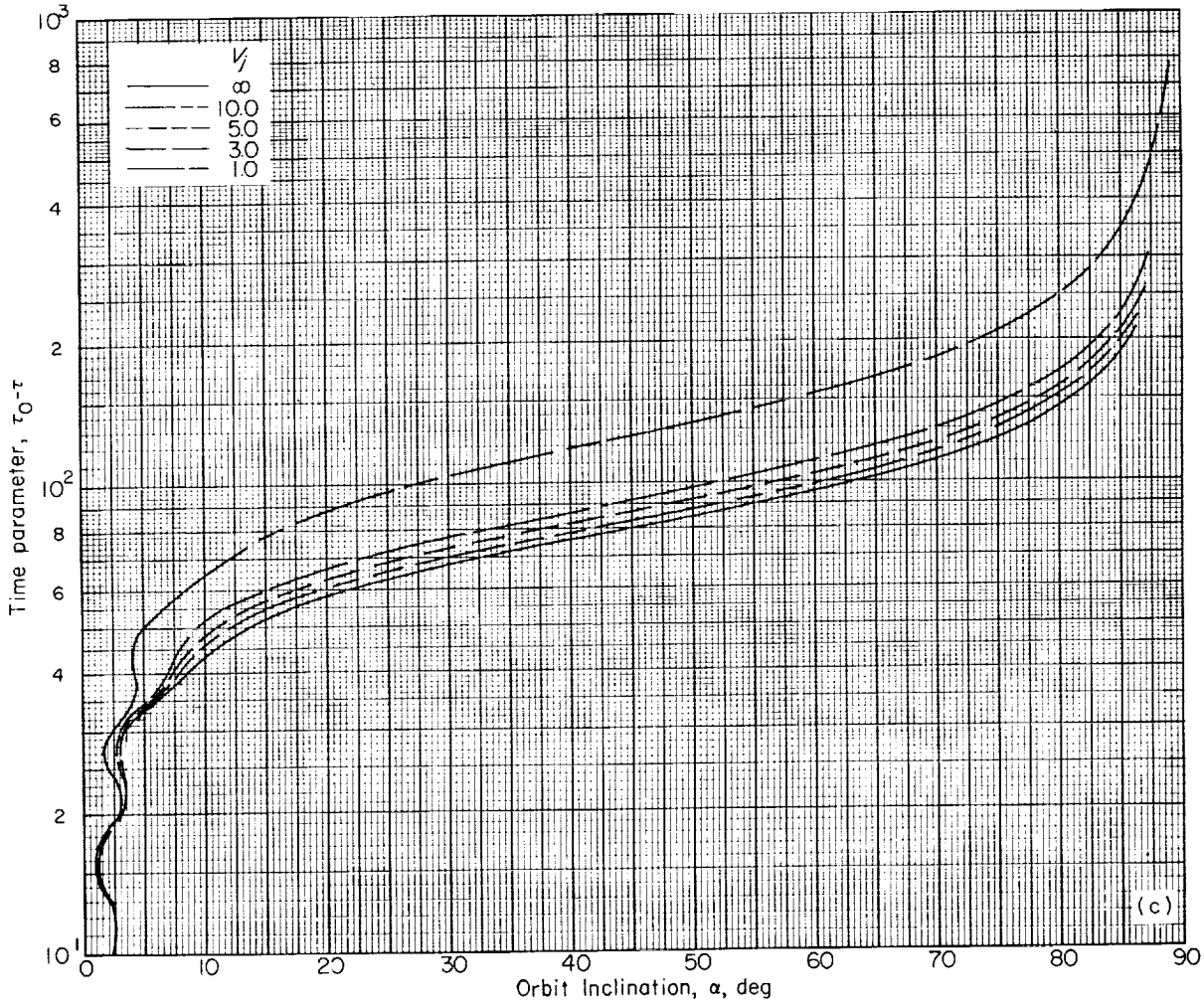

(c) a_0, 10^{-2}.

FIGURE 10.—Continued. Inclination to circumferential direction as a function of time for inward paths.

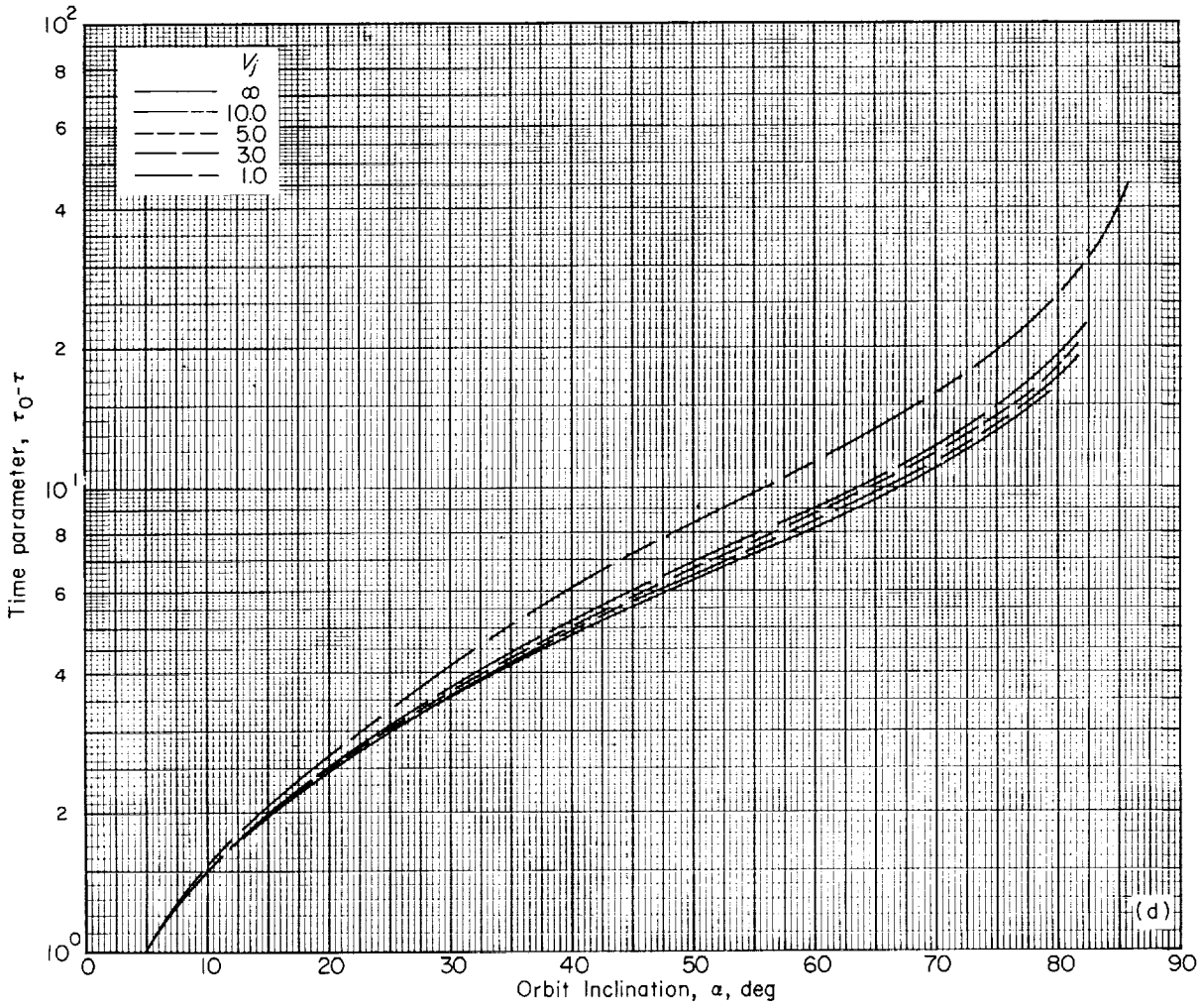

(d) a_0, 10^{-1}.

FIGURE 10.—Continued. Inclination to circumferential direction as a function of time for inward paths.

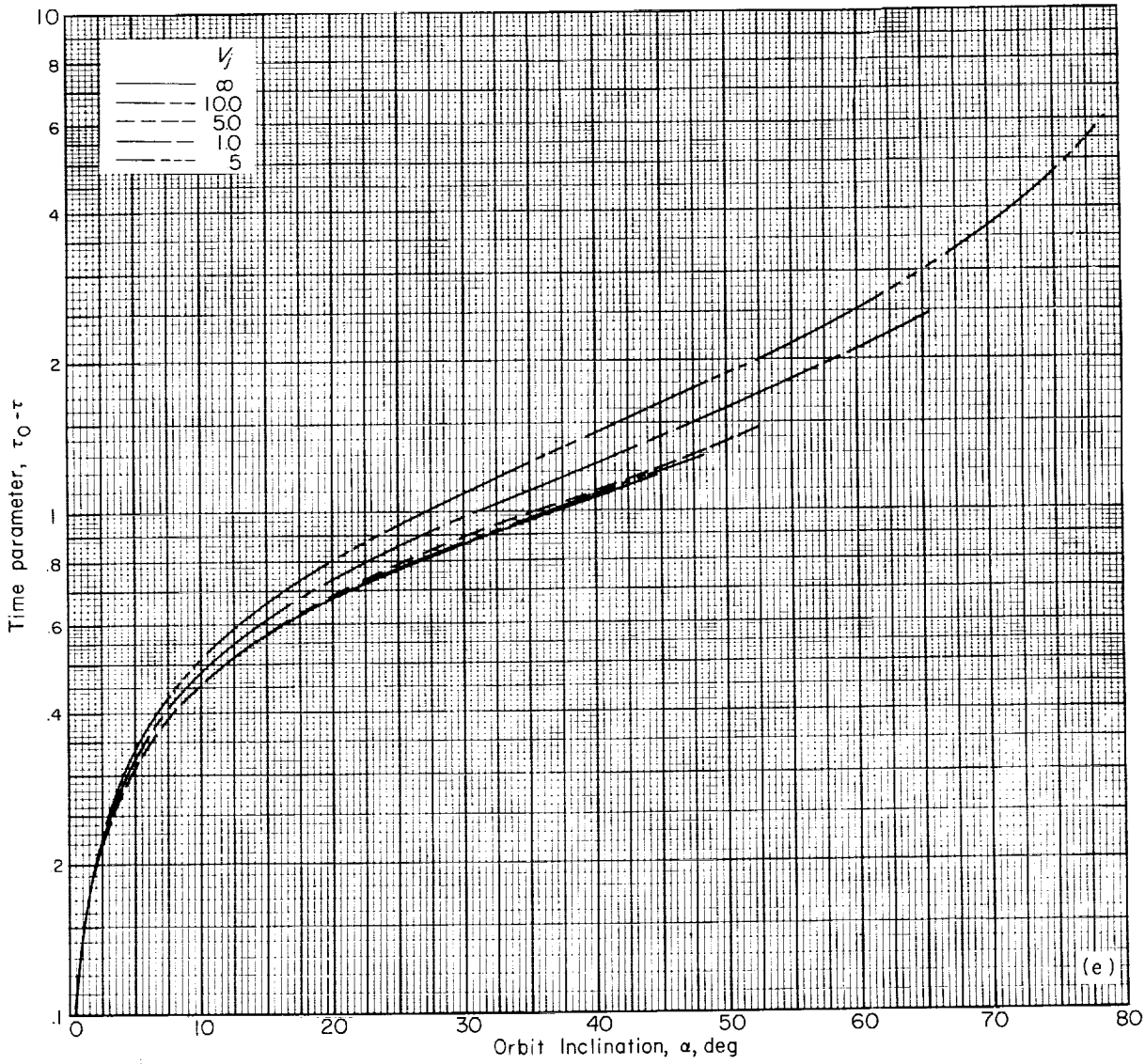

(c) a_0, 1.0.

FIGURE 10.—Continued. Inclination to circumferential direction as a function of time for inward paths.

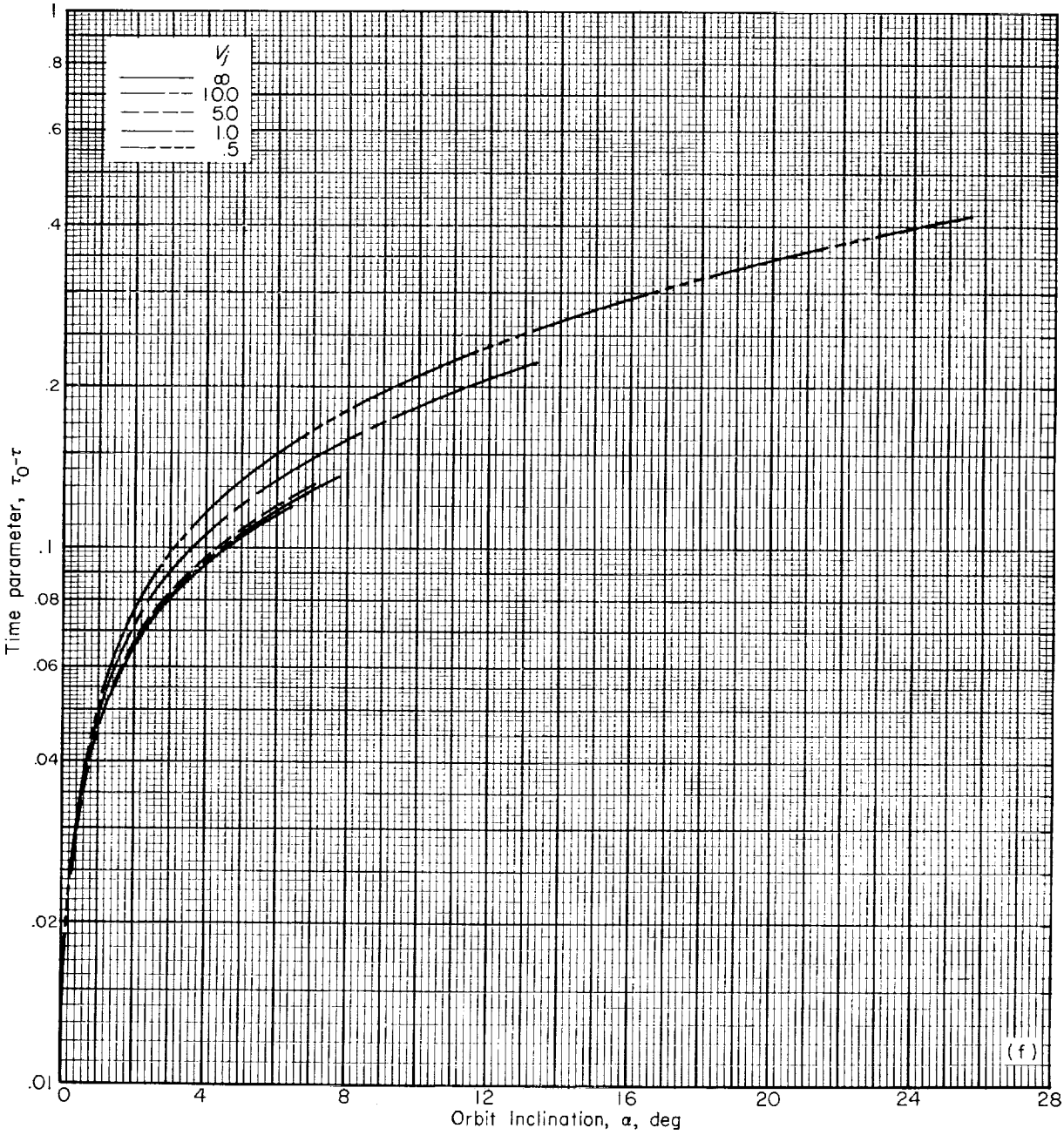

(f) a_0, 10.0.

FIGURE 10.—Concluded. Inclination to circumferential direction as a function of time for inward paths.

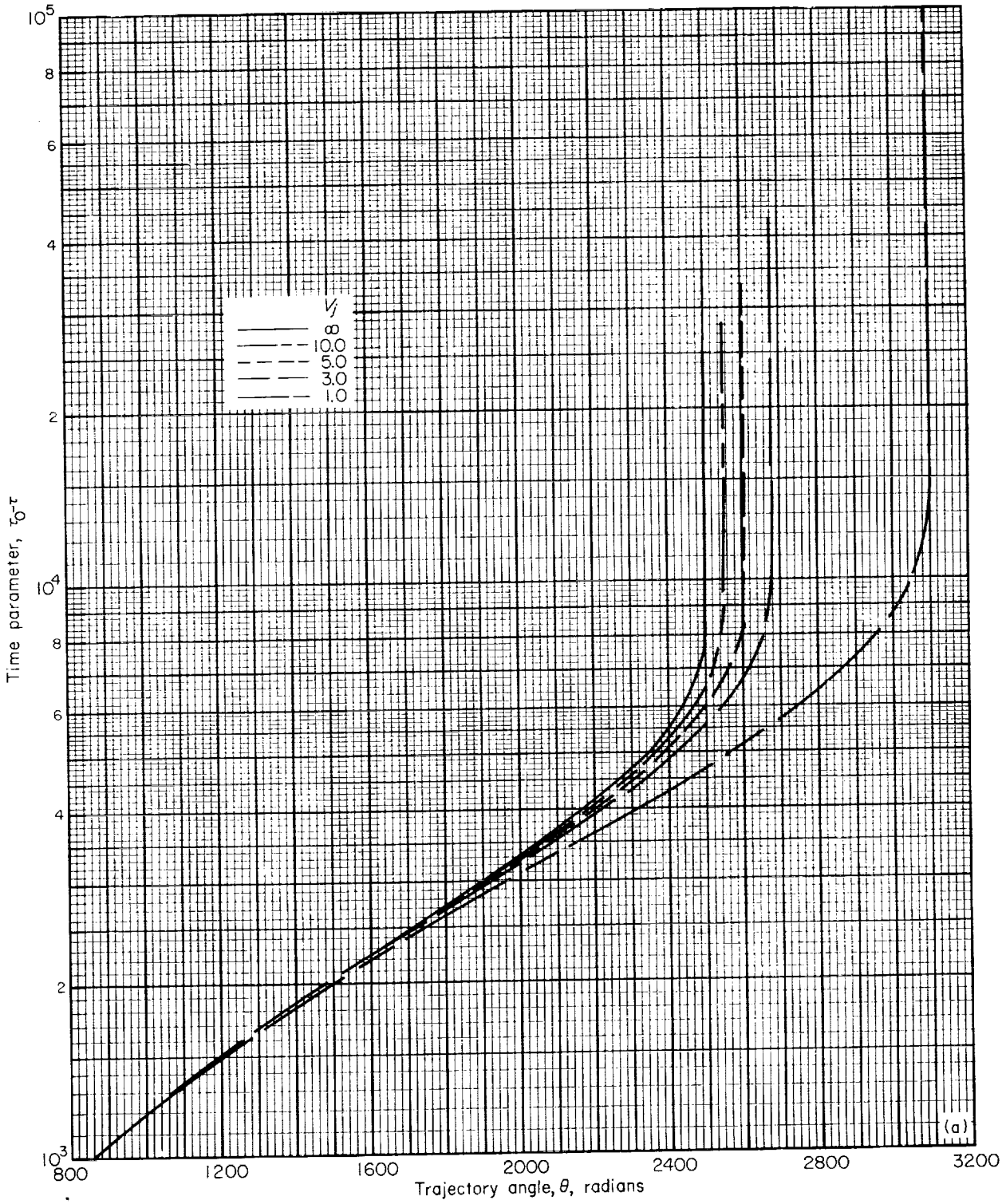

(a) a_0, 10^{-4}.

FIGURE 11.—Trajectory angle as a function of time for inward paths.

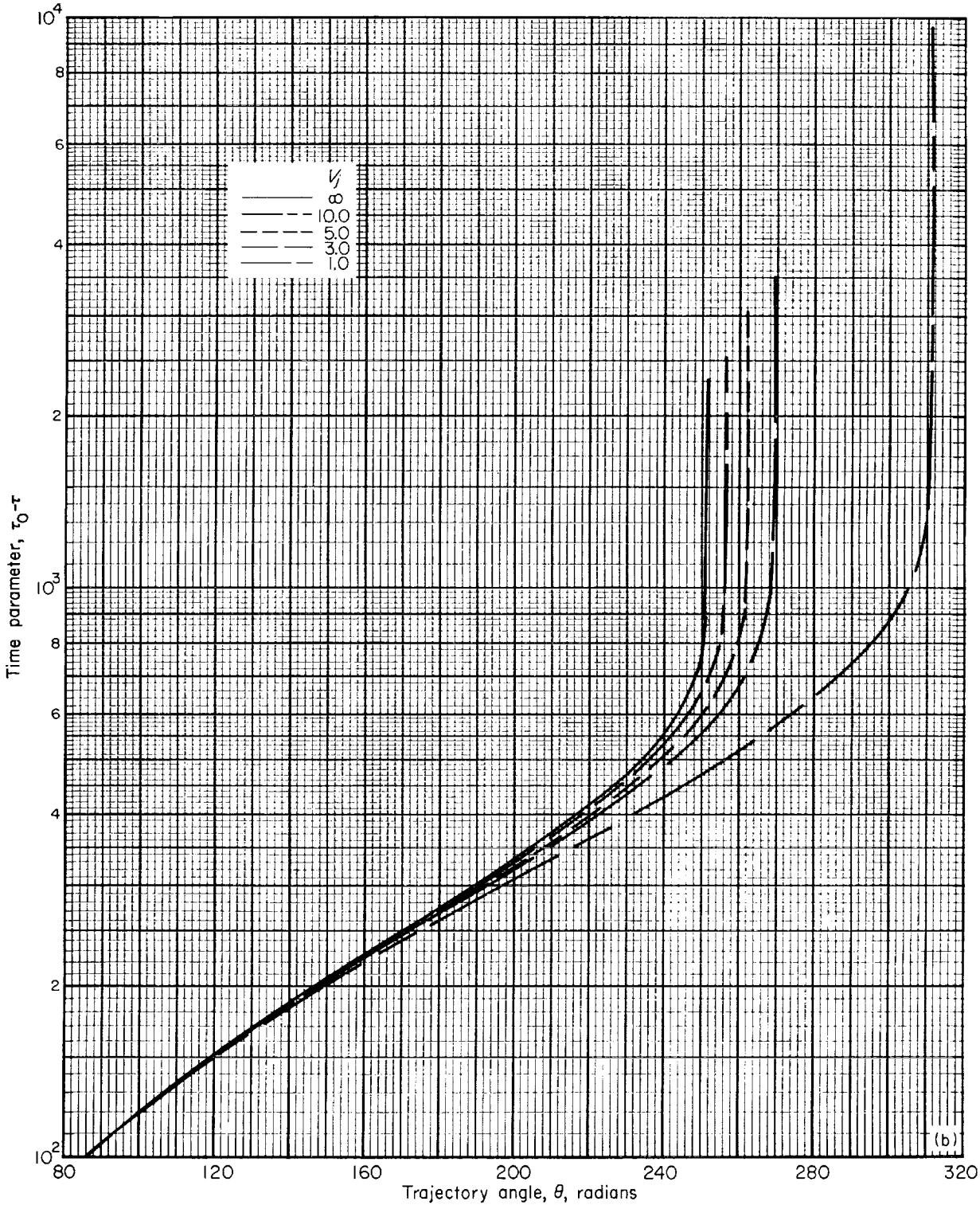

(b) a_0, 10^{-3}.

FIGURE 11.—Continued. Trajectory angle as a function of time for inward paths.

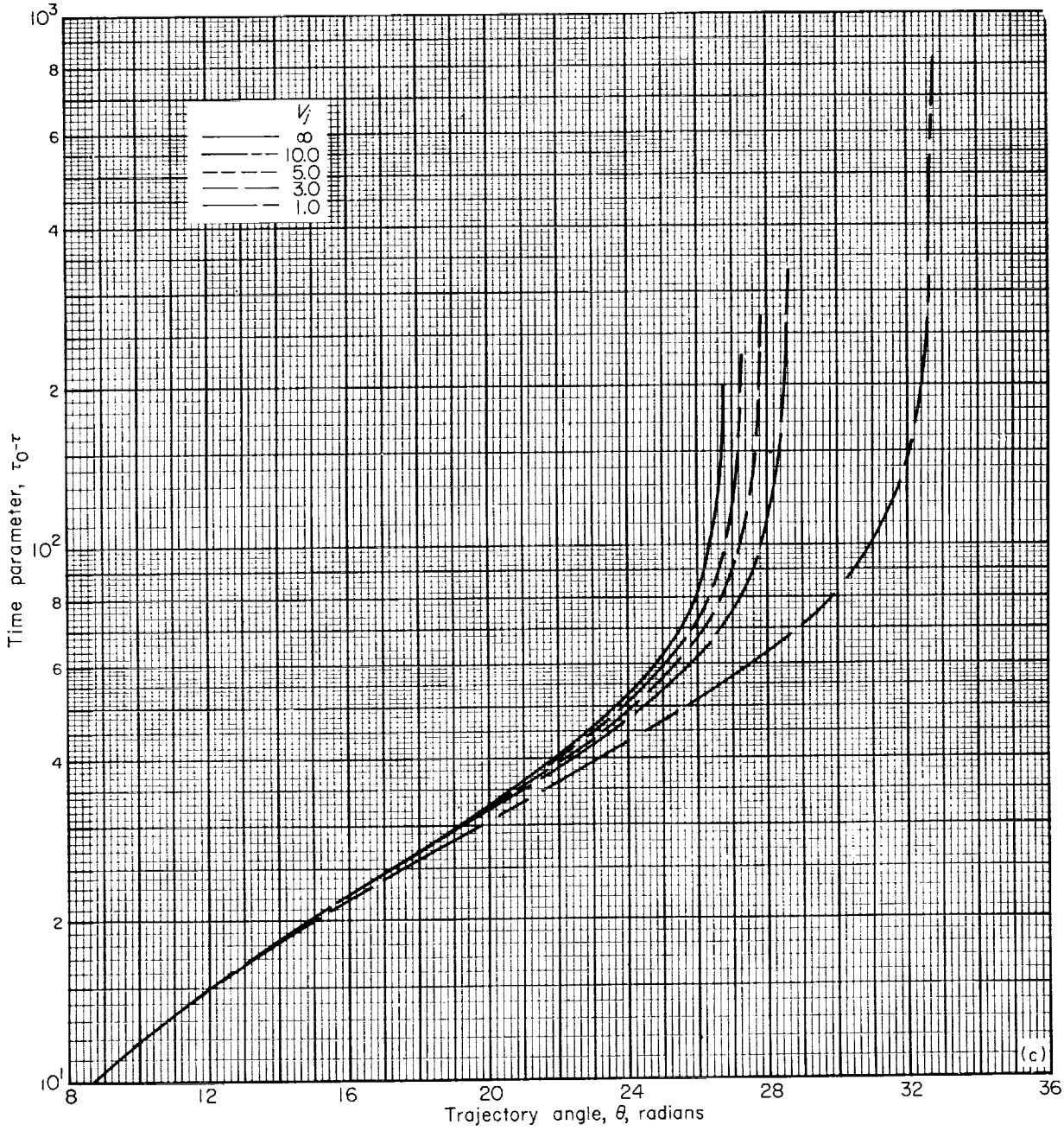

(c) a_0, 10^{-2}.

FIGURE 11.—Continued. Trajectory angle as a function of time for inward paths.

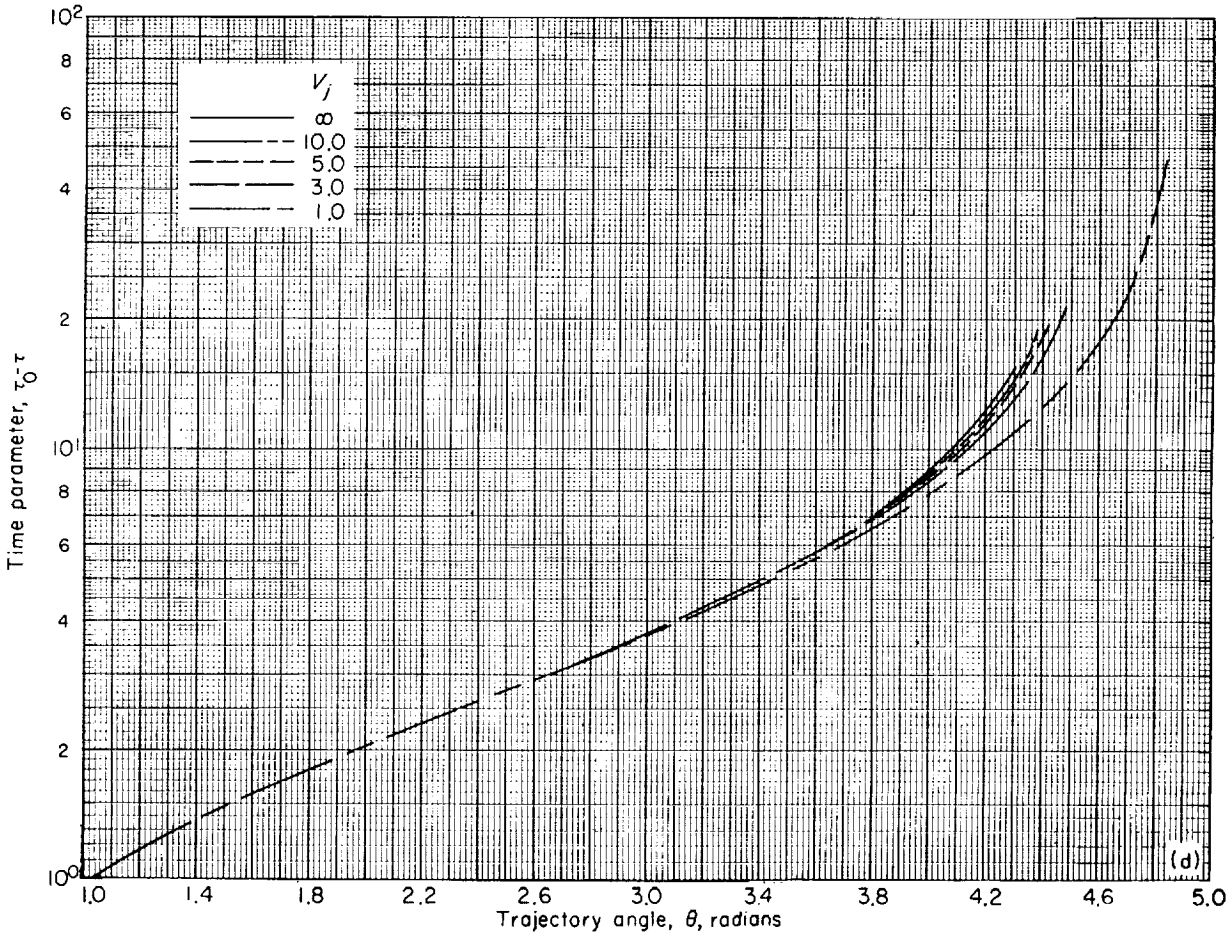

(d) a_0, 10^{-1}.

FIGURE 11.— Continued. Trajectory angle as a function of time for inward paths.

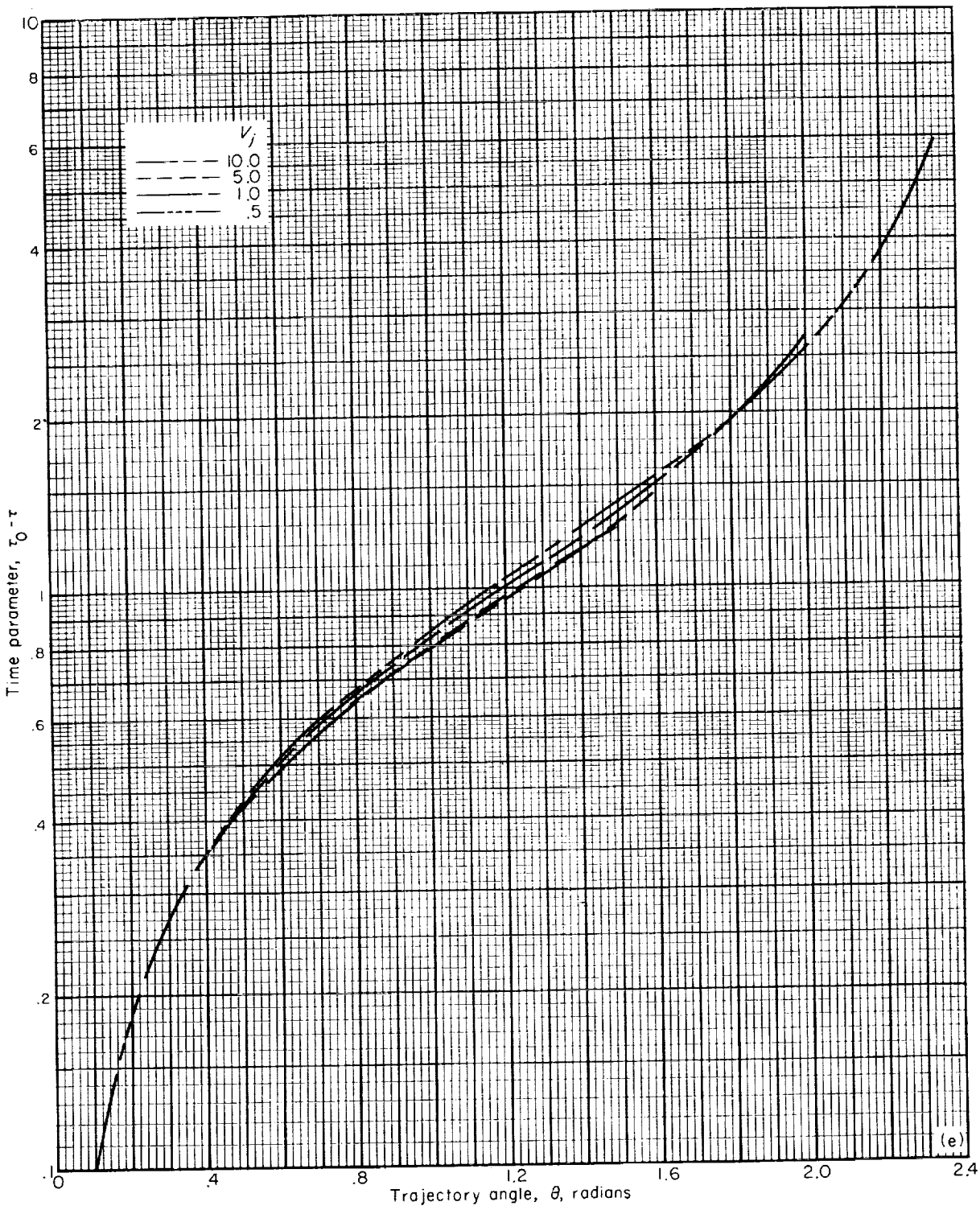

(e) a_0, 1.0.

FIGURE 11.—Continued. Trajectory angle as a function of time for inward paths.

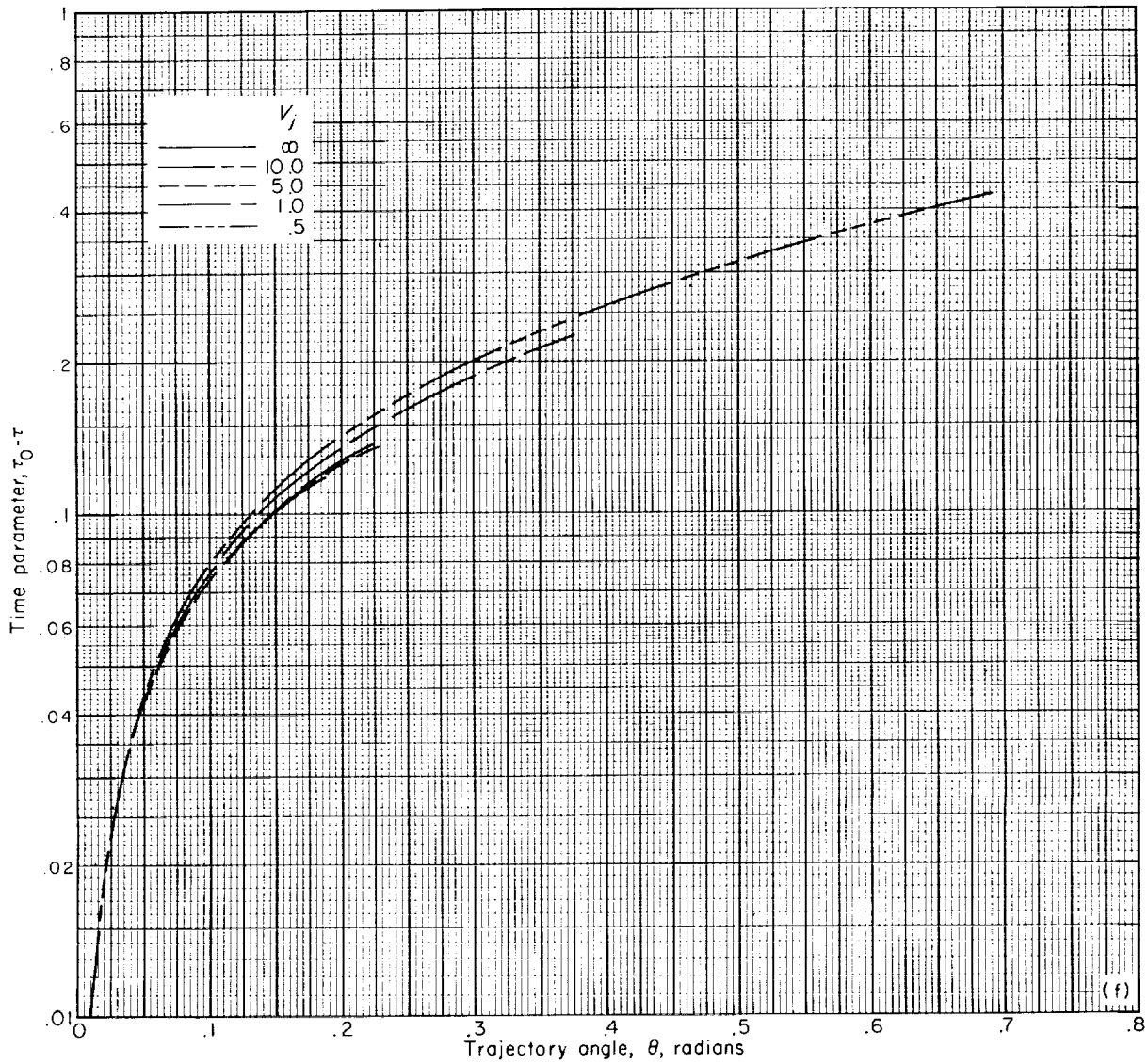

(f) a_0, 10.0.

FIGURE 11.—Concluded. Trajectory angle as a function of time for inward paths.

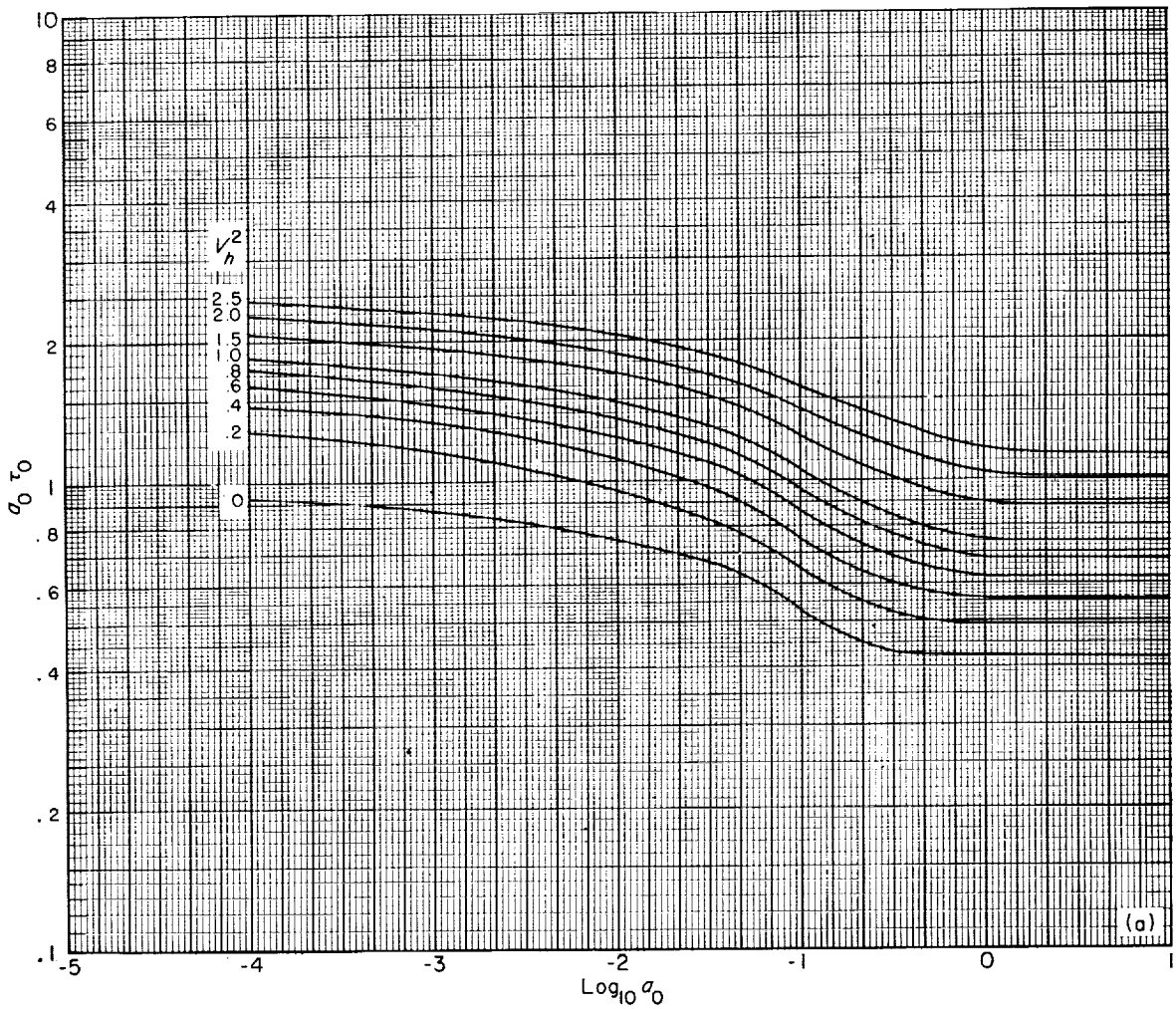

(a) $V_i = \infty$ (same for outward and inward paths).

FIGURE 12.— Propulsion time as a function of initial acceleration.

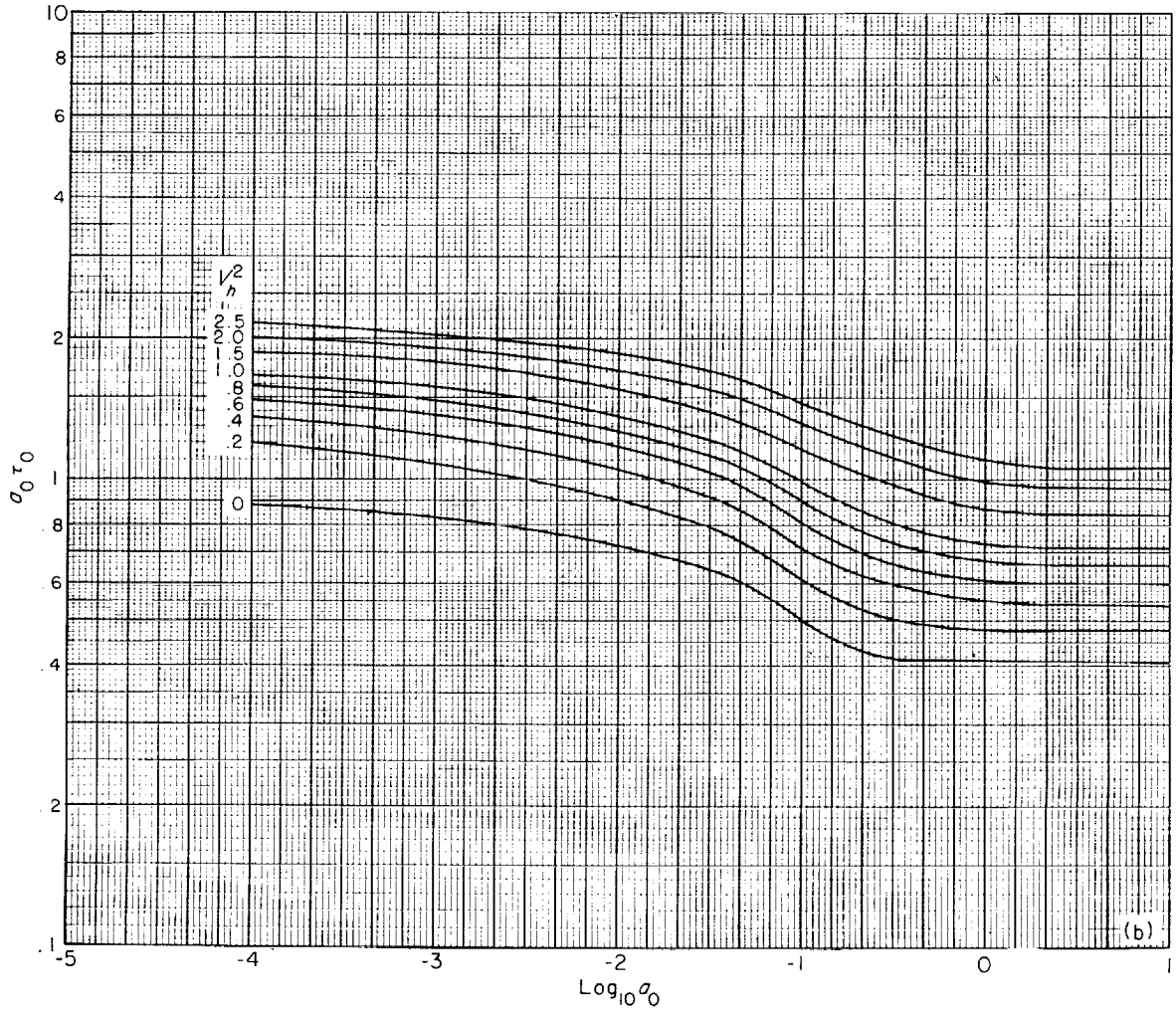

(b) $V_j=10$, outward path.

FIGURE 12.—Continued. Propulsion time as a function of initial acceleration.

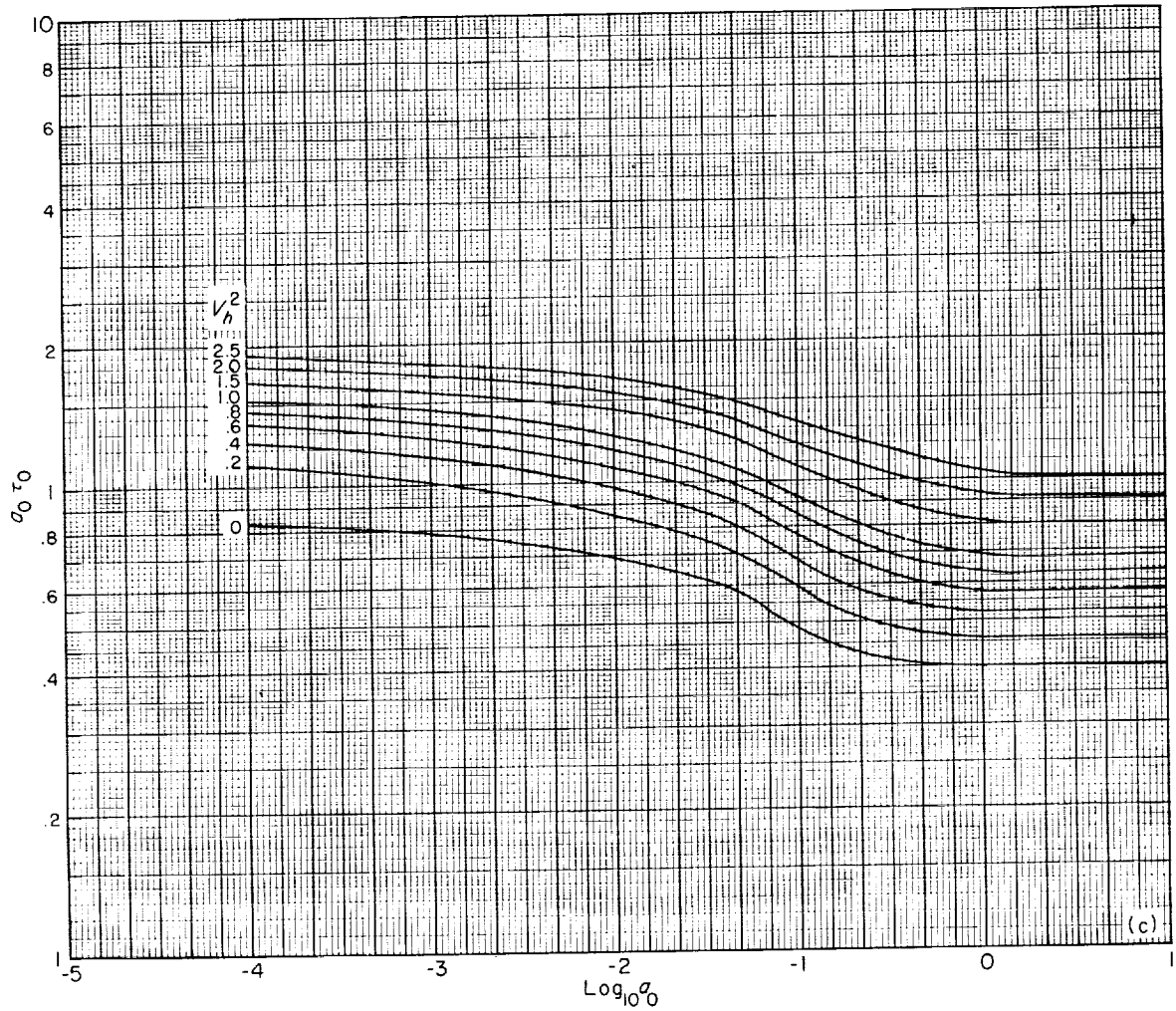

(c) $V_j=5$, outward path.

FIGURE 12.—Continued. Propulsion time as a function of initial acceleration.

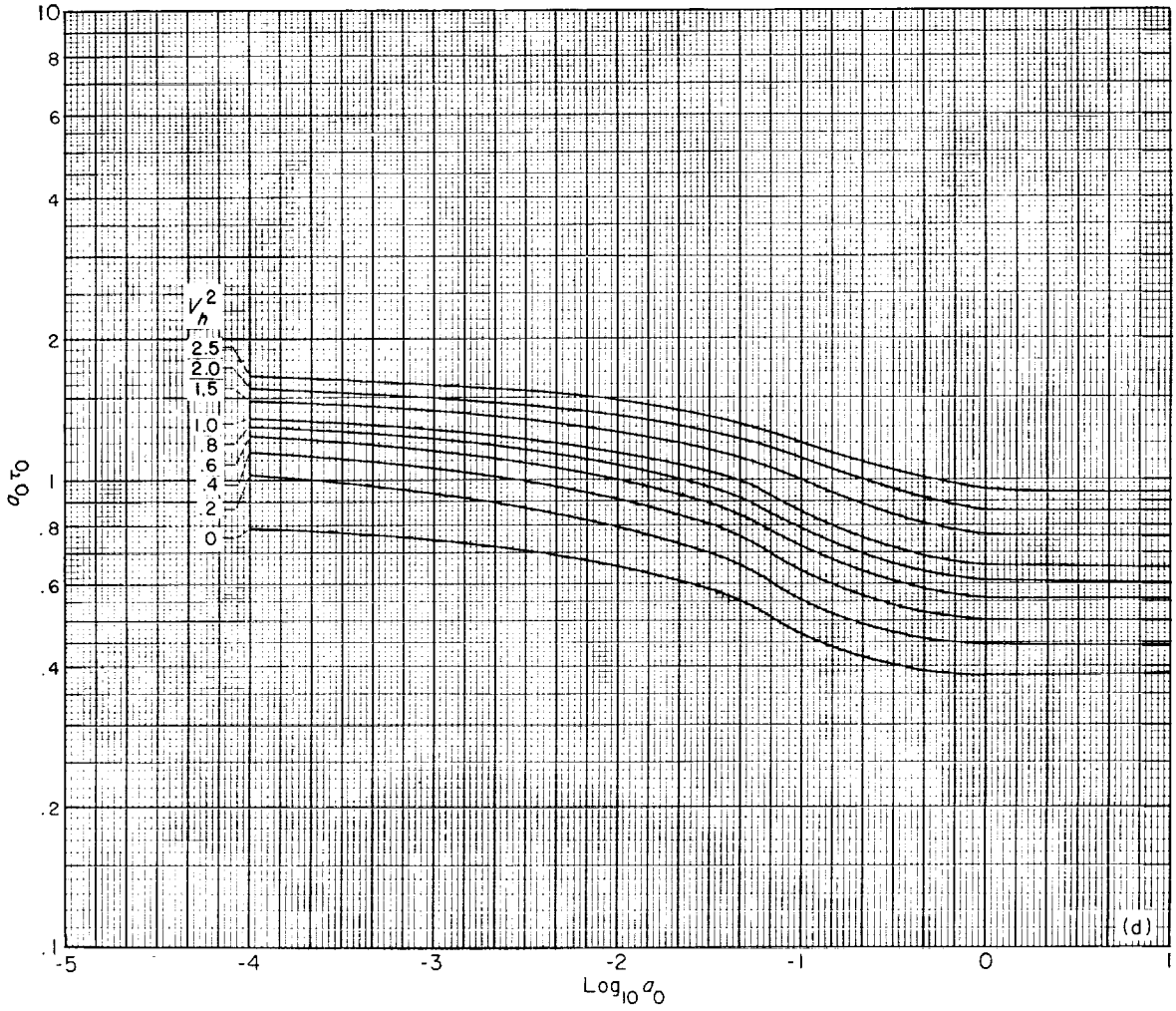

(d) $V_i=3$, outward path.

FIGURE 12.—Continued. Propulsion time as a function of initial acceleration.

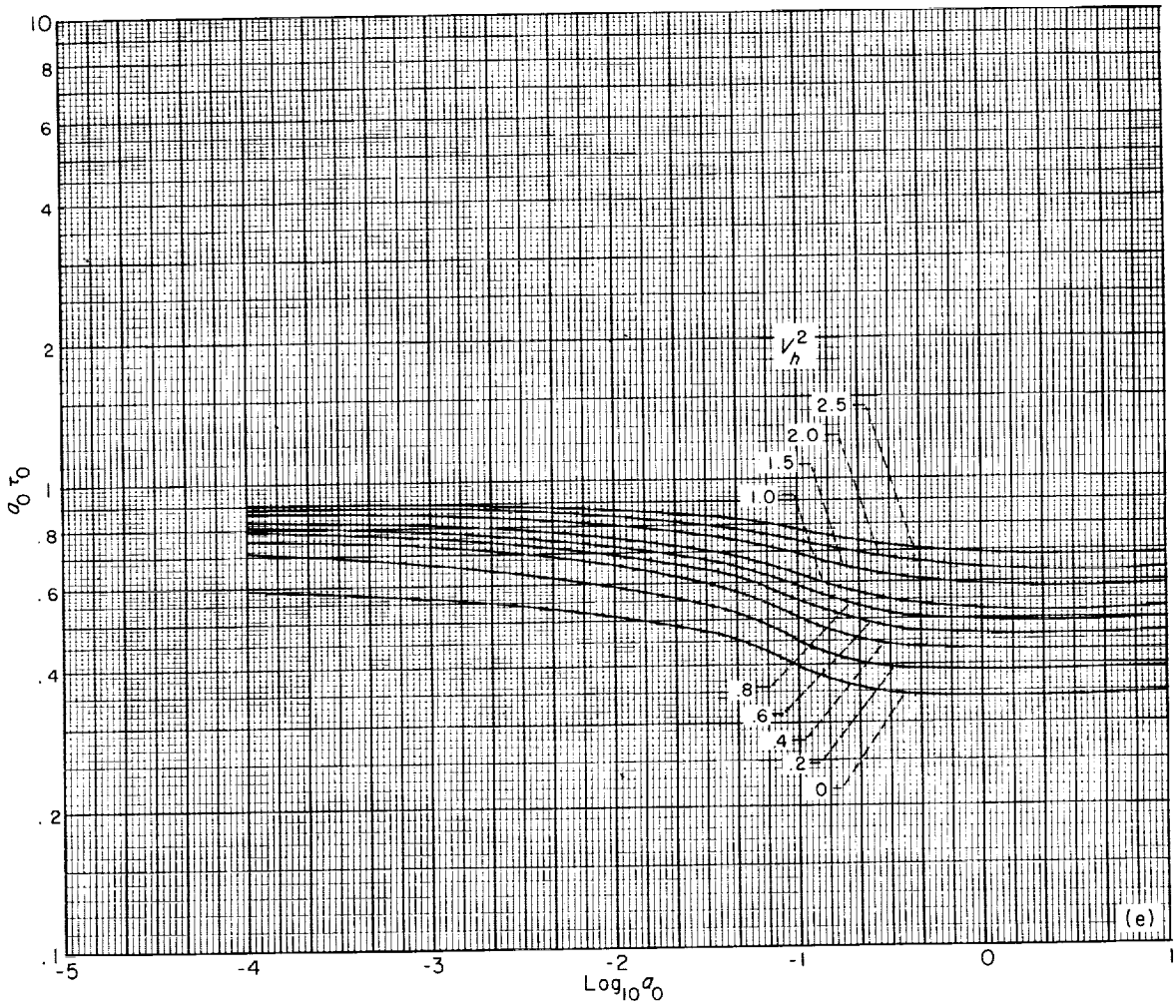

(c) $V_j=1$, outward path.

FIGURE 12.—Concluded. Propulsion time as a function of initial acceleration.

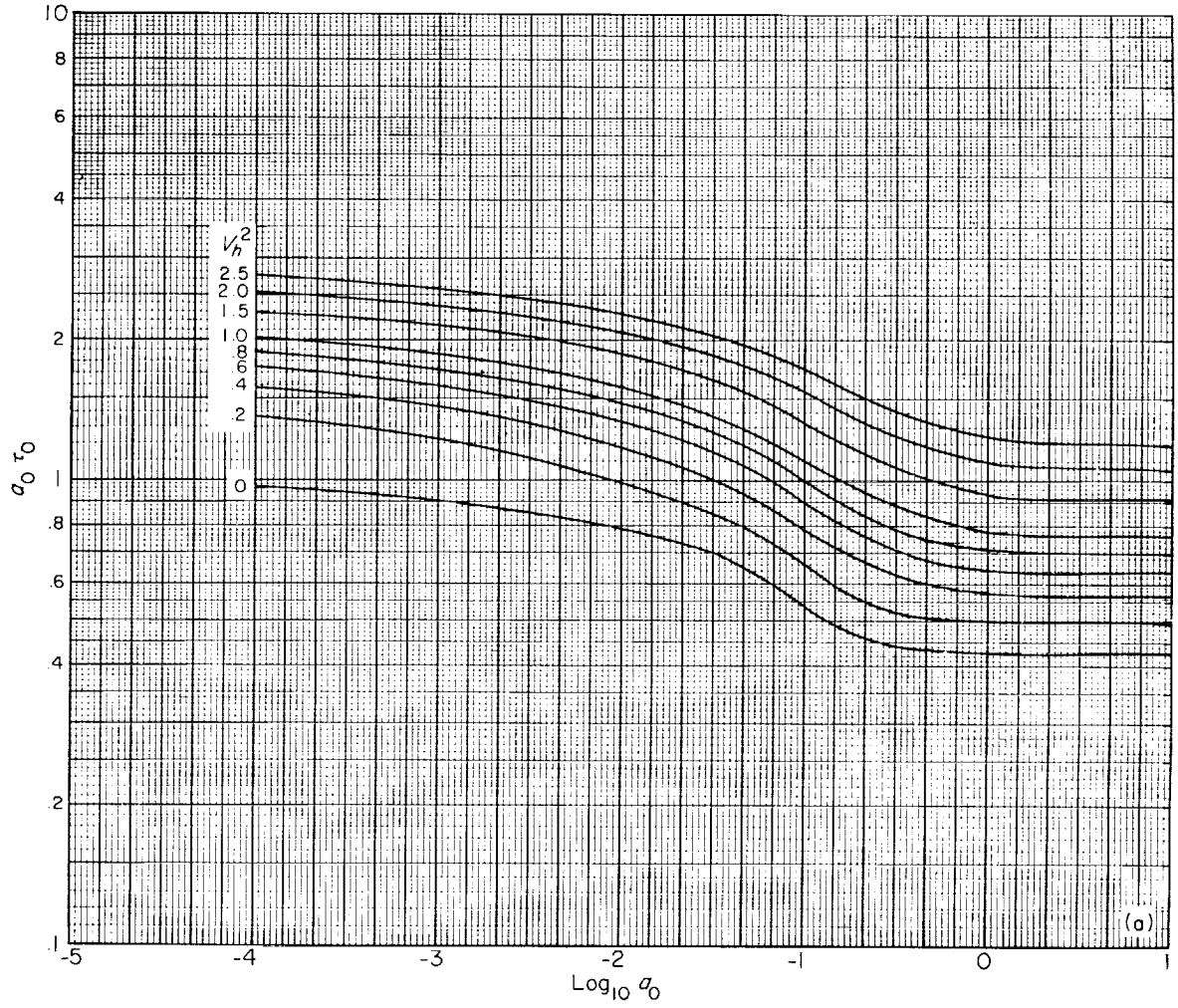

(a) $V_i = 10$, inward path.

FIGURE 13.—Propulsion time as a function of final acceleration.

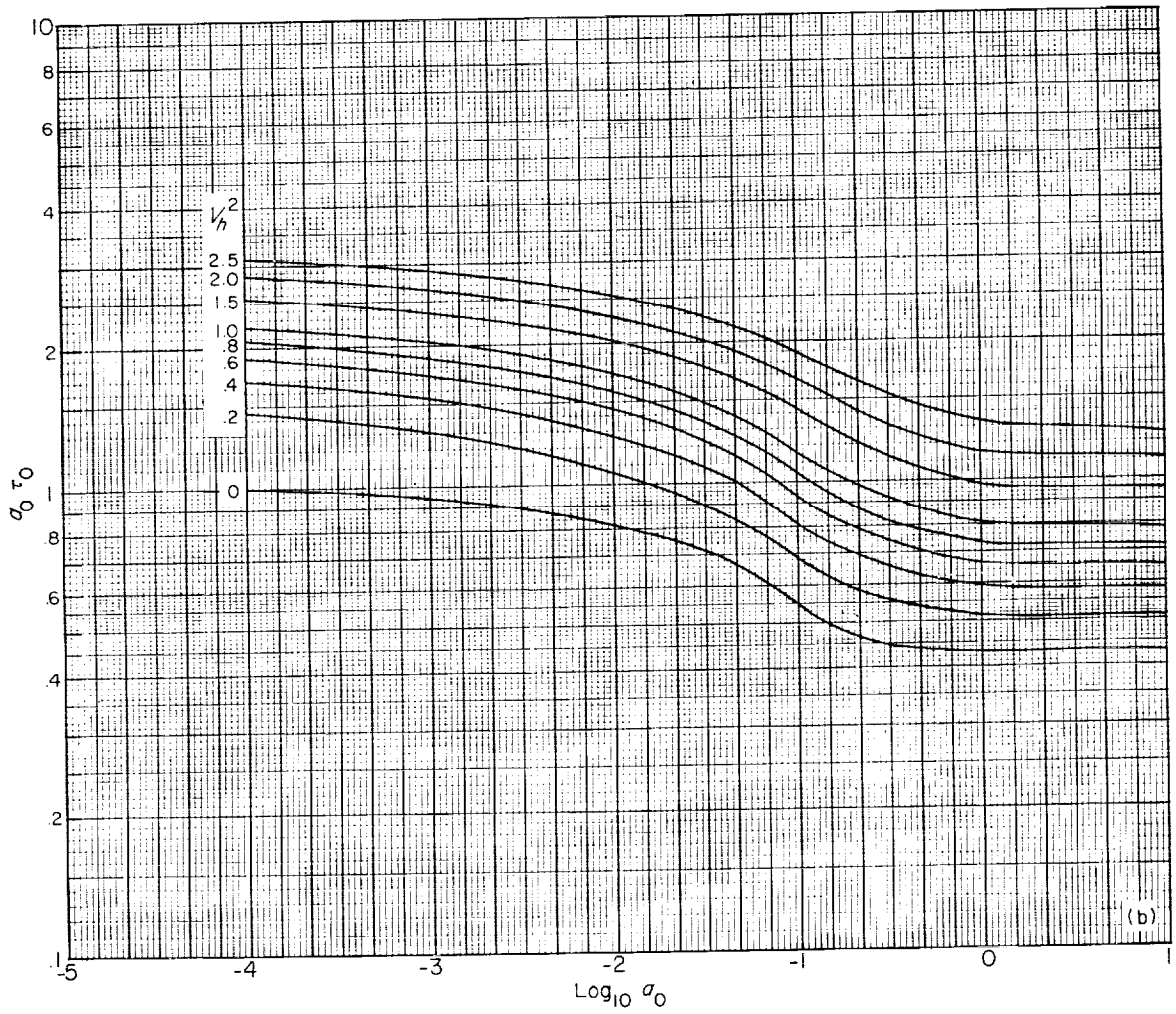

(b) $V_j=5$, inward path.

FIGURE 13.—Continued. Propulsion time as a function of final acceleration.

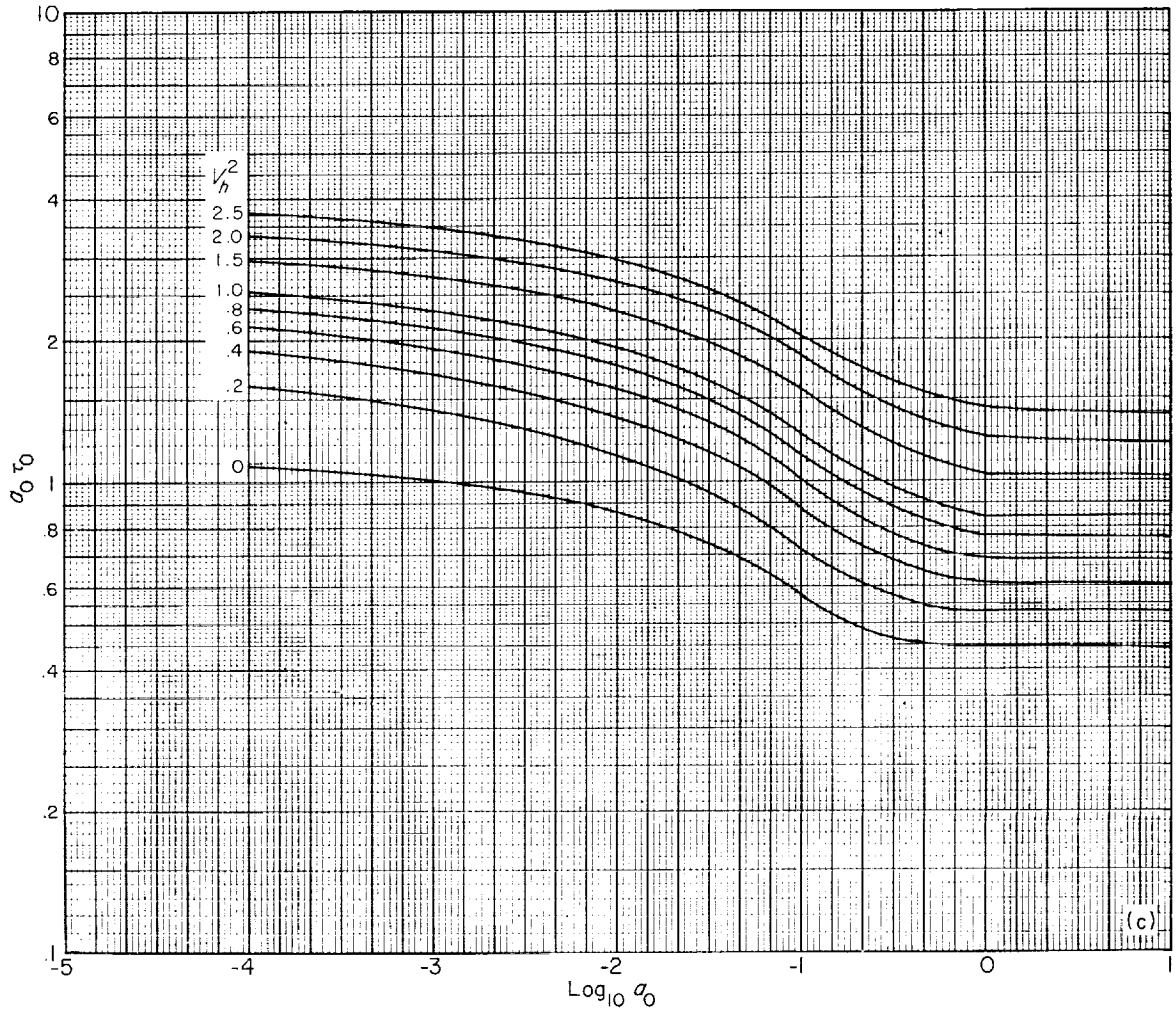

(c) $V_i=3$, inward path.

FIGURE 13.—Continued. Propulsion time as a function of final acceleration.

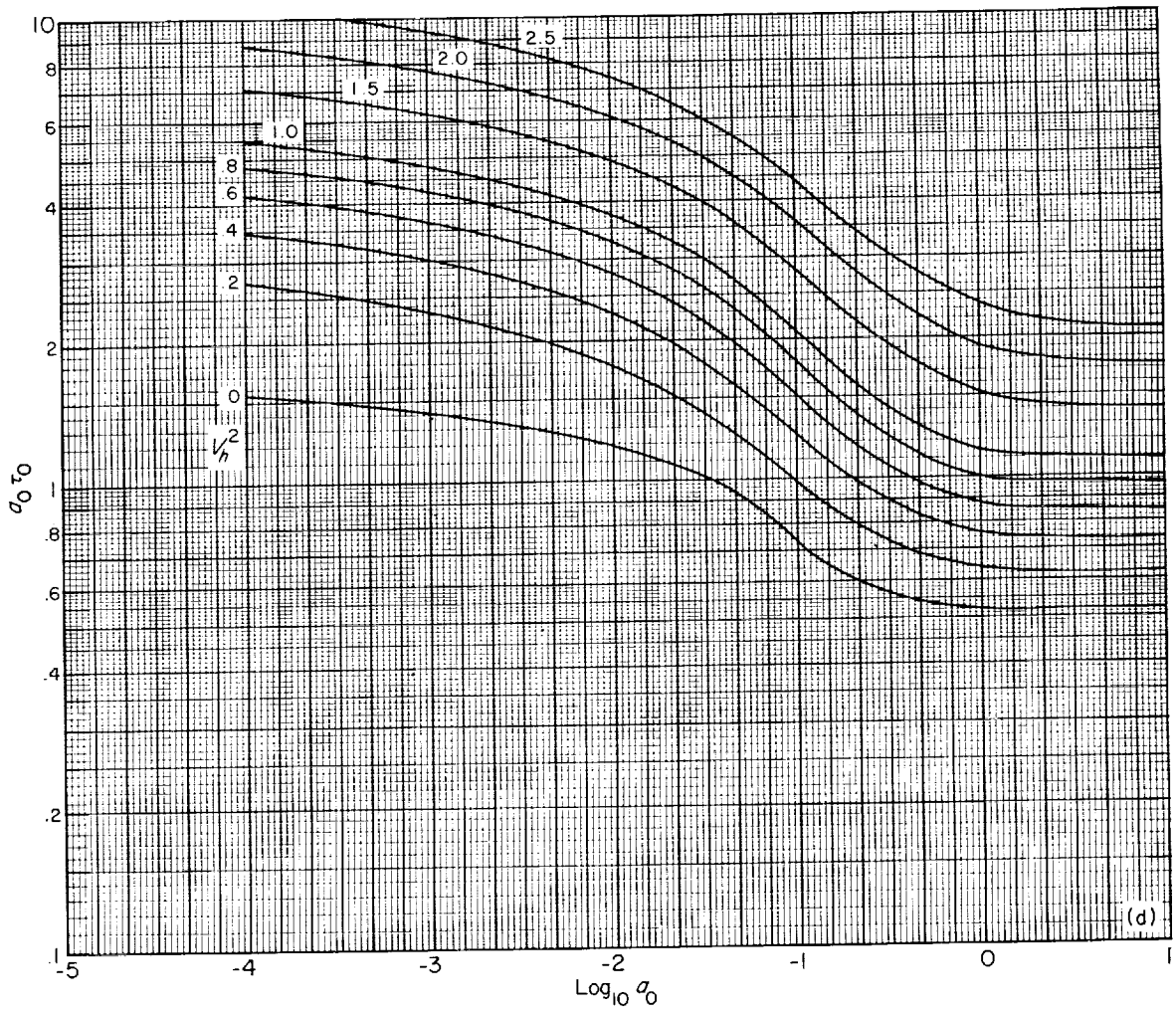

(*d*) $V_i = 1$, inward path.

FIGURE 13.—Concluded. Propulsion time as a function of final acceleration.

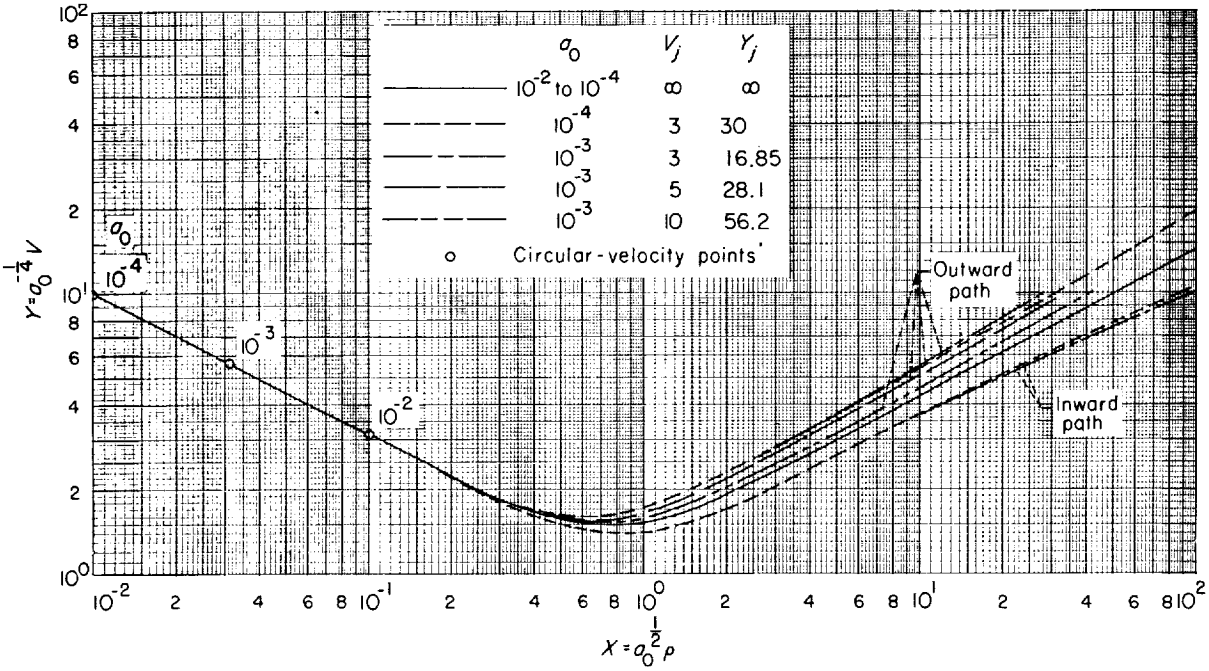

FIGURE 14.—Correlation of velocity-distance parameters.

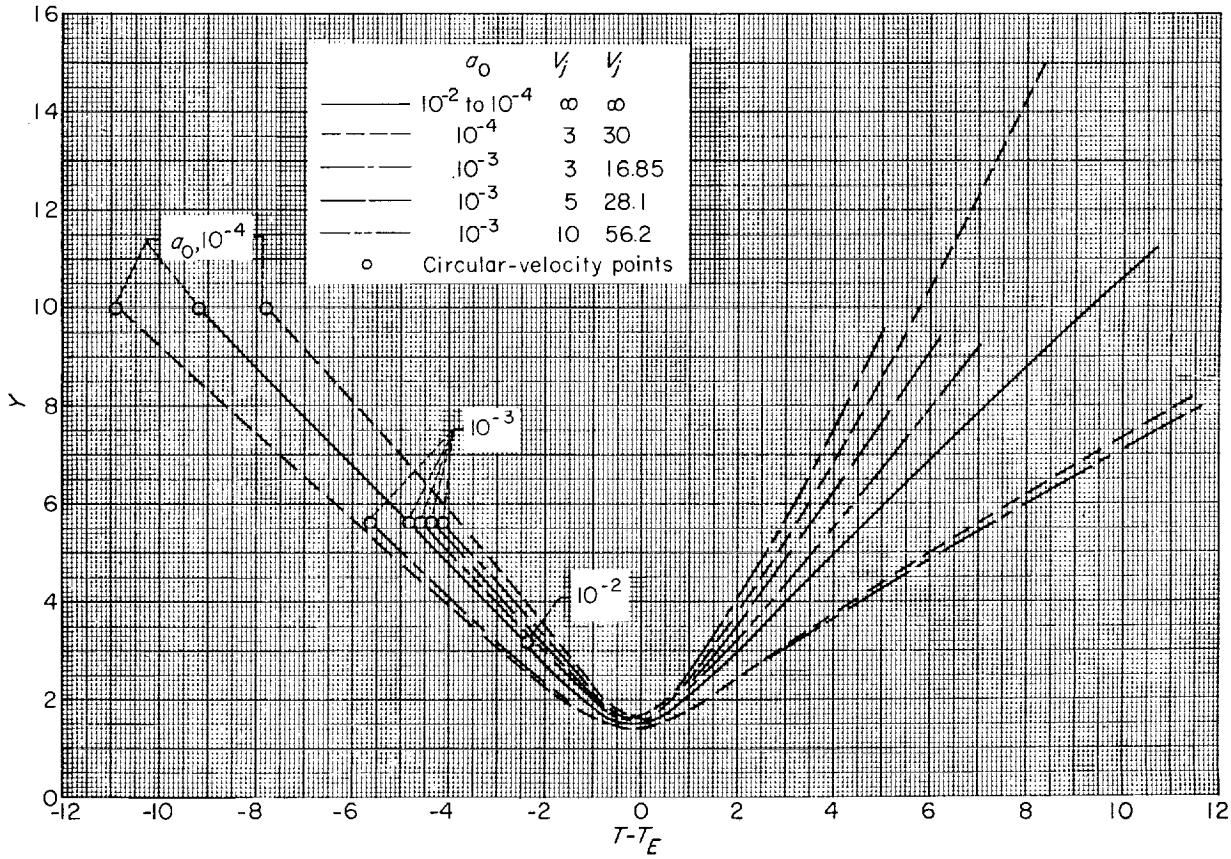

FIGURE 15.—Correlation of velocity-time parameters.

U.S. GOVERNMENT PRINTING OFFICE: 1960